

Design of Robust Controllers for Multivariable Nonlinear Plants

Javier Andres Villegas

A Thesis
presented for the degree of
Master of Electronic Engineering

Supervised by Dr Anthony M Holohan
School of Electronic Engineering
Dublin City University

December 2002

I hereby certify that this material, which I now submit for assessment on the programme of study leading to the award of Master of Electronic Engineering is entirely my own work and has not been taken from the work of others save and to the extent that such work has been cited and acknowledged within the text of my work.

Signed: Javier Villegas

ID: 99145855

Date: 07-02-2003

Abstract

This thesis deals with design techniques for robust non-linear multivariable systems. It describes and discusses some design techniques for such systems.

First, one-loop-at-a-time design using the root locus method is considered. The disadvantages of this approach are outlined. Next, some gain-scheduling controllers are designed for each loop. Then, a multivariable optimization approach is taken. Software to find the frequency domain solution of the two-block weighted-mixed-sensitivity problem using the Youla Parameterisation and Smith-McMillan form is developed. This two-variable problem decouples into two single-variable problems, corresponding to optimizing at the input and output of the plant.

The fundamental limitations and the trade-offs in design are studied at the input and output of the plant.

All controllers are tested and implemented on the inverted pendulum-cart apparatus, an unstable single-input two-output system.

Acknowledgments

I would sincerely like to thank my supervisor, Dr Anthony Holohan, for his constant guidance and encouragement during the past years, which I gratefully appreciated. He has always been ready to give his time generously to discuss ideas and difficulties, and to provide invaluable advice. He made my dream of following postgraduate studies come true.

I would also like to thank Professor Charles McCorkell and the School of Electronic Engineering for giving me the chance of studying at DCU and for funding my research.

I want to thank my friends Amra, Elodie, Prince, Li-Chuan, Val and all other friends from DCU. They made life in Dublin more enjoyable and memorable. Special thanks to Mariem, Gloria, Angela, Felipe, Jaime and Eury for their help and friendship from afar.

Finally, I want to thank my family, specially my mother, my brother and my uncle Jairo for their encouragement and support. Quiero dedicar esta tesis a mi madre por su paciencia, amor y apoyo.

Contents

1	Introduction	1
1 1	Motivation	1
1 2	Outline of the Thesis	2
2	Background	4
2 1	The Inverted Pendulum	4
2 1 1	Description	4
2 1 2	Physical Modelling	5
2 1 3	Conventional Linearization	8
2 1 4	Description of the Real System	11
2 1 5	Choice of Design Methods	12
2 2	The Smith-McMillan Form	12
2 2 1	Smith-McMillan Form of the Inverted Pendulum	14
2 3	Poles and Zeros of a Transfer-Function Matrix	16
2 3 1	Poles and Zeros	17
2 3 2	Input and Output Directions	17
3	Youla Parameterization	19
3 1	Solving the Generalised Bezout Equation - Approach 1	20
3 2	Solving the Generalised Bezout Equation - Approach 2	22
3 3	Generalized Bezout Equation of the Inverted Pendulum	23
3 3 1	State Space Realization of the Plant	24
3 3 2	Design of a Stabilizing Controller for the Plant	24
3 3 3	Design of an Observer for the Plant	25
3 3 4	Solution of the Generalized Bezout Equation	28
4	One-Loop-at-a-Time Method - Approach 1	31
4 1	Controller Design	31
4 1 1	Controller Design for the Angular Rotation	32
4 1 2	Controller Design for the Displacement	35
4 2	Discussion	37
5	Fundamental Limitations - SISO case	40
5 1	Some Facts About SISO Systems	40
5 2	Time Domain Limitations	43
5 3	Frequency Domain Limitations	46
5 4	Limitations and the Inverted Pendulum	47
5 4 1	Limitations of the Angular Rotation	48

5 4 2	Limitations of the Displacement	49
5 5	Discussion	50
6	One-Loop-at-a-Time Method - Approach 2	52
6 1	Controller Design - Approach 2	52
6 1 1	Controller Design for the Angular Rotation	53
6 1 2	Controller Design for the Displacement	54
6 2	Discussion	55
7	Gain Scheduling	60
7 1	Non-Linear Transfer Functions	61
7 2	GS Controller Design	62
7 2 1	GS Controller Design for the Angular Rotation	62
7 2 2	GS Controller Design for the Displacement	62
7 3	Discussion	64
8	\mathcal{H}_2 Optimization and Multivariable Control	65
8 1	Introduction	65
8 2	Finding the \mathcal{H}_2 Controller - Approach 1	67
8 2 1	Solution via Completion of Squares	68
8 2 2	Optimal Q at the Output	73
8 3	Finding the \mathcal{H}_2 Controller - Approach 2	78
8 4	\mathcal{H}_2 Control of the Inverted Pendulum	82
8 5	Discussion	84
9	Fundamental Limitations on Control - MIMO case	89
9 1	Interpolation Constraints	90
9 2	Limitations in Terms of the Elements of S and T	91
9 3	Input vs Output Properties	93
9 4	Discussion	95
10	Discussion and Conclusions	97
	Bibliography	100

List of Tables

7 1	Variation of poles of G_{eq}	63
9 1	Frequency vs direction of the plant	95

List of Figures

2 1	Inverted pendulum	5
2 2	Forces acting on the pendulum	6
4 1	Feedback system	32
4 2	Root locus of the angular rotation, G_2 without controller	33
4 3	Root locus with another unstable pole	33
4 4	Root locus with the new pole-zero pair	34
4 5	Step response of the angle control system	35
4 6	Bode diagram of the angle control system	35
4 7	Sensitivity functions of the angle control system	36
4 8	Equivalent control system for the displacement	37
4 9	Step response of the displacement system	38
4 10	Bode diagram of the displacement system	38
4 11	Sensitivity functions of the displacement system	39
5 1	Control loop	41
6 1	New feedback system	53
6 2	Step response of the angle loop	54
6 3	Bode diagram of the angle loop	55
6 4	Sensitivity functions of the angle loop	55
6 5	Step response of the displacement loop	56
6 6	Bode diagram of the displacement loop	57
6 7	Sensitivity functions of the displacement loop	57
6 8	Response of the real system	59
8 1	Control loop	66
8 2	Sensitivity function at the input $ S_i(jw) $	83
8 3	Complementary sensitivity function at the input, $ T_i(jw) $	84
8 4	Sensitivity function, $ (S_o(jw))_{i,j} $	85
8 5	Complementary sensitivity function, $ (T_o(jw))_{i,j} $	86
8 6	Singular values of S_o and T_o	87
8 7	Step response of the system $d(t)$ (upper plot) and $\phi(t)$ (lower plot)	88
9 1	Frequency vs plant/controller alignment	95

Chapter 1

Introduction

This thesis deals with design techniques for multivariable systems. Design of controllers for single-input single-output (SISO) systems can usually be done very effectively by using various traditional techniques, such as root locus methods and methods based on Nyquist and Bode plots. But the design of controllers for non-linear (NL) multi-input multi-output (MIMO) systems is a different matter. This is still an important open problem and it attracts a good deal of research.

1.1 Motivation

Sometimes when dealing with SISO systems other signals in the control loop are considered to be disturbances. However, it often happens that these disturbances originate in other loops. This effect is known as interaction or coupling. In some cases, interaction can be ignored, either because the coupling signals are weak or because a clear time-scale or frequency-scale separation exists. However, in other cases it can be necessary to consider all signals simultaneously. Then, the problem has to be tackled entirely as a multivariable design. Consequently a good knowledge and understanding of MIMO systems is important, since, in most situations, the tools used for analysing SISO systems are no longer applicable. Simple definitions like poles and zeros, among others, have a different meaning when dealing with multivariable processes and since matrices are involved, some functions (e.g. sensitivity) have a different interpretation at the input versus the output of the plant.

Rosenbrock [1, 2, 3] was the first researcher to emphasize that the MIMO case is much more challenging than the SISO case, and to recognize that new theoretical foundations would be required. Despite all the advances and improvements in MIMO control theory, multivariable design is still a subject under research, and it is still, in some sense, an unsolved problem, as discussed in Section 2.1.5.

The aim of this thesis is to study some design techniques for multivariable systems. Design methods which allow for certain levels of inaccuracy in the model of the plant to be controlled are emphasized. This is called robustness. Among these design techniques, this thesis focuses mainly on some frequency domain optimization techniques, such as minimizing a quadratic cost function in order to get a controller that gives a robust performance.

This thesis also discusses some advantages and disadvantages of the design methods used. It also treats trade-offs and fundamental limitations in multivariable controller design, including the approach of treating the MIMO problem as several SISO problems.

Throughout the thesis the inverted pendulum is used as an application example. Since this system is multivariable with right half plane poles and zeros, which is non-linear and non-square, it gives more insight about the inherent limitations when facing a control design. All controllers are implemented and tested on this apparatus.

1.2 Outline of the Thesis

In Chapter 2, some important background used throughout the thesis is presented. First, a discussion of the inverted pendulum is given. Then some important definitions concerning MIMO systems are stated. In Chapter 3, the Youla parameterization is presented, and two approaches to solving the generalised Bezout equation are presented and discussed.

Next, in Chapter 4, a one-loop-at-a-time design technique is used. The plant is

viewed as a set of SISO plants and some SISO controllers are designed for each loop using the root locus method. Then in Chapter 5, using the results of these designs, the fundamental limitations imposed by right half plane (RHP) poles and zeros and the impact of these limitations on the closed-loop performance are studied. Also, fundamental limitations for general SISO systems are discussed for both the time and the frequency domain. With the benefit of these limitations for designing control systems, the one-loop-at-a-time approach is further analyzed in Chapter 6. Within this one-loop-at-a-time framework, some gain-scheduled controllers are designed for each loop in Chapter 7.

In Chapter 8, a multivariable optimization approach is taken. First a novel approach is attempted. Indeed a frequency domain solution of the \mathcal{H}_2 problem based on the Youla Parameterization using frequency domain (Matlab) software is developed. The \mathcal{H}_2 problem is recast as a two-block weighted-mixed-sensitivity problem, which results in an optimization problem with two variables. Then by optimising at the input and then at the output of the plant this particular problem can be reduced to two decoupled single-variable problems. Next the standard two-norm optimization in the frequency domain using the Youla Parameterization for SISO systems is adapted to the multivariable case. Then, in Chapter 9 the fundamental limitations and the trade-offs when designing a multivariable controller are studied as well as the difference between optimizing transfer function matrices at the input and at the output. In Chapter 10, general conclusions are given.

Chapter 2

Background

In this chapter some basic definitions and some background material that are used throughout the thesis are stated. It starts with a brief discussion about the inverted pendulum which is used as a practical example. Then several definitions and some results that apply to MIMO systems are given.

2.1 The Inverted Pendulum

The inverted pendulum has been a classic tool in control system laboratories. It has been used to demonstrate various control design techniques, see [4], [5] and the references therein. For example, it was used to illustrate much of the material presented in the book by Kwakernaak and Sivan [6]. In this thesis the Digital Pendulum Mechanical Unit 33-200 manufactured by Feedback (see [7]) is used as an application example. A description of the well-known inverted pendulum apparatus is given.

2.1.1 Description

Consider the inverted pendulum of Figure 2.1. The pivot of the pendulum is mounted on a carriage which can move in the horizontal direction. The carriage is driven by a motor. The control problem is to move the carriage to a desired position while keeping the pendulum up and when the desired position has been

reached the pendulum should stay in the fully upright position ($\phi = 0$). The output (measurements) will be the position of the carriage (displacement) and the angular rotation of the pendulum (angle)

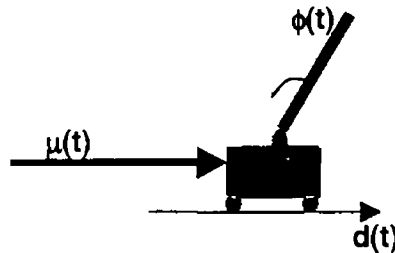


Figure 2.1 Inverted pendulum

Next, we develop a physical model for this system

2.1.2 Physical Modelling

Figure 2.2 shows the forces acting on the system. $\mu(t)$ is the force exerted by the motor, at time t , on the carriage. This force is the input variable to the system. The displacement of the cart at time t is $d(t)$ while the angular rotation at time t of the pendulum is $\phi(t)$. The mass of the pendulum is m , the distance from the pivot to the centre of gravity is L and the moment of inertia with respect to the centre of gravity is J . The carriage has mass M . The forces exerted on the pendulum are the gravitational force mg acting at the centre of gravity, a horizontal reaction force $H(t)$, and a vertical reaction force $V(t)$. Here g is the gravitational acceleration. Friction is accounted for only in the motion of the carriage and not at the pivot. F_r represents the friction coefficient.

From Newton's second law $\sum F = ma$ the sum of the horizontal components of the forces must be equal to the product of the mass m by the acceleration a acting on the pendulum, which is due to the acceleration of the carriages and the acceleration of the pendulum. Thus

$$m \frac{d^2}{dt^2} [d(t) + L \sin \phi(t)] = H(t) \quad (2.1.1)$$

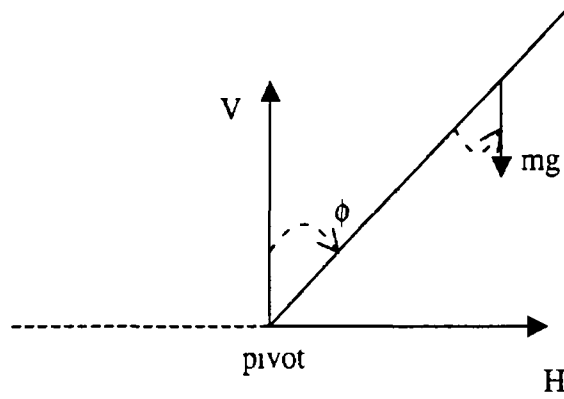


Figure 2 2 Forces acting on the pendulum

where $L \sin \phi(t)$ is the lever arm of the force acting on the pendulum. The lever arm of a force F about a chosen axis is the perpendicular distance from the line along that force to the axis. Stanford [8 page 93]. Similarly for the vertical components,

$$m \frac{d^2}{dt^2} [L \cos \phi(t)] = V(t) - mg \quad (2.1.2)$$

For this system the moment of inertia is constant. Hence

$$\sum \tau = J \frac{d\omega}{dt} \quad (2.1.3)$$

Equation (2.1.3) may be thought of as the rotational form of Newton's second law, Stanford [8 page 185], where ω is the angular velocity of the pendulum and τ is the torque. Using Equation (2.1.3) for this system yields,

$$J \frac{d^2}{dt^2} \phi(t) = LV(t) \sin \phi(t) - LH(t) \cos \phi(t) \quad (2.1.4)$$

For the forces acting on the carriage,

$$M \frac{d^2}{dt^2} d(t) = \mu(t) - H(t) - F_r \frac{d}{dt} d(t) \quad (2.1.5)$$

Performing the differentiations above yields

$$md(t) + L\phi(t) \cos \phi(t) - L\phi^2(t) \sin \phi(t) = H(t) \quad (2.1.6)$$

$$mg - mL\phi^2(t) \cos \phi(t) - mL\phi(t) \sin \phi(t) = V(t) \quad (2.1.7)$$

$$J\phi(t) = LV(t) \sin \phi(t) - LH(t) \cos \phi(t) \quad (2.1.8)$$

$$Md(t) = \mu(t) - H(t) - F_r d(t) \quad (2.1.9)$$

In order to eliminate $H(t)$ and $V(t)$ from Equation (2.1.8), Equations (2.1.6) and (2.1.7) are substituted into Equation (2.1.9), giving

$$J\ddot{\phi}(t) = mgL \sin \phi(t) - mL^2\dot{\phi}(t) \sin^2 \phi(t) - mL^2\dot{\phi}^2(t) \sin \phi(t) \cos \phi(t) - mLd(t) \cos \phi(t) - mL^2\phi(t) \cos^2 \phi(t) + mL^2\phi^2(t) \sin \phi(t) \cos \phi(t)$$

Simplifying we obtain

$$[J + mL^2]\ddot{\phi}(t) - mgL \sin \phi(t) + mLd(t) \cos \phi(t) = 0 \quad (2.1.10)$$

Division of this equation by $J + mL^2$ yields

$$\ddot{\phi}(t) = \frac{g}{L'} \sin \phi(t) - \frac{1}{L'} d(t) \cos \phi(t), \quad (2.1.11)$$

where

$$L' = \frac{J + mL^2}{mL} \quad (2.1.12)$$

This quantity has the significance of "effective pendulum length" since a pendulum of length L' that is not on a car would also yield Equation (2.1.11), Kwakernaak [6, page 6]

To simplify the equations, assume that m is small with respect to M and therefore neglect the horizontal reaction force, $H(t)$, on the motion of the carriage. This allows us to replace Equation (2.1.9) with

$$Md(t) = \mu(t) - F_r d(t) \quad (2.1.13)$$

In brief the equations which govern the system are (2.1.13), (2.1.11) and (2.1.12)

$$d(t) = \frac{1}{M} \mu(t) - \frac{F_r}{M} d(t)$$

and

$$\ddot{\phi}(t) = \frac{g}{L'} \sin \phi(t) - \frac{1}{L'} d(t) \cos \phi(t),$$

where

$$L' = \frac{J + mL^2}{mL}$$

2 1 3 Conventional Linearization

In order to get a linearized model, the system must first be described in state space form

Non-linear State Space Model

We define the states as follows,

$$x_1 = d(t), \quad x_2 = \dot{d}(t), \quad x_3 = \phi(t), \quad x_4 = \dot{\phi}(t), \quad (2 1 14)$$

and the input is

$$u = \mu(t) \quad (2 1 15)$$

Now, differentiating each component with respect to t , gives

$$\begin{aligned} \dot{x}_1 &= x_2, \\ \dot{x}_2 &= \ddot{d}(t), \\ \dot{x}_3 &= \dot{\phi}(t), \\ \dot{x}_4 &= \ddot{\phi}(t) \end{aligned}$$

Or, using Equations (2 1 13), (2 1 11) and (2 1 14),

$$\begin{aligned} \dot{x}_1 &= x_2, \\ \dot{x}_2 &= \frac{1}{M}u - \frac{F_r}{M}x_2, \\ \dot{x}_3 &= x_4, \\ \dot{x}_4 &= \frac{g}{L'} \sin x_3 - \frac{1}{L'}x_2 \cos x_3 \end{aligned} \quad (2 1 16)$$

and using the second equation to eliminate x_2 from the fourth equation gives

$$\dot{x}_4 = \frac{g}{L'} \sin x_3 - \frac{1}{ML'}u \cos x_3 + \frac{F_r}{ML'}x_2 \cos x_3$$

A state space description can now be written down. Writing the above equations in matrix form gives

$$\begin{pmatrix} \dot{x}_1 \\ \dot{x}_2 \\ \dot{x}_3 \\ \dot{x}_4 \end{pmatrix} = \begin{pmatrix} x_2 \\ \frac{1}{M}u - \frac{F_r}{M}x_2 \\ x_4 \\ \frac{g}{L'} \sin x_3 - \frac{1}{ML'}u \cos x_3 + \frac{F_r}{ML'}x_2 \cos x_3 \end{pmatrix} \quad (2 1 17)$$

For this system the outputs are the displacement $d(t)$ and the angular rotation of the pendulum $\phi(t)$, so define the output vector as

$$y(t) = \begin{pmatrix} d(t) \\ \phi(t) \end{pmatrix} = \begin{pmatrix} x_1 \\ x_3 \end{pmatrix} \quad (2.1.18)$$

Equilibrium Points

Equilibrium points are points in state space where the system can remain “static”, stationary, where it can come to rest or settle down, for some constant input level. In other words, they are points where the derivatives of the states are zero ($\dot{x} = 0$). Then, Equation (2.1.16) yields

$$\begin{aligned} x_2 &= 0, \\ \frac{1}{M}u - \frac{F_r}{M}x_2 &= 0 \Rightarrow u = 0, \\ x_4 &= 0, \\ \frac{g}{L'} \sin x_3 - \frac{1}{L'}x_2 \cos x_3 &= 0 \Rightarrow \frac{g}{L'} \sin x_3 = 0 \Rightarrow x_3 = 0 \text{ or } x_3 = \pi \end{aligned}$$

The set of equilibrium points is therefore described by $x_2 = 0$, $x_3 = 0$ or $x_3 = \pi$, $x_4 = 0$, $u = 0$ and x_1 is arbitrary.

These equations say that for an equilibrium point, the carriage and the pendulum must be stationary (i.e. have zero velocity) and the pendulum must have a vertical position, either upwards or downwards. Clearly, $x_3 = 0$ (pendulum up) is an unstable equilibrium point and $x_3 = \pi$ (pendulum down) is a stable one. With the pendulum in equilibrium, the carriage can be at any location. This is expected from physical considerations.

Linearized Model

Differentiating each row of Equation (2.1.17) with respect to each state and the input u and then evaluating at the equilibrium point (with $x_3 = 0$) we get the

linearized model for the inverted pendulum

$$\dot{x} = \begin{pmatrix} 0 & 1 & 0 & 0 \\ 0 & -\frac{F_r}{M} & 0 & 0 \\ 0 & 0 & 0 & 1 \\ 0 & \frac{F_r}{ML'} & \frac{g}{L'} & 0 \end{pmatrix} x + \begin{pmatrix} 0 \\ \frac{1}{M} \\ 0 \\ -\frac{1}{ML'} \end{pmatrix} u \quad (2.1.19)$$

$$y = \begin{pmatrix} 1 & 0 & 0 & 0 \\ 0 & 0 & 1 & 0 \end{pmatrix} x \quad (2.1.20)$$

where $x = (x_1 \ x_2 \ x_3 \ x_4)^T$

The state space representation of the system is then

$$A = \begin{pmatrix} 0 & 1 & 0 & 0 \\ 0 & -\frac{F_r}{M} & 0 & 0 \\ 0 & 0 & 0 & 1 \\ 0 & \frac{F_r}{ML'} & \frac{g}{L'} & 0 \end{pmatrix} \quad B = \begin{pmatrix} 0 \\ \frac{1}{M} \\ 0 \\ -\frac{1}{ML'} \end{pmatrix} \quad C = \begin{pmatrix} 1 & 0 & 0 & 0 \\ 0 & 0 & 1 & 0 \end{pmatrix}$$

Transfer Functions

The transfer functions can now be calculated Using the formula

$$G(s) = C(sI - A)^{-1}B, \quad (2.1.21)$$

where $G(s)$ is the transfer function of the system, gives

$$G(s) = \begin{pmatrix} G_1 \\ G_2 \end{pmatrix} = \begin{pmatrix} \frac{\frac{1}{M}}{s(s + \frac{F_r}{M})} \\ \frac{-\frac{1}{ML'}s}{(s + \frac{F_r}{M})(s^2 - \frac{g}{L'})} \end{pmatrix} \quad (2.1.22)$$

Let

$$\begin{aligned} a &= \frac{F_r}{M} \\ b &= \sqrt{\frac{g}{L'}} \\ k_1 &= \frac{1}{M} \\ k_2 &= \frac{1}{ML'} \end{aligned} \quad (2.1.23)$$

This gives the following linearized model

$$G(s) = \begin{pmatrix} G_1 \\ G_2 \end{pmatrix} = \begin{pmatrix} \frac{k_1}{s(s+a)} \\ \frac{-k_2s}{(s+a)(s+b)(s-b)} \end{pmatrix} \quad (2.1.24)$$

where the following values were obtained after several identification experiments

$$\begin{aligned}a &= 3.33 \\b &= 5.46 \\k_1 &= 11 \\k_2 &= 30\end{aligned}\tag{2.1.25}$$

and using Equation 2.1.23 yields,

$$\begin{aligned}F_r &= 0.303\text{Kg/s}, \\M &= 0.091\text{Kg} \\L' &= 0.328298\text{m}, \\g &= 9.8\text{m/s}^2\end{aligned}\tag{2.1.26}$$

This is the model which will be used for all the experimental work reported here

2.1.4 Description of the Real System

In this section the Digital Pendulum Mechanical Unit 33-200 manufactured by Feedback, [7], is briefly described. The pendulum-cart set-up consists of a pole mounted on a cart in such a way that the pole can swing free only in the vertical plane. The cart is driven by a DC motor. The cart is allowed to move on a rail of limited length.

The pendulum-cart set-up utilises two optical encoders as angle and position detectors. The first one is installed on the pendulum axis and the second one on the DC motor axis. The control signal is limited to be within a normalized range from -1 to 1. That is, it has a saturation at the input of the plant. Another non-linearity exists due to the cart friction which is a non-linear function of the velocity of the cart. Omitting or simplifying the friction on the mathematical model results in poor compatibility between the real system and the simulation model. Notice that the non-linear friction model was not taken into account during the modeling stage, which implies that a highly robust system has to be aimed for when designing controllers. This is acknowledged by the manufacturer. "Due to

the presence of disturbances and parameter uncertainties, a robust behavior is more important than the optimal character of the control strategy", [7]

2.1.5 Choice of Design Methods

It was said earlier that the inverted pendulum has been used as a classical tool in the control system laboratories. Many methods for designing controllers has been used and implemented with this system. Those include, Linear Quadratic Regulator (LQR), \mathcal{H}_∞ , Fuzzy Logic and Neural Networks. It must be acknowledged that each of these methods will control the pendulum successfully.

This thesis focuses mainly on two design methods, the gain scheduling (GS) approach and the \mathcal{H}_2 optimization approach as well as the analysis of limitations that exist on any system, specifically the pendulum system. GS is chosen because it has become a very popular method for designing controllers for non-linear systems and it is still a subject under research. \mathcal{H}_2 optimization is chosen because 2-norm-optimization based controller design has become very popular and it is still an unsolved problem in the sense of its transparency (there are no algebraic equations for the design of the controllers design is an iterative process) and its design time (involves the selection of some weights, which is done sometimes by trial and error).

2.2 The Smith-McMillan Form

The Smith-McMillan form of a multivariable plant transforms the plant's transfer function into a diagonal transfer function matrix by pre- and post-multiplying by unimodular matrices. A polynomial matrix is called *unimodular* if it has an inverse which is also a polynomial matrix. It follows that its determinant is a constant (independent of the variable s). It is possible to analyze the position and number of poles and zeros from the diagonal equivalent transfer matrix. The Smith-McMillan form, [9, §2] [10] relies on the fact that every rational transfer

function matrix can be expressed as a polynomial matrix, divided by a common denominator polynomial. For more information about the Smith-McMillan form see Maciejowski [9, §2] and Tadeo [10].

An *elementary matrix* is a matrix which represents an elementary row (column) operation. “Represents” means that multiplying on the left (right) by the elementary matrix performs the row (column) operation. We say that two (polynomial or rational) matrices $P(s)$ and $Q(s)$ are *equivalent* (symbolized $P(s) \sim Q(s)$) if there exist sequences of left and right elementary matrices $\{L_1(s), \dots, L_l(s)\}$ and $\{R_1(s), \dots, R_r(s)\}$ such that

$$P(s) = L_l(s)L_{l-1}(s) \dots L_1(s)Q(s)R_1(s) \dots R_r(s)$$

The next theorem is a result given in Maciejowski [9, §2.2].

Theorem 2.2.1 (Smith-McMillan Form) *If $G(s)$ is a rational matrix of normal rank r , then $G(s)$ may be transformed by a series of elementary row and column operations into a pseudo-diagonal rational matrix $M(s)$ of the form*

$$M(s) = \text{diag} \left\{ \frac{\varepsilon_1(s)}{\psi_1(s)}, \frac{\varepsilon_2(s)}{\psi_2(s)}, \dots, \frac{\varepsilon_r(s)}{\psi_r(s)}, 0, \dots, 0 \right\} \quad (2.2.1)$$

in which the monic polynomials $\{\varepsilon_i(s), \psi_i(s)\}$ are coprime for each i (i.e. they have no common factors) and satisfy the divisibility properties

$$\left. \begin{array}{l} \varepsilon_i(s) | \varepsilon_{i+1}(s) \\ \psi_{i+1}(s) | \psi_i(s) \end{array} \right\} \quad i = 1, \dots, r-1 \quad (2.2.2)$$

$M(s)$ is the Smith-McMillan form of $G(s)$.

This theorem says that any transfer function matrix can be factorized as

$$G = U \Lambda V$$

where U and V are unimodular matrices and Λ is a diagonal transfer function matrix with the structure given in Equation 2.2.1.

2 2 1 Smith-McMillan Form of the Inverted Pendulum

In this section the inverted pendulum is used as an example of how to find the Smith-McMillan form of a transfer function matrix

First, the rational matrix $G(s)$ Equation (2 1 24), is expressed as a polynomial matrix, divided by a common denominator polynomial, as follows

$$G(s) = \frac{1}{s(s+a)(s^2-b^2)} G_p \quad (2 2 3)$$

where

$$G_p = \begin{pmatrix} k_1(s^2 - b^2) \\ -k_2 s^2 \end{pmatrix}$$

Using elementary matrices the polynomial matrix G_p in the equation above, can be transformed into a diagonal matrix pre-multiplied (row operations) and post-multiplied (column operations) by unimodular matrices. Notice that an elementary matrix is unimodular, and the product of unimodular matrices is a unimodular matrix. Thus G_p can be transformed as follows,

- 1 Interchange row 1 and 2

$$G_1 = L_1 G_p = \begin{pmatrix} -k_2 s^2 \\ k_1(s^2 - b^2) \end{pmatrix}$$

where

$$L_1 = \begin{pmatrix} 0 & 1 \\ 1 & 0 \end{pmatrix}$$

- 2 Replace row 2 with row 2 plus $\frac{k_1}{k_2}$ times row 1,

$$G_2 = L_2 G_1 = \begin{pmatrix} -k_2 s^2 \\ -k_1 b^2 \end{pmatrix}$$

where

$$L_2 = \begin{pmatrix} 1 & 0 \\ \frac{k_1}{k_2} & 1 \end{pmatrix}$$

3 Interchange row 1 and 2,

$$G_3 = L_3 G_2 = \begin{pmatrix} -k_1 b^2 \\ -k_2 s^2 \end{pmatrix}$$

where

$$L_3 = \begin{pmatrix} 0 & 1 \\ 1 & 0 \end{pmatrix}$$

4 Replace row 2 with row 2 plus $-\frac{k_2 s^2}{k_1 b^2}$ times row 1,

$$G_4 = L_4 G_3 = \begin{pmatrix} -k_1 b^2 \\ 0 \end{pmatrix}$$

where

$$L_4 = \begin{pmatrix} 1 & 0 \\ -\frac{k_2 s^2}{k_1 b^2} & 1 \end{pmatrix}$$

5 Replace row 1 with $-\frac{1}{k_1 b^2}$ times row 1

$$G_5 = L_5 G_4 = \begin{pmatrix} 1 \\ 0 \end{pmatrix}$$

where

$$L_5 = \begin{pmatrix} -\frac{1}{k_1 b^2} & 0 \\ 0 & 1 \end{pmatrix}$$

Now, G_5 is the "diagonal" matrix after the transformation

Thus, in this case, the product of the sequence of left elementary matrices is

$$L = L_5 L_4 L_3 L_2 L_1 = \begin{pmatrix} -\frac{1}{k_1 b^2} & -\frac{1}{k_2 b^2} \\ -\frac{k_2 s^2}{k_1 b^2} & -\frac{1}{b^2}(s^2 - b^2) \end{pmatrix} \quad (2.2.4)$$

It can be checked that its determinant is a constant, $-\frac{1}{k_1 b^2}$, which indicates that L is a unimodular matrix. Moreover, its inverse, L^{-1} , is a polynomial matrix, which is

$$L^{-1} = \begin{pmatrix} k_1(s^2 - b^2) & -\frac{k_1}{k_2} \\ -k_2 s^2 & 1 \end{pmatrix} \quad (2.2.5)$$

Notice that, in this case, the matrix of right elementary matrices is equal to the identity matrix, since no column operations were performed. Hence, $G_5 \sim G_p$ (where G_p is given in Equation (2.2.3)), and therefore

$$LG_p = G_5 = \begin{pmatrix} 1 \\ 0 \end{pmatrix}$$

and it follows from the equation above and Equation (2.2.3) that

$$LG(s) = \frac{1}{s(s+a)(s^2-b^2)} \begin{pmatrix} 1 \\ 0 \end{pmatrix}$$

Thus

$$G(s) = L^{-1} \begin{pmatrix} \lambda(s) \\ 0 \end{pmatrix} \quad (2.2.6)$$

where

$$\lambda(s) = \frac{1}{s(s+a)(s^2-b^2)}$$

and L^{-1} is given in Equation (2.2.5). The matrix

$$\begin{pmatrix} \lambda(s) \\ 0 \end{pmatrix} = \begin{pmatrix} \frac{1}{s(s+a)(s+b)(s-b)} \\ 0 \end{pmatrix} \quad (2.2.7)$$

is then the *Smith-McMillan form* of $G(s)$.

2.3 Poles and Zeros of a Transfer-Function Matrix

In the SISO case, the zeros of a system are defined as the solutions $s = z_i$ to $G(s) = 0$ and, similarly, the poles are defined as the solutions $s = p_i$ to $G^{-1}(s) = 0$. Moreover, in the scalar case the zeros and poles could be found easily from a transfer function representation. However, for multivariable systems things are not that easy. The main difficulty in the MIMO case is that one has to work with matrix, rather than scalar, transfer functions. It is well known that the principal difference between scalars and matrices is the presence of directions and that directions are relevant for vectors and matrices, but not for scalars. Thus,

as is shown next, the zeros and poles of MIMO plants not only involve a scalar value (i.e. $s = z_i$) but also directions

2.3.1 Poles and Zeros

As stated at the beginning of Section 2.2 the poles and zeros of a multivariable system can be found from the Smith-McMillan form. The result is as follows (see Maciejowski [9, §2.3])

Definition 2.3.1 Let $G(s)$ be a rational transfer-function matrix with Smith-McMillan form

$$M(s) = \text{diag} \left\{ \frac{\epsilon_1(s)}{\psi_1(s)}, \dots, \frac{\epsilon_r(s)}{\psi_r(s)}, 0, \dots, 0 \right\}$$

and define the **pole polynomial** and **zero polynomial** as

$$p(s) = \psi_1(s) \psi_r(s)$$

$$z(s) = \epsilon_1(s) \epsilon_r(s)$$

respectively. The roots of $p(s)$ and $z(s)$ are called the **poles** and **zeros**, with their respective multiplicity, of $G(s)$, respectively.

Then from Equation (2.2.7) one can see that the pendulum system does not have any zeros, and it has four poles at $s = 0$, $s = -a$, $s = -b$ and $s = b$. It is therefore obvious that this system is unstable since $a > 0$ and $b > 0$.

2.3.2 Input and Output Directions

Definition 2.3.2 (Input and Output Zero Directions) If $G(s)$ has a zero at $s = z \in \mathbb{C}$ then there exist non-zero vectors called the **output zero direction** $y_z \in \mathbb{C}^l$ and the **input zero direction** $u_z \in \mathbb{C}^m$, such that $y_z^* y_z = 1$, $u_z^* u_z = 1$ and

$$y_z^* G(z) = 0, \quad G(z) u_z = 0 \tag{2.3.1}$$

where l is the number of outputs and m is the number of inputs of the system $G(s)$.

Definition 2 3 3 (Input and Output Pole Directions) If $G(s)$ has a pole at $s = p \in \mathbb{C}$ then there exist non-zero vectors called the output pole direction $y_p \in \mathbb{C}^l$ and the input pole direction $u_p \in \mathbb{C}^m$, such that $y_p^* y_p = 1$, $u_p^* u_p = 1$ and

$$y_p^* G(p) = \infty, \quad G(p) u_p = \infty \quad (2 3 2)$$

where l is the number of outputs and m is the number of inputs of the system $G(s)$

In the next definitions the linear time invariant (LTI) system in state space form

$$\dot{x} = Ax + Bu \quad (2 3 3)$$

$$y = Cx + Du \quad (2 3 4)$$

corresponding to a minimal realization is considered

Definition 2 3 4 Let z be a zero of $G(s)$ Then

$$\begin{bmatrix} A - zI & B \\ C & D \end{bmatrix} \begin{bmatrix} x_z \\ u_z \end{bmatrix} = 0 \quad (2 3 5)$$

has a solution with $u_z^* u_z = 1$ where x_z is the input zero state direction and u_z is the input zero direction

Definition 2 3 5 Let z be a zero of $G(s)$ Then

$$\begin{bmatrix} x_o^* & y_z^* \end{bmatrix} \begin{bmatrix} A - zI & B \\ C & D \end{bmatrix} = 0 \quad (2 3 6)$$

has a solution with $y_z^* y_z = 1$, where x_o is the output zero state direction and y_z is the output zero direction

For more information regarding zeros, poles and their directions see [11] and [12]

Chapter 3

Youla Parameterization

The Youla Parameterization technique gives a simple and elegant solution to the problem of describing the set of compensators that stabilize a given plant. This set is a function of the so-called “ Q ” parameter $Q = Q(s)$, which is an arbitrary stable proper transfer matrix of size $m \times l$ where m is the number of inputs and l is the number of outputs of the system. As shown later, the result is extremely important since instead of thinking in terms of the controller transfer matrix $K(s)$, it is generally much better to design $Q(s)$. However, in order to find the set, a coprime factorization of the multivariable plant is needed as well as a solution of the generalised Bezout identity. Maciejowski [9, §6] and Tadeo et al [10]

Theorem 3.0.1 (The Youla Parameterization) *Let $K_o = U_l V_l^{-1} = V_r^{-1} U_r$ be such that the generalised Bezout equation*

$$\begin{pmatrix} N_l & D_l \\ -V_r & U_r \end{pmatrix} \begin{pmatrix} U_l & -D_r \\ V_l & N_r \end{pmatrix} = \begin{pmatrix} I & 0 \\ 0 & I \end{pmatrix} \quad (3.0.1)$$

holds. For any $Q \in \mathcal{H}_\infty$ (that is, for any stable Q of compatible dimensions), define

$$\begin{aligned} X_r &= U_l - D_r Q & Y_r &= V_l + N_r Q \\ X_l &= U_r - Q D_l & Y_l &= V_r + Q N_l \end{aligned} \quad (3.0.2)$$

Then $K = Y_l^{-1} X_l = X_r Y_r^{-1}$ is a stabilizing controller for the plant $G = N_r D_r^{-1} = D_l^{-1} N_l$. Furthermore, any stabilizing controller has fractional representations as in Equation (3.0.2)

As can be seen, solving the generalised Bezout equation plays an important role in the Youla Parameterization. The next two sections show two possible procedures to find a solution to this equation.

3.1 Solving the Generalised Bezout Equation - Approach 1

Finding the solution of the Bezout equation of a multivariable system may not be an easy task. In this section a solution of the generalised Bezout equation is sought using the Smith-McMillan form, which was discussed previously. The procedure is demonstrated with an example, again the inverted pendulum is used.

First, start with a coprime factorization of the plant. From Equation (2.2.6) and finding a stable coprime factorization of $\lambda(s)$ (i.e. $\lambda_n(s)$ and $\lambda_d(s)$) gives

$$\begin{aligned} G(s) &= L^{-1} \begin{pmatrix} \frac{1}{s(s+a)(s+b)(s-b)} \\ 0 \end{pmatrix} \\ &= L^{-1} \begin{pmatrix} \left(\frac{1}{(s+a)(s+b)^3} \right) \left(\frac{s(s-b)}{(s+b)^2} \right)^{-1} \\ 0 \end{pmatrix} \\ &= L^{-1} \begin{pmatrix} \left(\frac{1}{(s+a)(s+b)^3} \right) \\ 0 \end{pmatrix} \left(\frac{s(s-b)}{(s+b)^2} \right)^{-1} \\ &= N_r D_r^{-1} \end{aligned}$$

where

$$N_r = L^{-1} \begin{pmatrix} \left(\frac{1}{(s+a)(s+b)^3} \right) \\ 0 \end{pmatrix} \quad (3.1.1)$$

$$D_r = \begin{pmatrix} \frac{s(s-b)}{(s+b)^2} \end{pmatrix} \quad (3.1.2)$$

and L^{-1} is given in Equation (2.2.5)

Similarly, a left coprime factorization of $G(s)$ can be found. Again, from Equa-

tion (2.2.6) and finding a stable coprime factorization of $\lambda(s)$ yields,

$$\begin{aligned}
 G(s) &= L^{-1} \begin{pmatrix} \left(\frac{s(s-b)}{(s+b)^2}\right)^{-1} \left(\frac{1}{(s+a)(s+b)^3}\right) \\ 0 \end{pmatrix} \\
 &= L^{-1} \begin{pmatrix} \left(\frac{s(s-b)}{(s+b)^2}\right)^{-1} & 0 \\ 0 & 1 \end{pmatrix} \begin{pmatrix} \frac{1}{(s+a)(s+b)^3} \\ 0 \end{pmatrix} \\
 &= \left(\begin{bmatrix} \frac{s(s-b)}{(s+b)^2} & 0 \\ 0 & 1 \end{bmatrix} L \right)^{-1} \begin{pmatrix} \frac{1}{(s+a)(s+b)^3} \\ 0 \end{pmatrix} \\
 &= D_l^{-1} N_l
 \end{aligned}$$

where L is given in Equation (2.2.4)

$$\begin{aligned}
 D_l &= \begin{pmatrix} \frac{s(s-b)}{(s+a)^2} & 0 \\ 0 & 1 \end{pmatrix} L \\
 &= \begin{pmatrix} -\frac{s(s-b)}{k_1 b^2 (s-a)^2} & -\frac{s(s-b)}{k_2 b^2 (s+a)^2} \\ -\frac{k_2}{k_1 b^2} s^2 & -\frac{1}{b^2} (s^2 - b^2) \end{pmatrix} \quad (3.1.3)
 \end{aligned}$$

and

$$N_l = \begin{pmatrix} \frac{1}{(s+a)^3 (s+b)} \\ 0 \end{pmatrix} \quad (3.1.4)$$

Now solve the first Bezout equation $N_l U_l + D_l V_l = I$ as follows. Recall that

$$D_l = \begin{pmatrix} \frac{s(s-b)}{(s+a)^2} & 0 \\ 0 & 1 \end{pmatrix} L$$

thus, let

$$V_l = L^{-1} \begin{pmatrix} V_1 & 0 \\ 0 & V_2 \end{pmatrix} \quad (3.1.5)$$

and $U_l = [U_{l1} \quad U_{l2}]$. Thus

$$\begin{aligned}
N_l U_l + D_l V_l &= \begin{pmatrix} \frac{1}{(s+a)^3(s+b)} \\ 0 \end{pmatrix} [U_{l1} \ U_{l2}] + \begin{pmatrix} \frac{s(s-b)}{(s+a)^2} & 0 \\ 0 & 1 \end{pmatrix} \begin{pmatrix} V_1 & 0 \\ 0 & V_2 \end{pmatrix} \\
&= \begin{pmatrix} \frac{1}{(s+a)^3(s+b)} U_{l1} & \frac{1}{(s+a)^3(s+b)} U_{l2} \\ 0 & 0 \end{pmatrix} + \begin{pmatrix} \frac{s(s-b)}{(s+a)^2} V_1 & 0 \\ 0 & V_2 \end{pmatrix} \\
&= \begin{pmatrix} 1 & 0 \\ 0 & 1 \end{pmatrix}
\end{aligned}$$

Notice that now the elements of U_l and V_l can be found by solving four scalar Bezout equations given in the equation above. Similarly, we can solve $U_r N_r + V_r D_r = I$. The only problem with this approach is that some of the elements of some of the matrices involved in the Youla parameterization may be improper (see Equation (3.13)). As Tadeo said ([13]) “el unico problema es que si bien las matrices de transferencia (N_r, D_r , etc) son causales (en el sentido que tiene menos ceros de transmision que polos), no se asegura que cada uno de sus componentes individuales sea causal” (‘the only problem is that, even though the transfer function matrices (N_r, D_r , etc) are causal (in the sense that they have less transmission zeros than poles), it cannot be assured that every individual element will be causal’).

3.2 Solving the Generalised Bezout Equation - Approach 2

Because of the problem found above, an alternative approach is needed. Here the approach used in Nett et al [14] is adopted. In this paper, the authors describe how to find the solution of the generalised Bezout equation using a state-space realization. This involves constant matrices K and F . The result is as follows.

Theorem 3.2.1 *Suppose $G(s) = C(sI - A)^{-1}B \in \mathbb{R}^{l \times m}$ where $A \in \mathbb{R}^{n \times n}$, $B \in \mathbb{R}^{n \times m}$, $C \in \mathbb{R}^{l \times n}$, (C, A) is detectable and (A, B) is stabilizable. Select*

$K \in \mathbb{R}^{m \times n}$, $F \in \mathbb{R}^{n \times l}$ such that $A - BK$ and $A - FC$ are stable. Define

$$\begin{aligned}
 N_r &= C(sI - A + BK)^{-1}B & D_r &= I - K(sI - A + BK)^{-1}B \\
 U_r &= K(sI - A + FC)^{-1}F & V_r &= I + K(sI - A + FC)^{-1}B \\
 D_l &= I - C(sI - A + FC)^{-1}F & N_l &= C(sI - A + FC)^{-1}B \\
 V_l &= I + C(sI - A + BK)^{-1}F & U_l &= K(sI - A + BK)^{-1}F
 \end{aligned} \tag{3.2.1}$$

Then

- (i) all eight matrices described by (3.2.1) are stable
- (ii) D_r and D_l are nonsingular
- (iii) $G = N_r D_r^{-1} = D_l^{-1} N_l$
- (iv) The transfer functions in (3.2.1) fulfill the generalized Bezout equation (3.0.1)

As can be seen, the solution to the Bezout equation may not be unique and in this case approach, there are many choices for the matrices K and F . Next, this method is applied to the inverted pendulum.

3.3 Generalized Bezout Equation of the Inverted Pendulum

In this section the solution of the Bezout equation of the inverted pendulum is found, so that the Youla Parameterization of this system can be used subsequently. The approach given in Section 3.2 is followed. First, the controller canonical form of the plant is obtained, which is more convenient to facilitate the selection of the matrices K and F .

3.3.1 State Space Realization of the Plant

Based on Equation (2.2.3) the controller canonical form of the plant can be found, see Maciejowski [9, §2.5]. Notice that

$$s(s+a)(s^2-b^2) = s^4 + as^3 - b^2s^2 - ab^2s. \quad (3.3.1)$$

Thus the state-space realization of the plant of Equation (2.1.24) is

$$\dot{x} = Ax + Bu \quad \text{and} \quad y = Cx + Du \quad (3.3.2)$$

where

$$A = \begin{pmatrix} 0 & 1 & 0 & 0 \\ 0 & 0 & 1 & 0 \\ 0 & 0 & 0 & 1 \\ 0 & ab^2 & b^2 & -a \end{pmatrix} \quad B = \begin{pmatrix} 0 \\ 0 \\ 0 \\ 1 \end{pmatrix}$$

$$C = \begin{pmatrix} -b^2k_1 & 0 & k_1 & 0 \\ 0 & 0 & -k_2 & 0 \end{pmatrix} \quad D = 0.$$

3.3.2 Design of a Stabilizing Controller for the Plant

Next, at least one stabilizing controller is needed. Thus in this section a gain matrix, K , is designed such that the matrix $(A - BK)$ is stable. First notice that for a single-input system in controller canonical form, as in Equation (3.3.2),

$$BK = \begin{pmatrix} 0 \\ \vdots \\ 0 \\ 1 \end{pmatrix} (k_n \quad k_{n-1} \quad \dots \quad k_1) = \begin{pmatrix} 0 & 0 & \dots & 0 \\ \vdots & & \ddots & \\ 0 & 0 & & 0 \\ k_4 & k_{n-1} & \dots & k_1 \end{pmatrix}.$$

Thus for the system described by Equation (3.3.2) one obtains

$$A_c = A - BK = \begin{pmatrix} 0 & 1 & 0 & 0 \\ 0 & 0 & 1 & 0 \\ 0 & 0 & 0 & 1 \\ -k_4 & (ab^2 - k_3) & (b^2 - k_2) & (-a - k_1) \end{pmatrix}. \quad (3.3.3)$$

Hence, the gains k_1, k_2, \dots are simply "added" to the coefficients of the open-loop matrix A to give the closed-loop matrix A_c , [15]. Thus, for a single-input system in the controller canonical form, the gain matrix elements are given by

$$-a_i - k_i = -\bar{a}_i \quad \text{or} \quad k_i = \bar{a}_i - a_i \quad (3.3.4)$$

where the a_i 's are the coefficients of the open-loop characteristic polynomial (o l c p) and the \bar{a}_i 's are the coefficients of the desired closed-loop characteristic polynomial (c l c p), i.e. $s^n + \bar{a}_1 s^{n-1} + \dots + \bar{a}_n$. Therefore, for this system, it is necessary to define the desired closed-loop characteristic polynomial. In order to reduce the order of the transfer functions given in Theorem 3.2.1 (see Remark 3.3.1 below), the desired pole locations are chosen as $s = -a$, $s = -a$, $s = -b$, $s = -b$. Then, the c l c p is

$$(s + a)^2(s + b)^2 = s^4 + \bar{a}_1 s^3 + \bar{a}_2 s^2 + \bar{a}_3 s + \bar{a}_4$$

Thus, it follows that $\bar{a}_1 = 17\,594$, $\bar{a}_2 = 113\,81$, $\bar{a}_3 = 320\,42$ and $\bar{a}_4 = 331\,68$. The coefficients of the open-loop characteristic polynomial are $a_1 = 3\,3333$, $a_2 = -29\,851$, $a_3 = -99\,503$ and $a_4 = 0$ (see Equations (2.1.25) and (3.3.1)). Then the coefficients of the gain matrix K can be obtained as follows

$$\begin{aligned} k_1 &= \bar{a}_1 - a_1 = 17\,594 - 3\,3333 = 14\,261 \\ k_2 &= \bar{a}_2 - a_2 = 113\,81 - (-29\,851) = 143\,66 \\ k_3 &= \bar{a}_3 - a_3 = 320\,42 - (-99\,503) = 419\,92 \\ k_4 &= \bar{a}_4 - a_4 = 331\,68 - 0 = 331\,68 \end{aligned}$$

and then the gain matrix, $K = [k_4 \quad k_3 \quad k_2 \quad k_1]$, is given by

$$K = [331\,68 \quad 419\,92 \quad 143\,66 \quad 14\,261] \quad (3.3.5)$$

Now a matrix F need to be designed such that $(A - FC)$ is stable

3.3.3 Design of an Observer for the Plant

The fact that the system has one input (i.e. the matrix B has one column) makes the design of the controller K relatively easy. However, the selection of the matrix F is more difficult, since the design of the observer involves the matrix C which has two rows (i.e. the system has two outputs). Thus, the observer problem must be solved, which is equivalent to find a matrix F such that $(A - FC)$ is stable. The form of the observer selected is

$$\hat{x} = \hat{A}\hat{x} + \hat{B}u + Fy \quad (3.3.6)$$

where u and y are the input and the output respectively. The matrices \hat{A} , \hat{B} and F have to be selected in a way that the error

$$e = x - \hat{x} \quad (3.3.7)$$

is acceptably small. Then using Equations (3.3.2), (3.3.6) and (3.3.7) gives

$$e = x - \hat{x} = (Ax + Bu) - (\hat{A}\hat{x} + \hat{B}u + Fy) = Ax + Bu - \hat{A}(x - e) - \hat{B}u - FCx$$

and thus

$$e = \hat{A}e + (A - \hat{A} - FC)x + (B - \hat{B})u \quad (3.3.8)$$

Now, it is desired that the error goes to zero asymptotically, independent of x and u , therefore the coefficients of x and u must be zero and \hat{A} must be the dynamic matrix of a stable system. Thus

$$\hat{A} = A - FC \quad (3.3.9)$$

and

$$\hat{B} = B \quad (3.3.10)$$

Notice that A , B and C are known matrices; therefore it is only needed to design F . Now if Equations (3.3.9) and (3.3.10) are satisfied then Equation (3.3.8) becomes

$$e = \hat{A}e$$

The only thing left is to make the matrix $\hat{A} = A - FC$ stable. It is known that every eigenvalue of \hat{A} can be located at any desired location whatsoever if the matrix

$$O = \begin{bmatrix} C \\ C A \\ \vdots \\ C(A)^{n-1} \end{bmatrix}$$

has full column rank n , i.e. if the system is observable. Recall that \hat{A} and A are $n \times n$ matrices, F is $n \times m$ and C is $m \times n$. Remember also that the eigenvalues of \hat{A} are the solution to the equation $|\lambda I_n - \hat{A}| = 0$ and that the o.l.c.p. is equal

to $|sI - A|$, where $| \cdot |$ stands for the determinant of a matrix. That is

$$\begin{aligned} \text{c l c p} &= |\lambda I_n - \hat{A}| = 0 \\ \Rightarrow |\lambda I_n - A + FC| &= 0 \\ \Rightarrow |\lambda I_n - A| |I_n + (\lambda I_n - A)^{-1} FC| &= 0 \\ \Rightarrow a(\lambda) |I_n + (\lambda I_n - A)^{-1} FC| &= 0 \end{aligned}$$

where $a(\lambda)$ is the open loop characteristic polynomial evaluated at λ . Now let the $n \times n$ matrix

$$\Phi(\lambda) = (\lambda I_n - A)^{-1} \quad (3.3.11)$$

and using the fact that $|I_n + \Phi(\lambda)FC| = |I_n + C\Phi(\lambda)F|$ yields

$$\text{c l c p} = a(\lambda) |I_m + C\Phi(\lambda)F| = 0 \quad (3.3.12)$$

Hence a matrix F needs to be chosen such that $|I_m + C\Phi(\lambda)F| = 0$ for each desired eigenvalue λ_i with $i = 1, \dots, n$ or equivalently, such that the matrix $I_m + C\Phi(s)F$ is singular for each desired λ_i . Thus the idea is to make one row of the matrix $C\Phi(\lambda_i)F$ equal to the negative of the corresponding row of the identity matrix I_m . That is, it is desired that $\text{row}_k(C\Phi(\lambda_i)F) = -\text{row}_k(I_m)$, where $\text{row}_k(\cdot)$ stands for the k -th row of a matrix. Notice that in this way one row of the matrix $I_m + C\Phi(\lambda)F$ is equaled to zero which makes this matrix singular. It is known that if \mathcal{O} has full column rank, n linearly independent rows can be selected from the rows of $C\Phi(\lambda) = C(\lambda I - A)^{-1}$ (or its derivatives if necessary when repeated eigenvalues are desired) for each desired λ_i . Therefore Equation (3.3.12) can be made zero for n specified eigenvalues λ_i by requiring

$$\text{row}_k(C\Phi(\lambda_i)F) = -\text{row}_k(I_m) \quad \text{or} \quad \left. \frac{d}{d\lambda} \text{row}_k(C\Phi(\lambda)F) \right|_{\lambda=\lambda_i} F = 0^T \quad (3.3.13)$$

where 0^T is the $1 \times m$ zero row vector. Using one equation like Equation (3.3.13) for each desired eigenvalue and defining the $n \times n$ non-singular matrix

$$G_c = \begin{bmatrix} \text{row}_j(C\Phi(\lambda_1)F) \\ \vdots \\ \text{row}_k(C\Phi(\lambda_n)F) \end{bmatrix}$$

and letting \mathfrak{S}_c be the $n \times m$ matrix whose rows are either $\text{row}(I_m)$ or 0^T , leads to

$$\begin{aligned} G_c F &= -\mathfrak{S}_c \\ \Rightarrow F &= -G_c^{-1} \mathfrak{S}_c \end{aligned} \quad (3.3.14)$$

Now for the system described by Equations (2.1.25) and (3.3.2), and using Equation (3.3.12) gives

$$\Phi(\lambda) = \begin{pmatrix} \lambda & -1 & 0 & 0 \\ 0 & \lambda & -1 & 0 \\ 0 & 0 & \lambda & -1 \\ 0 & -ab^2 & -b^2 & \lambda + a \end{pmatrix}^{-1}$$

and thus

$$\Phi(\lambda) = \begin{pmatrix} \frac{1}{\lambda} & \frac{1}{W\lambda^2}(W + ab^2) & \frac{1}{W\lambda}(\lambda + a) & \frac{1}{W\lambda} \\ 0 & \frac{1}{W\lambda}(W + ab^2) & \frac{1}{W}(\lambda + a) & \frac{1}{W} \\ 0 & \frac{ab^2}{W} & \frac{\lambda}{W}(\lambda + a) & \frac{\lambda}{W} \\ 0 & \frac{ab^2\lambda}{W} & \frac{1}{W}(b^2\lambda + ab^2) & \frac{\lambda^2}{W} \end{pmatrix} \quad (3.3.15)$$

where

$$W = \lambda^3 + a\lambda^2 - b^2\lambda - ab^2$$

It is desired to locate the eigenvalues at $s = -a$, $s = -a$, $s = -b$ and $s = -b$. Since there are repeated poles the derivative of $\Phi(\lambda)$ is needed. Thus using Equations (3.3.12), (3.3.13) and (3.3.14) a matrix F which locates the eigenvalues of $A - FC$ at the desired positions is obtained. This F is as follows

$$F = - \begin{pmatrix} -0.026791 & -0.0098232 \\ -0.055464 & -0.05367 \\ -0.30303 & -0.29323 \\ -1.6556 & -1.6021 \end{pmatrix} \quad (3.3.16)$$

Now the solution of the generalized Bezout equation can be found

3.3.4 Solution of the Generalized Bezout Equation

Now the stabilizing controller, K , and the observer, F , can be used together with Theorem 3.2.1 to find a solution of the Generalized Bezout equation. Using the equations given in the theorem yields

$$N_r = \begin{pmatrix} \frac{k_1(s-b)}{(s+b)(s+a)^2} \\ \frac{-k_2 s^2}{(s+b)^2(s+a)^2} \end{pmatrix} \quad (3.3.17)$$

$$D_r = \frac{s(s-b)}{(s+b)(s+a)} \quad (3.3.18)$$

$$U_r = \begin{pmatrix} \frac{-99\,3201(s+0\,1852)}{(s+b)(s+a)} & \frac{-51\,7069}{(s+a)} \end{pmatrix} \quad (3.3.19)$$

$$V_r = \frac{(s^2 + 23\,06s + 239\,8)}{(s+b)(s+a)} \quad (3.3.20)$$

and

$$N_l = \begin{pmatrix} \frac{k_1}{(s+b)(s+a)} \\ \frac{-k_2}{(s+b)(s+a)} \end{pmatrix} \quad (3.3.21)$$

$$D_l = \begin{pmatrix} \frac{s}{(s+b)} & 0 \\ \frac{-9\,0909s}{(s+b)(s+a)} & \frac{s-b}{s+a} \end{pmatrix} \quad (3.3.22)$$

$$U_l = \begin{pmatrix} \frac{-99\,3201(s-0\,3036)}{(s+b)(s+a)} & \frac{-90\,768s}{(s+b)(s+a)} \end{pmatrix} \quad (3.3.23)$$

$$V_l = \begin{pmatrix} \frac{(s+16)(s^2+1\,594s+88\,31)}{(s+b)(s+a)^2} & \frac{998\,4483}{(s+b)(s+a)^2} \\ \frac{9\,0909(s+26\,31)(s-3\,854)(s+0\,5986)}{(s+b)^2(s+a)^2} & \frac{(s-1\,281)(s+0\,4653)(s^2+27\,21s+339\,4)}{(s+a)^2(s+b)^2} \end{pmatrix} \quad (3.3.24)$$

Remark 3.3.1 Notice that the matrices K and F , were chosen in order to locate the eigenvalues of the matrices $A - BK$ and $A - FC$ at $s = -a$ and $s = -b$. This was done to place the poles of the transfer matrices (3.3.17)-(3.3.24) at these locations. These pole locations were chosen because in this way more cancellations between poles and zeros are obtained, which reduces the order of these transfer matrices.

Remark 3.3.2 *The observer F was designed in the way explained in Section 3.3.3 because this procedure makes the matrix D_1 lower triangular, see Equation (3.3.22). For other methods for designing observers see Kaulath [15].*

Now that the solution of the generalized Bezout equation has been found, the set of all stabilizing controllers for the pendulum is easily obtained. That set is given by Equation (3.0.2) (Theorem 3.0.1). Notice that the set depends on the parameter Q .

One way [16] to choose this parameter is by finding the optimal Q which minimizes the two norm of $\sqrt{|W_s S|^2 + |W_t T|^2}$, where W_s and W_t are weighting functions and S and T are the sensitivity and complementary sensitivity functions respectively. This approach is discussed later.

Chapter 4

One-Loop-at-a-Time Method - Approach 1

In multivariable controller design it is possible in some cases, to group some inputs and outputs so that the system can be seen as a collection of several SISO loops. This may be done when the interaction between the two loops is relatively low.

This chapter deals with the design of controllers using this approach. The method is illustrated by using a design example. Again the inverted pendulum system is taken to describe the approach. Therefore a one-loop-at-a-time method is used to design a controller for this plant. That is, SISO controllers are designed for each output, (i.e. angle of the pendulum and position of the cart).

4.1 Controller Design

The steps taken to design a controller for the inverted pendulum using this approach are explained next. Recall that the model of the system is given by Equations (2.1.24) and (2.1.25)

The pendulum system has one input and two outputs. Therefore, two controllers need to be designed, one for the angular rotation of the pendulum, $\phi(t)$, and one for the displacement of the carriage, $d(t)$. The command must only be followed by the displacement, since the angle of the pendulum should be ideally at zero.

degrees (upright position) and the goal is to control the position of the cart. The general idea is to introduce a feedback system as shown in Figure 4.1

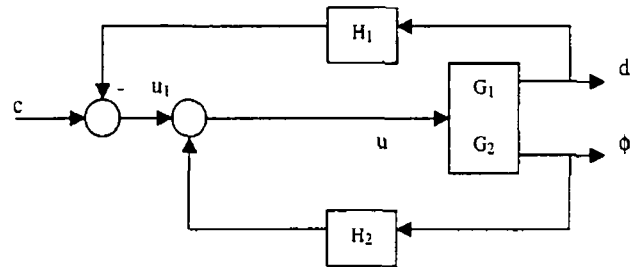


Figure 4.1 Feedback system

4.1.1 Controller Design for the Angular Rotation

For this part of the system, a controller $H_2(s)$, for the plant $G_2(s)$ (see Equation (2.1.24)) must be designed, that is, to implement the controller for the angle. One way to do this is by using the root locus method, which is a plot of the poles of the closed loop transfer function as the constant gain of a given controller is varied. The characteristic equation of the closed loop is

$$1 + kG_2(s)H_2(s) = 0$$

where k varies from 0 to ∞ . The system is stable when all the poles lie in the OLHP for a specific gain k . The root locus of the plant G_2 is shown in Figure 4.2

Clearly, the plant is unstable for any k (i.e. there is always a portion of the root locus in the RHP). Now, a controller has to be designed in order to make the system stable. First, a first order controller with a negative gain is tried. That is, an unstable pole is placed between the zero at the origin and the unstable pole, and another zero is placed in the LHP to attract the two unstable poles towards the LHP. In this case this zero is cancelling the pole at $a = -3.33$. Figure 4.3 shows the new root locus.

It can be noticed in this figure that a portion of the plot is always in the RHP, which indicates that the system is still unstable. So we need to place another

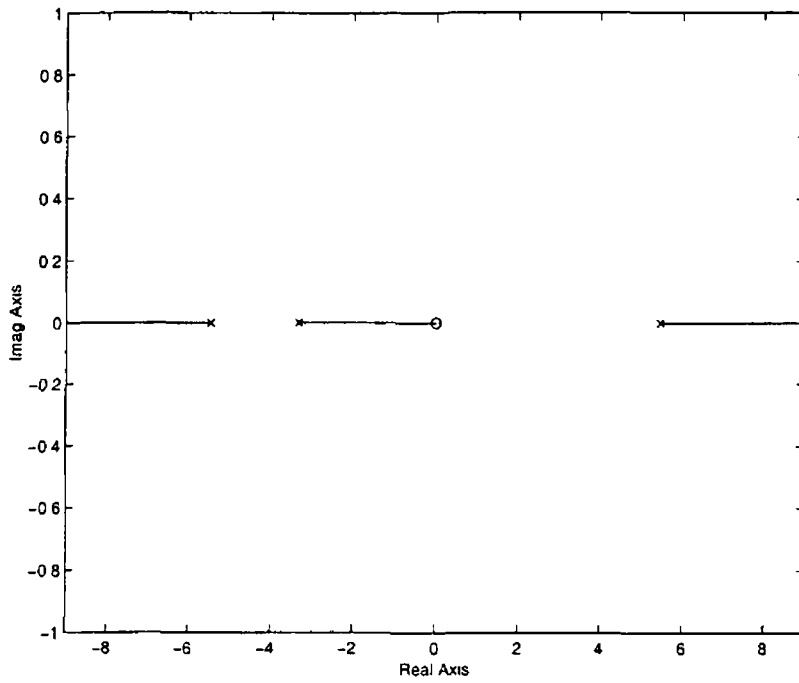


Figure 4 2 Root locus of the angular rotation, G_2 without controller

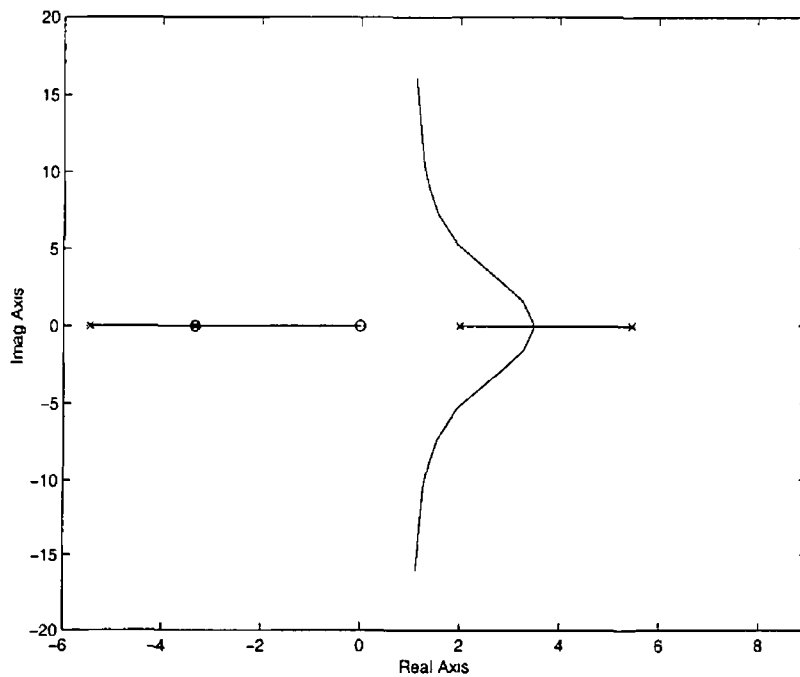


Figure 4 3 Root locus with another unstable pole

(stable) pole-zero pair so that the new root locus is pulled into the LHP. In this case, the plant pole at $b = -5.46$ is being cancelled by the new zero. The new root locus is shown in Figure 4 4. A sufficiently large gain, k , is chosen from the

plot in order to place all the closed-loop poles in the LHP

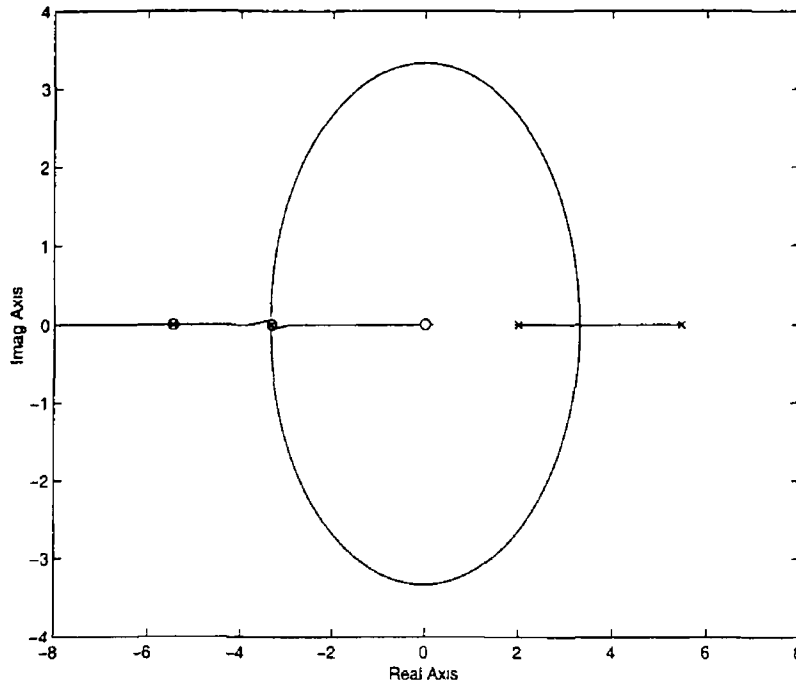


Figure 4 4 Root locus with the new pole-zero pair

In this controller, a pole was placed at -50 , which is not shown in Figure 4 4. The transfer function for the controller $H_2(s)$ is,

$$H_2 = k \frac{(s + a)(s + b)}{(s + 50)(s - 2)} \quad (4.11)$$

where $k = -400$ was chosen in order to get an appropriate trade-off between transient response and robustness.

For this controller the gain and phase margins are good as well as the sensitivity and complementary sensitivity functions. As can be seen in Figure 4 6 the system has good stability margins. The sensitivity and complementary sensitivity are shown in Figure 4 7.

As was said earlier, the gain k is chosen with the performance of the system in mind. A smaller gain would have given a system with faster response but with little robustness, whereas a larger gain would have given a robust system with a slower response. Now that a controller was designed for the angular rotation, the controller for the displacement must be designed.

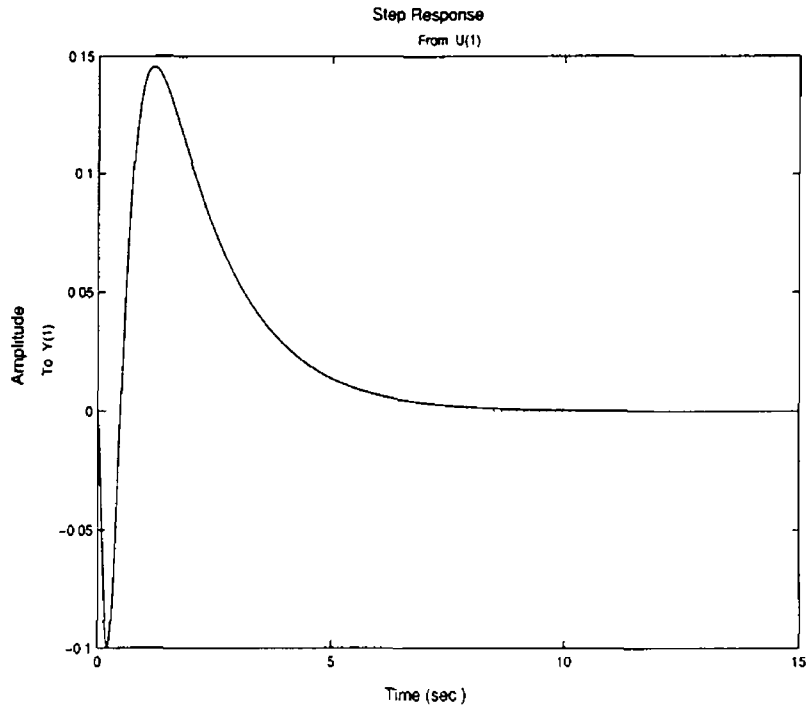


Figure 4 5 Step response of the angle control system

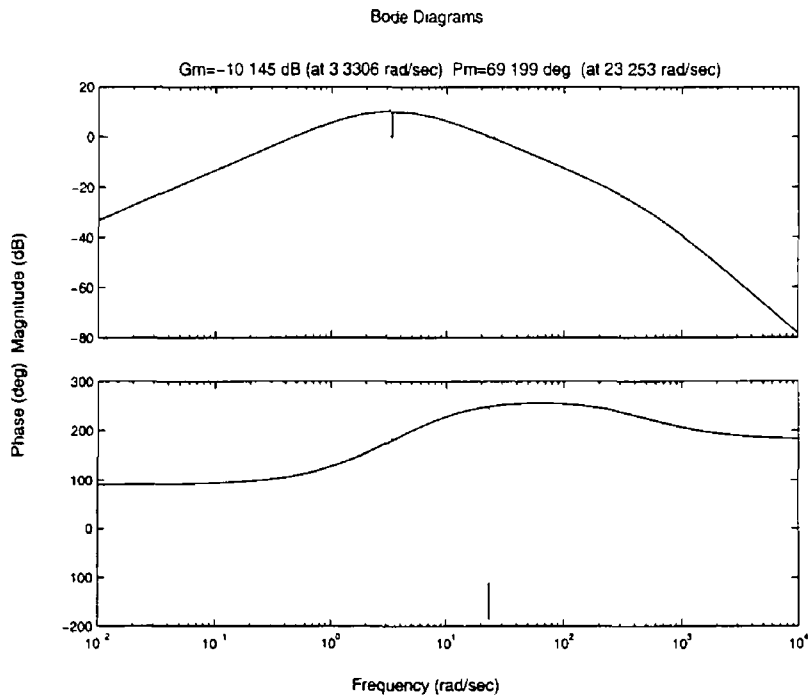


Figure 4 6 Bode diagram of the angle control system

4 1 2 Controller Design for the Displacement

It can be seen from Figure 4 1 that the design of the controller for the displacement, H_1 , depends on the displacement and the angle transfer functions, as well

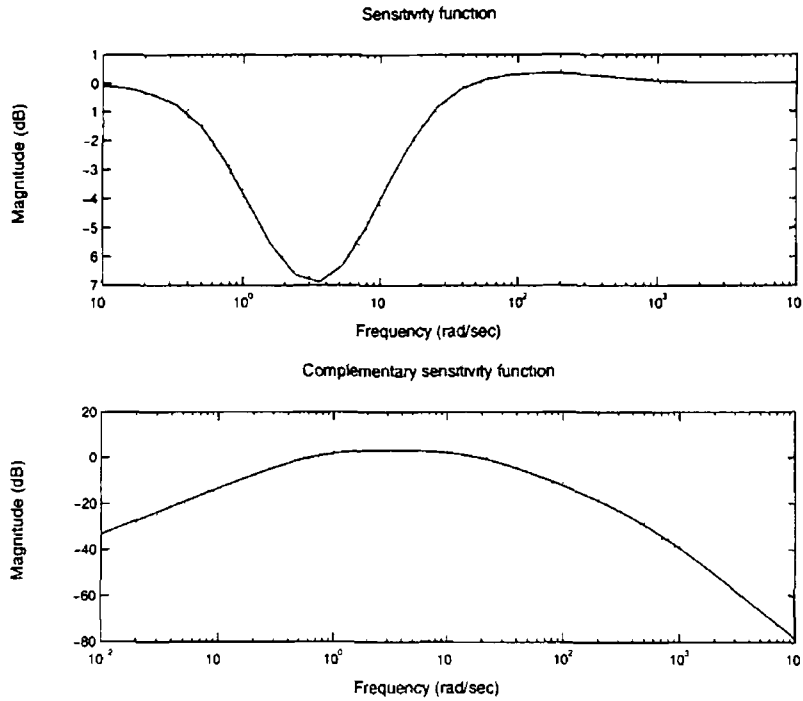


Figure 4.7 Sensitivity functions of the angle control system

as on H_2 . This means that the stabilization of the angle has to be taken into account when designing a stabilizing controller for the displacement rather than designing a controller for only G_1 . In order to do this, the equivalent plant which is seen by the controller H_1 has to be found. It is clear from Figure 4.1 that

$$d = uG_1(s) \quad (4.1.2)$$

$$\phi = uG_2(s) \quad (4.1.3)$$

$$u = u_1 - \phi H_2(s) \quad (4.1.4)$$

Substituting Equation (4.1.3) into Equation (4.1.4) gives

$$\frac{u}{u_1} = \frac{1}{1 + G_2 H_2} \quad (4.1.5)$$

Substituting Equation (4.1.5) into Equation (4.1.2) gives the transfer function for the equivalent plant,

$$G_{eq}(s) = \frac{d}{u_1} = \frac{G_1}{1 + G_2 H_2} \quad (4.1.6)$$

Notice, from Equation (4.1.6), that any unstable pole in the angle system (G_2 or H_2) turns into a non-minimum phase zero of the equivalent plant and, clearly,

any non-minimum phase zero or unstable pole in G_1 becomes a RHP zero or pole respectively, of the equivalent plant. The control system for the displacement is shown in Figure 4.8. Equations (2.1.24), (2.1.25) and (4.1.1) are substituted into

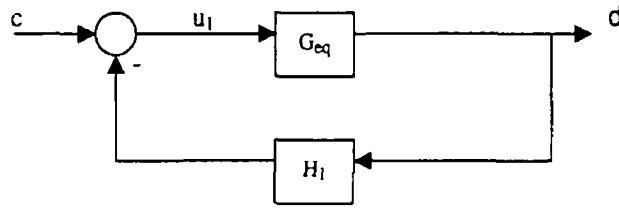


Figure 4.8 Equivalent control system for the displacement

Equation (4.1.6), to obtain the transfer function for the equivalent plant, G_{eq}

$$G_{eq}(s) = \frac{11(s + 500)(s - b)(s - 2)}{s(s + 475.1)(s + 16.71)(s + a)(s + 0.688)} \quad (4.1.7)$$

The same procedure used for designing the controller for the angle is used to design this controller. One possible controller is

$$H_1 = \frac{35(s + a)(s + 0.6888)}{(s + 20)(s + 25)} \quad (4.1.8)$$

The step response, the bode plot and the sensitivity and complementary sensitivity functions are shown in Figures 4.9, 4.10, and 4.11 respectively.

4.2 Discussion

With the above controller, (H_1, H_2) the linear system has acceptable stability margins, but it is not fast enough, in the sense that around 8 seconds for the settling of the linear model of the pendulum is too much, it may lead to instability of the real system. It would be desirable if it could be settled in less than 5 seconds. Aiming for a fast and robust closed-loop system is not easy with this plant. In fact, this controller cannot stabilize the real plant. Thus more insight about the system is required in order to improve the performance as much as possible. That is why in the next chapter limitations that exist in this system and in many other systems are investigated. Then, the approach studied in this chapter is further discussed in Chapter 6.

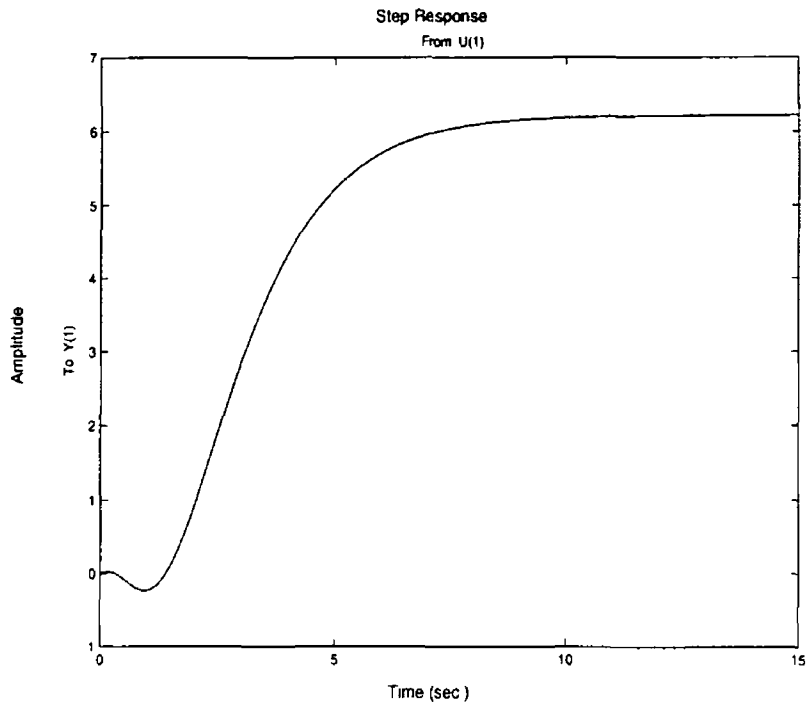


Figure 4 9 Step response of the displacement system

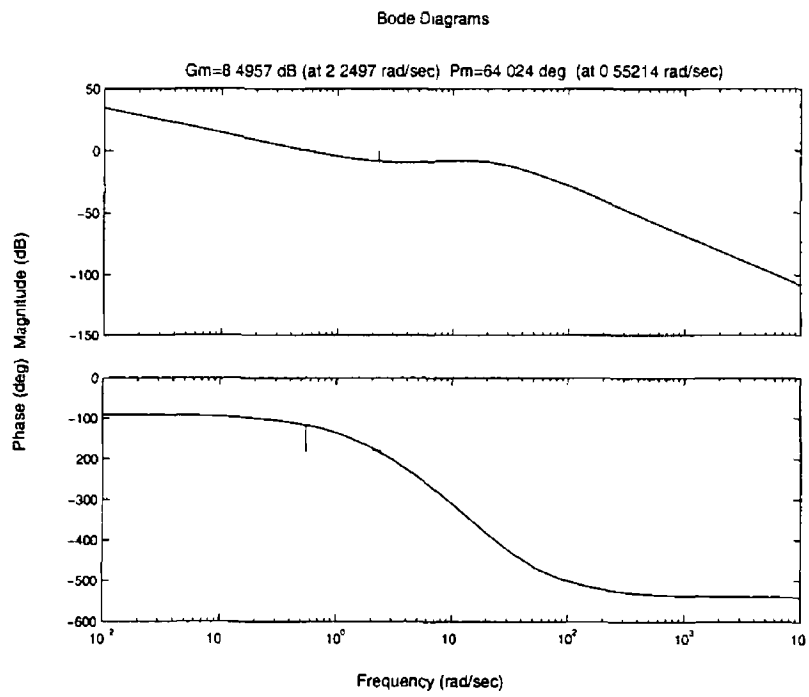


Figure 4 10 Bode diagram of the displacement system

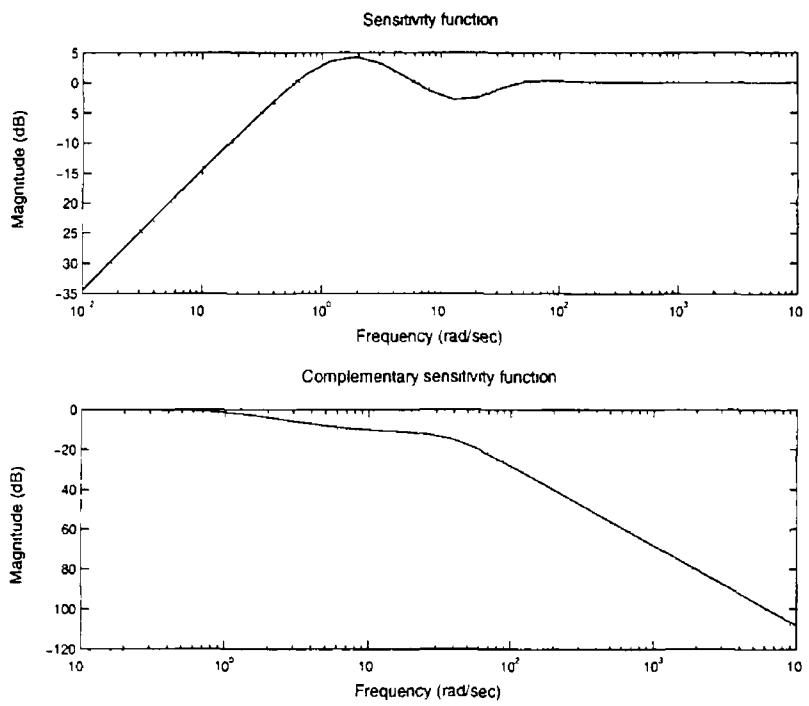


Figure 4.11 Sensitivity functions of the displacement system

Chapter 5

Fundamental Limitations - SISO case

Before starting to design any controller for any system, it is important to be aware of factors that limit the achievable performance. As we saw in the previous chapter, the plant is unstable i.e. the transfer function has a pole in the RHP and another on the imaginary axis. Nowadays it is known that RHP poles and RHP zeros make the control design problem more difficult, [17], [18], [19], [20]. In this chapter some limitations that apply to SISO systems are discussed. First some basic results about linear SISO systems are given.

5.1 Some Facts About SISO Systems

The results given in this section are used in later sections and chapters. They are based on the definition of the Laplace transform.

Definition 5.1.1 (Laplace-transform) *The Laplace transform is defined as*

$$\mathcal{L}\{y(t)\} = Y(s) = \int_0^{\infty} y(t)e^{-st} dt$$

The transform is well defined if there exists $\sigma \in \mathbb{R}$ and a positive constant $k < \infty$ such that

$$|y(t)| < k e^{\sigma t} \quad \forall t \geq 0$$

The region $\mathcal{R}\{s\} \geq \sigma$ is known as the region of convergence

Lemma 5.1.1 (Goodwin et al [16], pp 81) *Let $H(s)$ be a strictly proper function of Laplace variable s with region of convergence $\mathcal{R}\{s\} > -\alpha$. Then for any z_o such that $\mathcal{R}\{s\} > -\alpha$, we have*

$$\int_0^{\infty} h(t)e^{-z_o t} dt = \lim_{s \rightarrow z_o} H(s) \quad (5.1.1)$$

Proof This is easily proved by using the definition of the Laplace-transform, [16] □

Consider the standard feedback control loop shown in Figure 5.1

Lemma 5.1.2 (Interpolation Constraints) *Let z_o and p_o be a closed right-half plane (CRHP) zero and a CRHP pole, respectively, of the plant $G(s)$. Then for the sensitivity function, $S(s)$, and complementary sensitivity function, $T(s)$, we have*

$$S(z_o) = 1 \quad \text{and} \quad S(p_o) = 0 \quad (5.1.2)$$

$$T(z_o) = 0 \quad \text{and} \quad T(p_o) = 1 \quad (5.1.3)$$

where

$$S(s) = \frac{1}{1 + L(s)} \quad \text{and} \quad T(s) = \frac{L(s)}{1 + L(s)} \quad (5.1.4)$$

and $L(s) = G(s)C(s)$

Proof Since CRHP poles and zeros cannot be canceled they have to appear in the loop gain, $L(s)$. The results follow from the definition of $S(s)$ and $T(s)$, Equation (5.1.4) and the definition of poles and zeros □

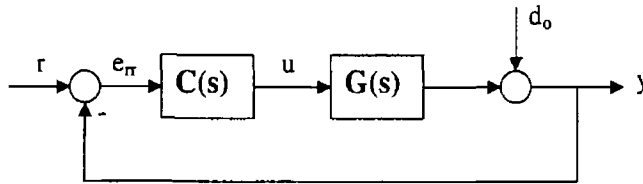


Figure 5.1 Control loop

A result similar to the next two lemmas is given in Middleton [20], for both the continuous and the discrete case

Lemma 5 1 3 (“Unstable” open loop pole) Let $e_{rr}(t)$ and $y(t)$ denote the responses for a unit step at the command input $r(t)$, and suppose there is an open loop CRHP pole at $s = p$. Then for any stable closed loop system

$$\int_0^{\infty} e_{rr}(t)e^{-pt} dt = 0 \quad (5 1 5)$$

and

$$\int_0^{\infty} y(t)e^{-pt} dt = \frac{1}{p} \quad (5 1 6)$$

Proof Let $E_{rr}(s)$ and $R(s)$ be the Laplace-transforms of $e_{rr}(t)$ and $r(t)$, respectively. Since $r(t)$ is a unit step it follows that $R(s) = \frac{1}{s}$. Then

$$E_{rr}(s) = S(s)R(s) = \frac{S(s)}{s}$$

Since the closed loop is stable $s = p$ is in the region of convergence $\mathcal{R}\{s\}$ of E_{rr} then using Lemma 5 1 1 gives

$$\begin{aligned} \int_0^{\infty} e_{rr}(t)e^{-pt} dt &= \lim_{s \rightarrow p} E_{rr}(s) = \lim_{s \rightarrow p} \frac{S(s)}{s} \\ &= \frac{S(p)}{p} \end{aligned}$$

and Equation (5 1 5) can be obtained from Lemma 5 1 2 and Equation (5 1 2)

To prove Equation (5 1 6) notice that

$$Y(s) = T(s)R(s) = \frac{T(s)}{s}$$

Again by Lemma 5 1 1

$$\begin{aligned} \int_0^{\infty} y(t)e^{-pt} dt &= \lim_{s \rightarrow p} Y(s) = \lim_{s \rightarrow p} \frac{T(s)}{s} \\ &= \frac{T(p)}{p} = \frac{1}{p} \quad (\text{bv Lemma 5 1 2, Equation (5 1 3)}) \end{aligned}$$

□

Lemma 5 1 4 (“Non-minimum phase” zero) Let $e_{rr}(t)$ and $y(t)$ denote the responses for $r(t)$ being a unit step and suppose there is an open loop CRHP zero at $s = z_0$. Then for any stable closed loop system

$$\int_0^{\infty} y(t)e^{-z_0 t} dt = 0 \quad (5 1 7)$$

and

$$\int_0^{\infty} e_{rr}(t)e^{-z_0 t} dt = \frac{1}{z_0} \quad (5.1.8)$$

Proof As for Lemma 5.1.3 except that $S(z_0) = 1$ and $T(z_0) = 0$ □

Remark 5.1.1 Since e^{-pt} is positive, it can be concluded from Equation (5.1.5) that any CRHP pole must produce a change in sign in the error signal, which implies that the output, $y(t)$, must overshoot. Furthermore, for a large CRHP pole, the exponential function decays fast relative to the settling time of the closed-loop. Hence, it is necessary that the error has a large negative value and/or the error changes sign rapidly at the beginning of the transient so that the weighted integral of the error is zero. Hence it can be argued that CRHP poles with a large magnitude are more difficult to control than CRHP poles with a small magnitude.

Remark 5.1.2 On the other hand, for a system with an open-loop CRHP zero one can see, from Equation (5.1.8), that for a step input, the error need not change sign, but for a small z_0 the integral of the error will be large and positive. Moreover, from Equation (5.1.7) it is obvious that the output must undershoot. Hence, large CRHP zeros are more difficult to control than small CRHP zeros.

Following these remarks it can be seen that CRHP poles and zeros impose fundamental limitations on the achievable performance of the closed-loop function. Next fundamental limitations for both the time and the frequency domain are discussed.

5.2 Time Domain Limitations

In this section, it is shown how RHP poles and zeros impose restrictions on the desired transient response of the closed-loop system. The following results are similar to those given in Middleton [20].

Lemma 5 2 1 (Middleton [20], Rise time, overshoot and real RHP poles)

- (a) A stable unit feedback system which has a real open loop RHP pole, must have overshoot in its step response
- (b) The amount of overshoot is related to the rise time and the location of the RHP pole, p , as follows Define the rise time, t_r , as

$$t_r = \sup_T \left\{ T \mid y(t) \leq \frac{t}{T} \text{ for } t \in [0, T] \right\} \quad (5 2 1)$$

Then, the overshoot,

$$y_{os} = \sup_t \{-e_{rr}(t)\} \quad (5 2 2)$$

satisfies

$$y_{os} \geq \frac{1}{pt_r} [(pt_r - 1)e^{pt_r} + 1] \quad (5 2 3)$$

Proof

- (a) Since $e^{-pt} > 0$, then it can be seen from Equation 5 1 5 that any open-loop RHP pole must produce a change in sign in the error and hence overshoot
- (b) From the rise time definition one can see that

$$e_{rr}(t) \geq \left(1 - \frac{t}{t_r}\right) \quad t \in [0, t_r] \quad (5 2 4)$$

Using Lemma 5 1 3, Equation (5 1 5) we have that

$$\begin{aligned} & \int_0^{\infty} e_{rr}(t)e^{-pt} dt = 0 \\ \Rightarrow & \int_0^{t_r} e_{rr}(t)e^{-pt} dt + \int_{t_r}^{\infty} e_{rr}(t)e^{-pt} dt = 0 \\ \Rightarrow & 0 \geq \int_0^{t_r} \left(1 - \frac{t}{t_r}\right) e^{-pt} dt + \int_{t_r}^{\infty} e_{rr}(t)e^{-pt} dt \quad (\text{by Eq (5 2 4)}) \\ \Rightarrow & y_{os} \int_{t_r}^{\infty} e^{-pt} dt \geq \int_0^{t_r} \left(1 - \frac{t}{t_r}\right) e^{-pt} dt \quad (\text{by Eq (5 2 2)}) \\ \Rightarrow & y_{os} \geq \frac{1}{pt_r} [(pt_r - 1)e^{pt_r} + 1] \end{aligned}$$

□

Lemma 5 2 2 (Settling time, undershoot and real RHP zeros)

(a) A stable closed loop system which has a real RHP open loop zero must have undershoot in its step response

(b) The amount of undershoot is related to the settling time and the location of the RHP zero, z , as follows Define the settling time, t_s , as

$$t_s = \inf_T \{T \mid y(t) \geq (1 - \delta) \text{ for } t \in [T, \infty] \text{ and } \delta \ll 1\} \quad (5 2 5)$$

Then, the undershoot,

$$y_{us} = \sup_t \{-y(t)\} \quad (5 2 6)$$

satisfies

$$y_{us} \geq \frac{1 - \delta}{e^{-zt_s} - 1} \quad (5 2 7)$$

Proof

(a) Recall that $e^{-zt} > 0$ Then it can be seen from Equation 5 1 7 that for an open-loop RHP zero the response to a step change in the set-point must produce a change in sign on the output, which implies undershoot

(b) (Similar to Lemma 5 2 1) From Equation 5 1 7 follows that

$$\begin{aligned} & \int_0^{t_s} y(t)e^{-zt} dt + \int_{t_s}^{\infty} y(t)e^{-zt} dt = 0 \\ \Rightarrow 0 & \geq \int_0^{t_s} y(t)e^{-zt} dt + (1 - \delta) \int_{t_s}^{\infty} e^{-zt} dt \quad (\text{by Eq (5 2 5)}) \end{aligned}$$

and using Equation (5 2 6) we obtain

$$\begin{aligned} \Rightarrow (1 - \delta) \int_{t_s}^{\infty} e^{-zt} dt & \leq - \int_0^{t_s} y(t)e^{-zt} dt \leq y_{us} \int_0^{t_s} e^{-zt} dt \\ \Rightarrow y_{us} & \geq \frac{1 - \delta}{e^{zt_s} - 1} \end{aligned}$$

□

Remark 5.2.1 *If $pt_r \gg 1$, then it can be seen from Equation 5.2.3 that $y_{os} > e^{pt_r}$. Thus two conclusions can be drawn from this. The first conclusion is that if the plant has an unstable pole then a fast response is desirable (i.e. t_r small) in order to avoid large overshoots. The second conclusion is that if the unstable pole is fast (i.e. $p \gg 0$) then the transient response of the close-loop system has to be fast (i.e. t_r small) in order to avoid large overshoots. In summary, RHP poles in the open loop system demand a fast closed-loop response.*

Remark 5.2.2 *Similar conclusions can be drawn for RHP zeros using Equation 5.2.7. Notice the trade-off between slow RHP zeros and the settling time t_s . A system with a slow RHP zero tends to have a large undershoot unless the settling time is very large, i.e. a slow response of the closed-loop system.*

5.3 Frequency Domain Limitations

As explained in the previous section, RHP poles and zeros impose fundamental limitations on the closed-loop response. In this section, limitations imposed in a frequency domain sense are studied. There are different results concerning limitations from a frequency domain point of view [20], [21], [12], [17]. The results shown here are based on those given in [17] since they are easier to apply and conclusions are easier to draw. In [17], Astrom investigates the general restrictions that RHP poles and zeros impose when designing a controller. It also shows restrictions on possible gain crossover frequencies.

One way to assess the crossover frequencies that can be achieved for a given system is the so-called *crossover frequency inequality*, [17, Section 4]. The achievable bandwidth is characterized by the gain crossover frequency ω_{gc} . The crossover frequency inequality is

$$\arg P_{nmp}(j\omega_{gc}) \geq -\pi + \varphi_m - \eta_{gc} \frac{\pi}{2}, \quad (5.3.1)$$

where φ_m is the desired phase margin in radians, η_{gc} is the slope of the minimum phase transfer function at the crossover frequency ω_{gc} , and the plant must be

factored as

$$P(s) = P_{mp}(s)P_{nmp}(s),$$

where P_{mp} is the minimum phase part and P_{nmp} is the non-minimum phase part. The factorization must be normalized in such a way that $|P_{nmp}(j\omega)| = 1$ and the sign is chosen so that P_{nmp} has negative phase. For example, for a system with a RHP pole the non-minimum phase part is thus

$$P_{nmp}(s) = \frac{s + p}{s - p}$$

where $p > 0$. Notice that

$$P_{nmp}(j\omega) = \frac{j\omega + p}{j\omega - p} = \frac{-\omega + jp}{-\omega - jp}$$

Then the magnitude is $|P_{nmp}(j\omega)| = 1$ and $\arg P_{nmp} = -2 \arctan \frac{p}{\omega}$. Therefore, the magnitude is 1 and the phase is negative. It follows from the crossover frequency inequality that

$$-2 \arctan \frac{p}{\omega_{gc}} \geq -\pi + \varphi_m - \eta_{gc} \frac{\pi}{2} = -2\alpha$$

where $\alpha = \frac{\pi}{2} - \frac{\varphi_m}{2} + \eta_{gc} \frac{\pi}{4}$. Hence

$$\omega_{gc} \geq \frac{p}{\tan \alpha}$$

This shows again that RHP poles impose a lower bound on the achievable bandwidth. This conclusion confirms the results stated in Remark 5.2.1. It can also be shown that RHP zeros impose an upper bound on the achievable bandwidth. In the next section, the crossover frequency inequality is applied to the inverted pendulum, giving some conclusions about the effect of RHP poles and zeros on the achievable bandwidths of this system.

5.4 Limitations and the Inverted Pendulum

As discussed in Chapter 4, the design of controllers for the pendulum system, following the procedure described in that chapter, has to deal with unstable

poles and RHP zeros. These RHP poles and zeros impose restrictions on the final closed-loop system. Next, the limitations that exist on the design of controllers for each loop is described.

5.4.1 Limitations of the Angular Rotation

Recall from Equation (2.1.24) that the transfer function of the plant is

$$G_2 = \frac{-k_2 s}{(s+a)(s+b)(s-b)}$$

It is worth mentioning that this plant, $G_2(s)$ cannot be stabilized by any stable controller due to the zero at the origin and the RHP pole, see [22]. This can be seen from the root locus of the plant shown in Figure 4.2 since the RHP pole cannot be moved into the LHP by changing the gain of any stable controller. A negative gain would move the RHP pole towards the zero at the origin, and a positive gain would move the pole towards infinity. Hence, in either case, we would always have a closed-loop pole in the RHP.

Now, the limitations of this plant are analyzed. Following the crossover frequency inequality, Equation (5.3.1), the plant must be factored as

$$G_2 = G_{2mp} G_{2nmp} = \left(\frac{-k_2 s}{(s+a)(s+b)^2} \right) \left(\frac{s+b}{s-b} \right)$$

For the non-minimum phase, one obtains

$$G_{2nmp}(j\omega) = \frac{j\omega + b}{j\omega - b} = \frac{-\omega + jb}{-\omega - jb}$$

and

$$\arg G_{2nmp}(j\omega) = -2 \arctan \frac{b}{\omega}$$

It follows from the crossover frequency inequality, Equation (5.3.1), that

$$\begin{aligned} -2 \arctan \frac{b}{\omega} &\geq -\pi + \varphi_m - \eta_{gc} \frac{\pi}{2} \\ \Rightarrow \frac{b}{\omega_{gc}} &\leq \tan \left(\frac{\pi}{2} - \frac{\varphi_m}{2} + \eta_{gc} \frac{\pi}{4} \right) \end{aligned}$$

$$w_{gc} \geq \frac{b}{\tan \alpha} \quad (5.4.1)$$

where

$$\alpha = \frac{\pi}{2} - \frac{\varphi_m}{2} + \eta_{gc} \frac{\pi}{4}$$

A RHP pole thus gives a lower bound on the crossover frequency. For systems with unstable poles the bandwidth must be sufficiently large. The range of achievable bandwidths is decreased with increasing frequency of the pole. It is thus more difficult to control fast unstable poles than slow unstable poles.

Choosing a controller that gives an $\eta_{gc} = -1$ or -20dB/dec (which is common for stability reasons) for the compensated minimum phase part, $G_{2mp}H_2$, and the phase margin, φ_m is chosen to be 45° ($\varphi_m = \pi/4$), hence

$$w_{gc} \geq \frac{b}{\tan \frac{\pi}{8}}$$

Using the values in Equation (2.1.25) gives

$$w_{gc} \geq 13.19 \text{ rad/sec}$$

It can be seen from Figure 4.6 that the bandwidth for the angle control is indeed larger than this lower bound.

5.4.2 Limitations of the Displacement

Next the fundamental limitations which apply to the second control loop, the displacement, are considered. As it is known, the compensator for the displacement is designed looking at the equivalent plant G_{eq} , Equation (4.1.7)

$$G(s) = \frac{11(s+50)(s-b)(s-2)}{s(s+475.1)(s+16.71)(s+a)(s+0.688)}$$

The plant must be factored as

$$G = G_{mp}G_{nmp} \\ = \left(\frac{11(s+50)(s+b)(s+2)}{s(s+475.1)(s+16.71)(s+a)(s+0.688)} \right) \left(\frac{(-s+b)(-s+2)}{(s+b)(s+2)} \right)$$

It follows for the non-minimum phase part that

$$G_{nmp}(j\omega) = \frac{(z_1 - j\omega)(z_2 - j\omega)}{(z_1 + j\omega)(z_2 + j\omega)}$$

where $z_1 = b$ and $z_2 = 2$, so

$$\arg G_{nmp}(j\omega) = -2 \arctan \frac{\omega}{z_1} - 2 \arctan \frac{\omega}{z_2}$$

It follows from the crossover frequency inequality, Equation (5.3.1), that

$$\begin{aligned} -2 \arctan \frac{\omega}{z_1} - 2 \arctan \frac{\omega}{z_2} &\geq -\pi + \varphi_m - \eta_{gc} \frac{\pi}{2} \\ \Rightarrow \arctan \frac{\frac{\omega}{z_1} + \frac{\omega}{z_2}}{1 - \frac{\omega^2}{z_1 z_2}} &\geq \frac{\pi}{2} - \frac{\varphi_m}{2} + \eta_{gc} \frac{\pi}{4} \\ \Rightarrow \omega \frac{z_1 + z_2}{z_1 z_2 - \omega^2} &\leq \tan \left(\frac{\pi}{2} - \frac{\varphi_m}{2} + \eta_{gc} \frac{\pi}{4} \right) \\ \beta \omega_{gc}^2 + \omega_{gc}(z_1 + z_2) - \beta z_1 z_2 &\leq 0 \end{aligned}$$

where $\beta = \tan \left(\frac{\pi}{2} - \frac{\varphi_m}{2} + \eta_{gc} \frac{\pi}{4} \right)$

Choosing a controller that gives an $\eta_{gc} = -1$ or -20 dB/dec for the compensated minimum phase part, $G_{mp}H_1$ and the phase margin, φ_m , is chosen to be 45 deg ($\varphi_m = \pi/4$), this yields

$$\omega_{gc} \leq 0.58729 \text{ rad/sec}$$

Unstable zeros thus give an upper bound on the crossover frequency. Slow RHP zeros are thus more difficult to control than fast RHP zeros.

5.5 Discussion

Limitations imposed by unstable poles and RHP zeros were studied in this chapter. Thus, it is important to be aware of how well a system can be controlled in terms of some performance requirements, i.e. bandwidths, settling time, rise time, etc. Systems with RHP poles and zeros are, by nature, more difficult to control.

From Figures 4.5 and 4.9 one can see the most noticeable characteristic of the RHP zeros. Figure 4.5 is the step response of the angle control closed-loop system,

which has a non-minimum phase zero at $s = 2$ due to the controller H_2 . Figure 4.9 is the closed-loop response of the displacement, which has two RHP zeros due to the plant G_{eq} . In the first case, the initial response of the system is in the opposite direction compared to its steady state value and the system has a large undershoot. In the second case, the initial response is in the same direction as its steady state value but eventually it changes the direction and reverses the sign to finally move back toward the steady state. In general, for a stable system with n_z RHP zeros, its step response will cross zero (its original value) n_z times; that is, the system will have undershoot. This result is a well known characteristic of RHP zeros (Holt and Morari [19]) and it is another way to verify that non-minimum phase zeros impose fundamental restrictions in the design of control systems. It was shown that RHP zeros close to the imaginary axis give a larger overshoot (see Lemma 5.2.2) which also illustrates the result obtained in this chapter. That is, slow non-minimum phase zeros are more difficult to control than fast RHP zeros.

Following Chapter 4 and this chapter, it can be concluded that the pendulum system is not easy to control since strong fundamental limitations apply to it. Now that these limitations are understood one can proceed to improve the design of Chapter 4.

Chapter 6

One-Loop-at-a-Time Method - Approach 2

In Section 4.1 some controllers were designed for good command following of the displacement control. The resulting response was not fast enough. It is now understood that this is because of the two slow RHP zeros in the equivalent plant $G_{eq}(s)$. This restrains the final response, as illustrated in the previous section. In this chapter we counter this restriction, in as much as this is possible, using a one-loop-at-a-time strategy.

6.1 Controller Design - Approach 2

It can be seen, from Equation (4.1.6), that RHP poles in the controller H_2 become RHP zeros in the equivalent plant. This plant has two RHP zeros (see Equation (4.1.7)). One is due to the plant G_2 and the other is due to the controller H_2 . It is obvious that the RHP zero that comes from the plant cannot be avoided, but one can avoid the RHP zero due to the controller H_2 . One way to do this is shown in Figure 6.1, which may be compared with Figure 4.1.

From this figure and using a similar procedure to that used to get Equation (4.1.6), the new equivalent plant, i.e. the plant seen by the controller H_1 can be obtained

$$G_{eq}(s) = \frac{d}{u_1} = \frac{G_1 H_2}{1 + G_2 H_2} \quad (6.1.1)$$

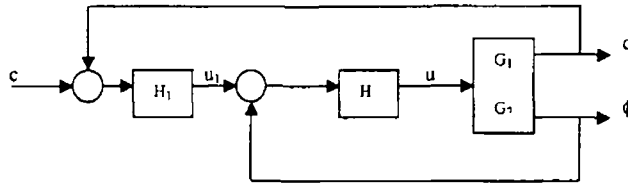


Figure 6.1 New feedback system

As can be noticed from the above equation, the poles of H_2 cancel with themselves when G_{eq} is calculated, which means that now there is only one RHP zero in the equivalent plant instead of two RHP zeros as was the case. In other words, unstable poles of H_2 resulting in RHP zeros in G_{eq} are avoided. Notice that in this way, unnecessary limitations on G_{eq} (i.e. displacement loop, not on the angle loop) are avoided.

Both controllers need to be redesigned. This is discussed in the following sections. It is important to notice that in order to have a good performance of the real system and since a precise mathematical model is not available, it has to be assured that the overall system is robust in order to cope with uncertainties and non-linearities existing in the real system. This is why good sensitivity and complementary sensitivity functions are required for this plant.

6.1.1 Controller Design for the Angular Rotation

The controller designed for this part of the system is

$$H_2(s) = -80 \frac{(s+a)(s+b)}{(s+100)(s-2)} \quad (6.1.2)$$

The step response, the Bode plot of the loop gain, the sensitivity and complementary sensitivity functions are shown in Figures 6.2, 6.3 and 6.4 respectively. From these figures one can see that there is no big difference between the response of this design and that of Section 4.1.1. This is because the limitation of the plant RHP pole is still imposed.

6 1 2 Controller Design for the Displacement

Before designing a controller for the displacement, the new equivalent plant has to be found. From Equations (2 1 24), (2 1 25), (6 1 1) and (6 1 2) one obtains

$$G_{eq}(s) = -880 \frac{(s + b)(s - b)}{s(s + 68.45)(s + 23.4)(s + 0.6821)} \quad (6 1 3)$$

Notice that there is only one RHP zero. The controller designed for this part of the system is

$$H_1(s) = 0.35 \frac{(s + 23.4)(s + 0.6821)}{(s + 15)(s + b)} \quad (6 1 4)$$

The step response, the Bode plots for the loop gain, the sensitivity and complementary sensitivity functions are shown in Figures 6 5, 6 6 and 6 7 respectively.

From these figures, one can see that with this controller good stability margins are obtained as well as a faster response, which was the objective.

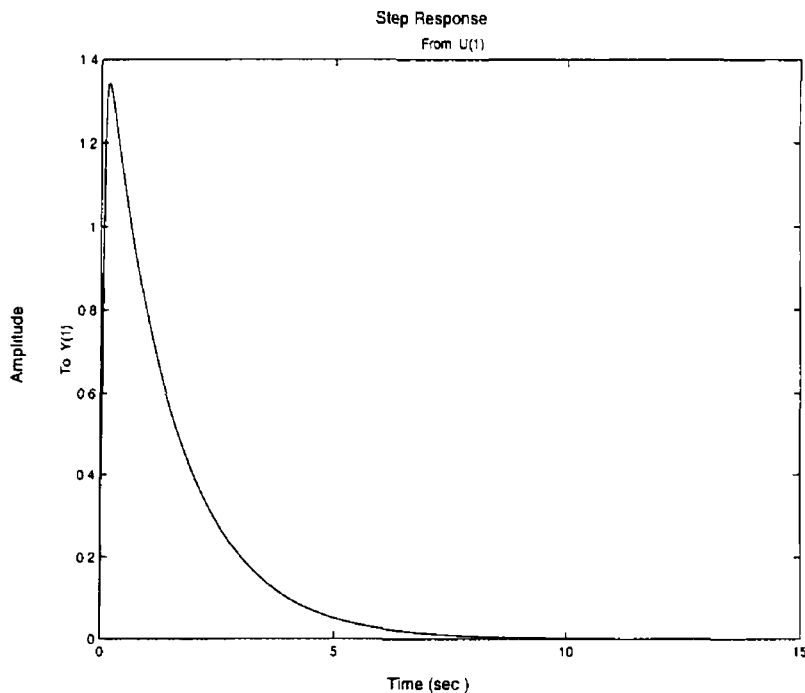


Figure 6 2 Step response of the angle loop

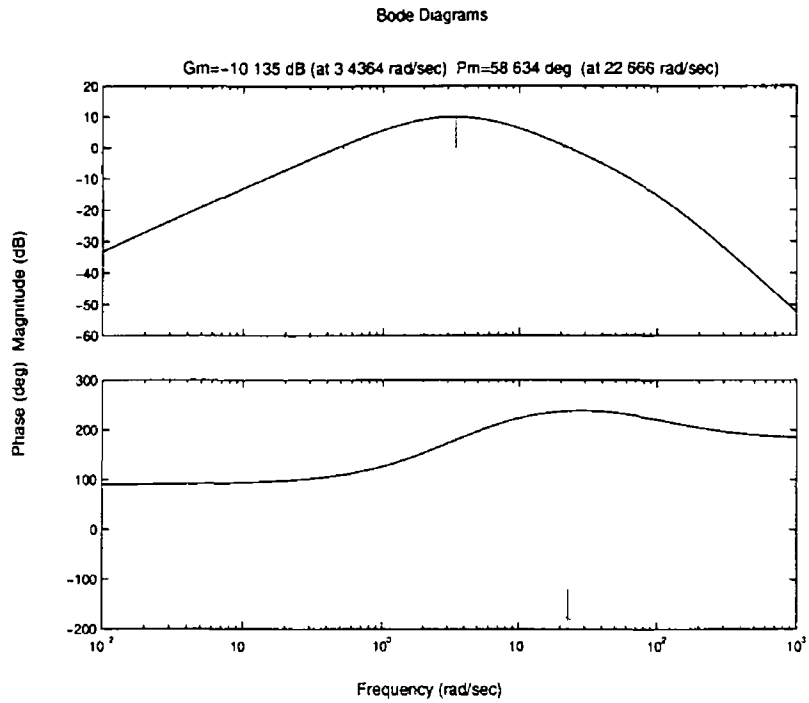


Figure 6.3 Bode diagram of the angle loop

6.2 Discussion

From Equation (6.1.3) it can be seen that with this new setup (see Figure 6.1) a RHP zero has been avoided when designing the control system for the displace-

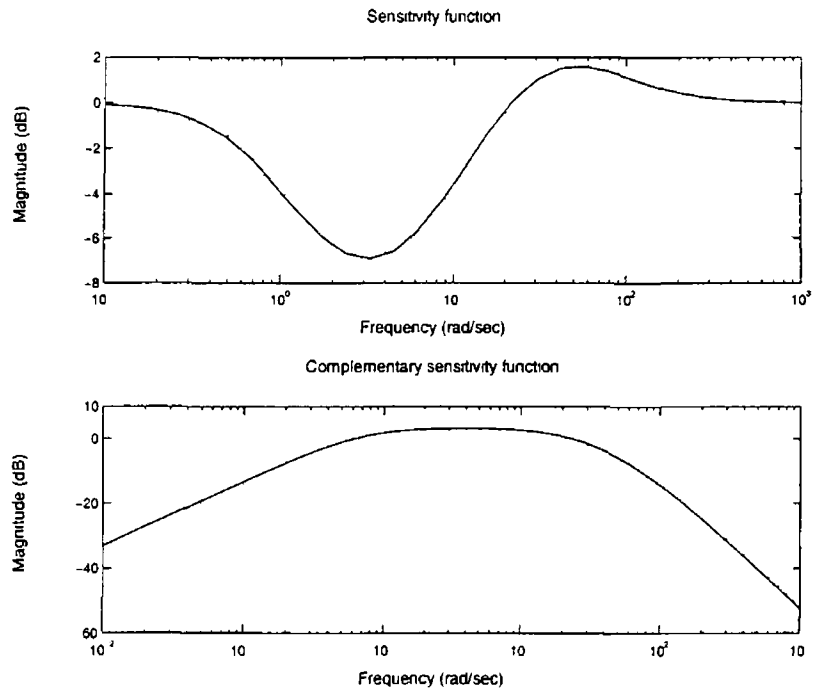


Figure 6.4 Sensitivity functions of the angle loop

ment This makes the design easier in the sense that the overall performance is not highly limited, bandwidths can be improved thus facilitating the shaping of the sensitivity and complementary sensitivity function All in all, this improves the performance and robustness of the system In fact as can be noticed from Figures 4 9, 4 10, 4 11, 6 5, 6 6 and 6 7 the performance was notably improved The system is much faster and more robust

In Chapter 5, it was stated that no stable controller could stabilize the angle plant and in the design process a controller with one RHP pole was chosen It is worth mentioning that a controller with one unstable pole gives a better response than controllers with two or more RHP poles To check this Lemma 5 1 3 can be used Hence, for the case of a controller with two unstable poles one obtains

$$\int_0^{\infty} e_{rr}(t)e^{-p_1t} dt + \int_0^{\infty} e_{rr}(t)e^{-p_2t} dt = 0$$

$$\Rightarrow \int_0^{\infty} e_{rr}(t) (e^{-p_1t} + e^{-p_2t}) dt = 0$$

Since the response of the error is equivalent to the response of the sensitivity function to a disturbance at the output of the plant, d_o (from Figure 5 1, $E(s) =$

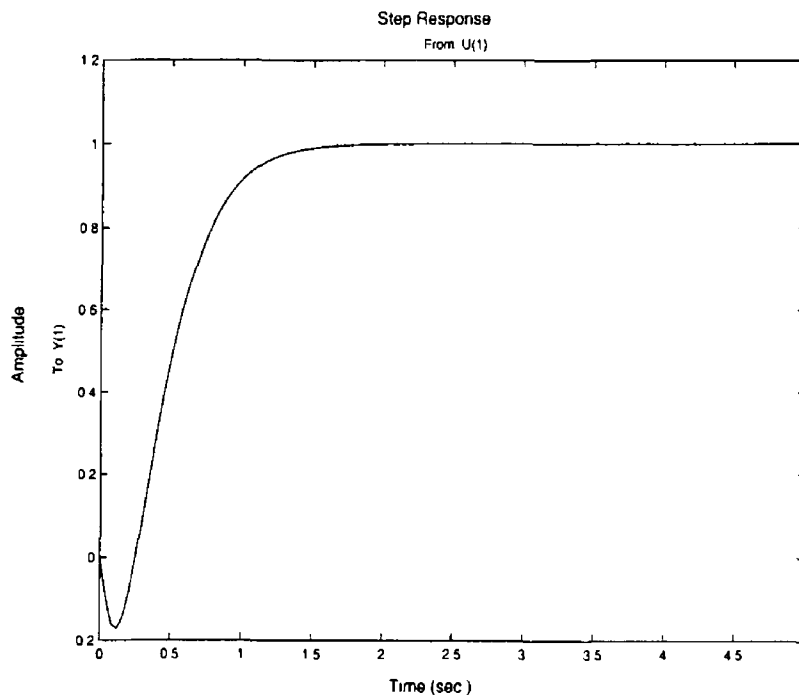


Figure 6 5 Step response of the displacement loop

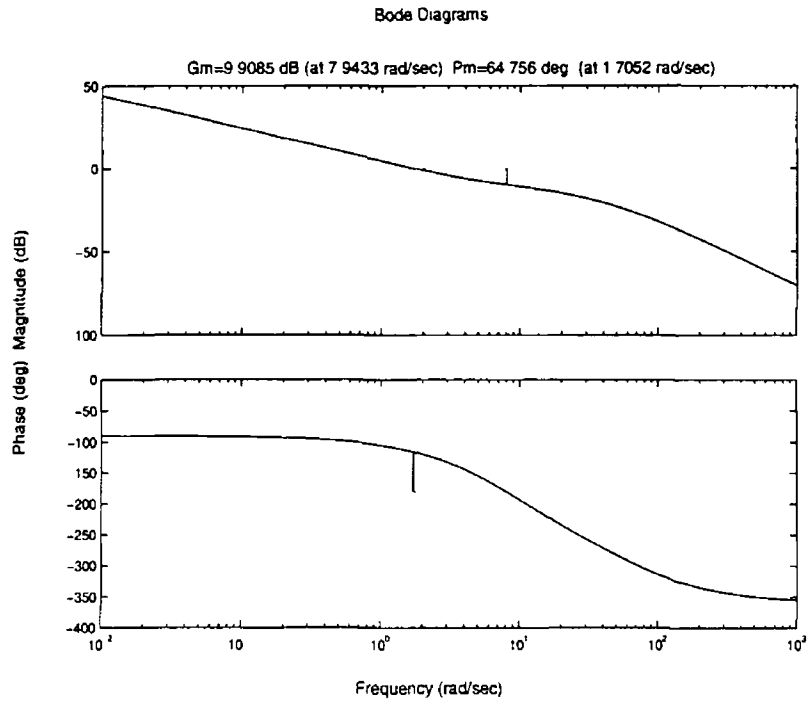


Figure 6 6 Bode diagram of the displacement loop

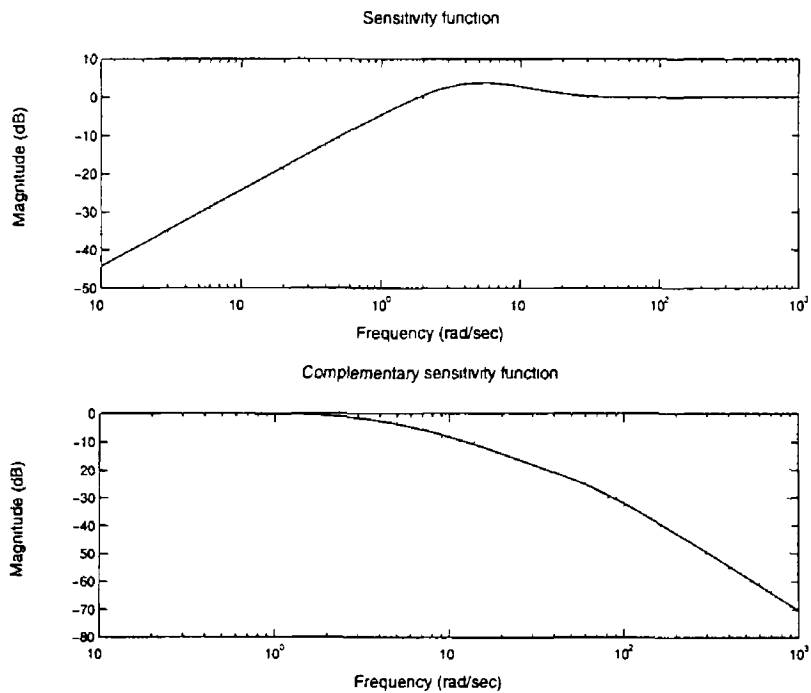


Figure 6 7 Sensitivity functions of the displacement loop

$S(s)R(s)$ and $Y(s) = S(s)D_o(s)$, it can be concluded from the above equation that a controller with more RHP poles would give a change in sign in the signal $y(t)$ and a higher overshoot in the transient response when a disturbance is applied

to the pendulum. Indeed, this is an undesirable effect. In other words, increasing the number of RHP poles that are added to the controller during the design has the effect of decreasing the level of disturbance attenuation.

Finally, the controllers were implemented in the real system and further tuning was needed. The gain of the controllers was increased in order to get more robustness in the control system. The linear model used to design the controllers is not accurate, that is why more robustness is required in order to deal with the uncertainty and non-linearities inherent in the system. The final controllers are

$$H_1 = 0.7 \frac{(s + 23.4)(s + 0.6821)}{(s + 15)(s + 5.464)} \quad (6.2.1)$$

and

$$H_2 = -150 \frac{(s + 5.464)(s + 3.333)}{(s + 100)(s - 2)} \quad (6.2.2)$$

The respective response is given in Figure 6.8. Notice from this figure the small oscillation on the responses of the system. This is due to the resolution of the discrete sensors (see Section 2.1.4) used in the system.

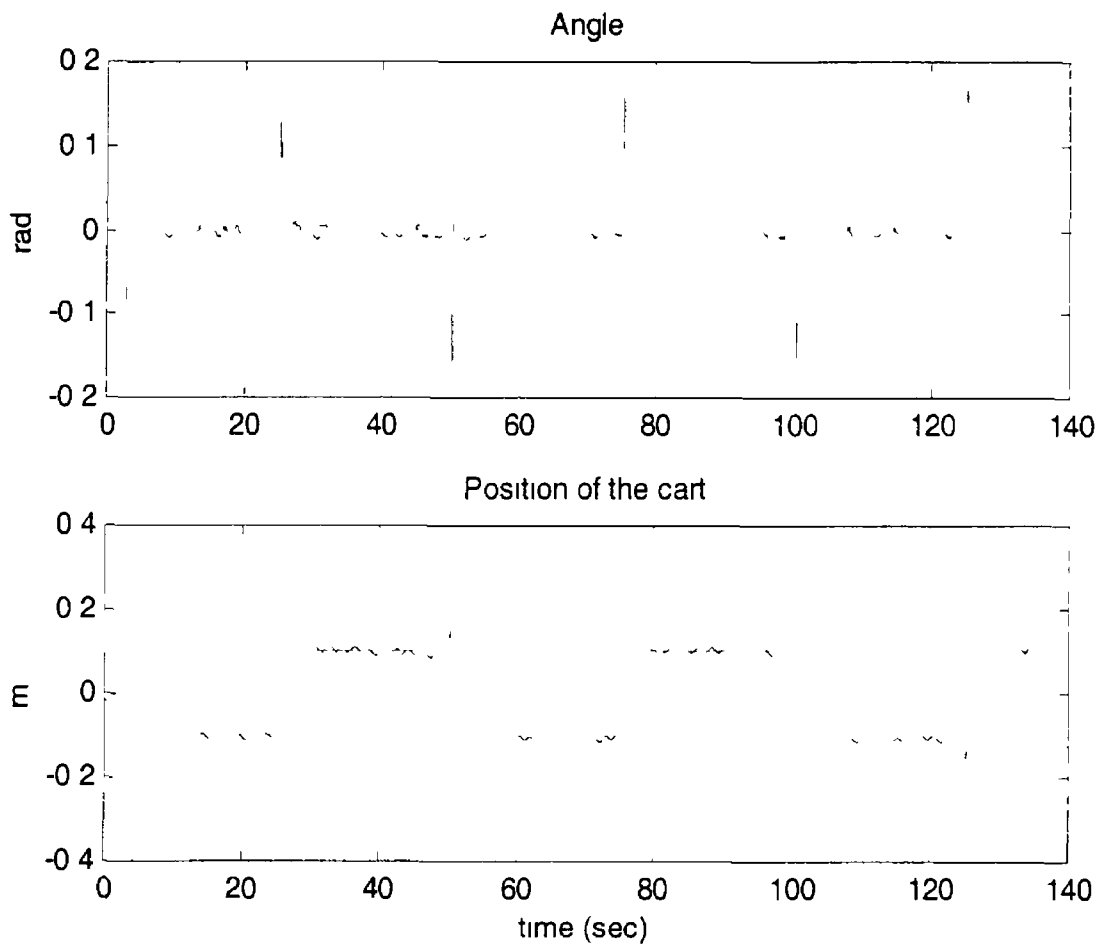


Figure 6 8 Response of the real system

Chapter 7

Gain Scheduling

Gain Scheduling (GS) design has become a popular method for designing controllers for non-linear plants specially during the last decade. It has special features that make it easy to apply compared with others design methods for non-linear plants. Among those features the most attractive is that GS employs linear design tools in the design stage. See Rugh and Shamma [23] for a survey on GS.

Many different design notions can be viewed as GS such as switching gain values according to operating conditions, precompensating a non-linear gain with the inverse gain function, etc. Techniques like switching controllers also fit a broad interpretation of GS. In this chapter the focus is on gain scheduling in the sense of continuously varying the controller coefficients according to the current value of a scheduling signal.

The design of GS controllers for non-linear plants can be summarized in four broad steps, [23]. The first step is to compute a linear parameter-varying (LPV) model for the plant. The second step is to use linear design methods to obtain linear controllers for the LPV model. The third step is to implement the families of controllers obtained in the second step in such a way that the controller coefficients vary according to the current value of the scheduled variable(s). The fourth step is performance assessment.

Again the inverted pendulum is used as an application example. The controllers that have already been designed for the inverted pendulum work properly for the

linearized plant at the equilibrium point with $x_3 = 0$ (pendulum in the upright position), but when applied to the nonlinear plant the system behaves differently when it is at a point that is not the equilibrium point. In order to see how the system behaves at every point in state space the non-linear transfer functions may be found

7.1 Non-Linear Transfer Functions

A representation of the plant is found which allows us to obtain a transfer function for points other than equilibrium points. To calculate the transfer functions it is necessary to get an appropriate non-linear state space form of the system. Finding a standard linearization of Equation (2.1.17), yields

$$x = \begin{pmatrix} 0 & 1 & 0 & 0 \\ 0 & -\frac{F}{M} & 0 & 0 \\ 0 & 0 & 0 & 1 \\ 0 & \frac{F}{ML'} \cos(x_3) & u & 0 \end{pmatrix} x + \begin{pmatrix} 0 \\ \frac{1}{M} \\ 0 \\ -\frac{1}{ML'} \cos(x_3) \end{pmatrix} u \quad (7.1.1)$$

and from Equation (2.1.20),

$$y = \begin{pmatrix} 1 & 0 & 0 & 0 \\ 0 & 0 & 1 & 0 \end{pmatrix} x \quad (7.1.2)$$

where

$$x = (x_1 \quad x_2 \quad x_3 \quad x_4)^T$$

and

$$w = \frac{g}{L'} \cos(x_3) + \frac{1}{ML'} u \sin(x_3) - \frac{F}{ML'} x_2 \sin(x_3) \quad (7.1.3)$$

Thus, x_3 can be chosen as the scheduled variable. Now, the transfer functions can be calculated using Equation (2.1.21). A few calculations gives

$$G_1 = \frac{\frac{1}{M}}{s \left(s + \frac{F}{M} \right)} \quad (7.1.4)$$

$$G_2 = -\frac{\frac{1}{ML'} \cos(x_3) s}{\left(s + \frac{F}{M} \right) (s^2 - w)} \quad (7.1.5)$$

From these transfer functions one can see that G_2 is nonlinear and its gain and two poles (i.e. $(s^2 - w)$) depend on the state of the plant $x(t)$. This model can be viewed as an LPV model. Now, the scheduled controller can be designed

7.2 GS Controller Design

Based on the controllers already designed in Chapter 6 one can design the GS controllers. Again two controllers are needed, one to control the displacement of the carriage and one to control the angular rotation.

7.2.1 GS Controller Design for the Angular Rotation

It can be seen from Equation (7.1.5) that the gain of the plant varies with the variation of the angle x_3 . To counteract that variation it is possible to vary the gain of the controller H'_2 . One way to deal with this is to replace the gain of H'_2 say h_2 by $h_2/\cos(x_3)$. It can be noticed from Equation (7.1.5) that the plant has two poles that change with the parameters of the plant $\pm\sqrt{w}$, where w is given in Equation (7.1.3). H_2 (Equation (6.1.2)) was designed aiming to cancel the two stable poles of G_2 , $(-\sqrt{w}$ and $-\frac{F}{M})$ at equilibrium. Hence for the GS controller one could have two zeros at the same location but varying as the poles of the plant varies. So the new controller for the angular rotation is

$$H'_2 = \frac{\frac{-80}{\cos(x_3)}(s + \frac{F}{M})(s + \sqrt{w})}{(s + 100)(s - 2)} \quad (7.2.1)$$

7.2.2 GS Controller Design for the Displacement

It can be noticed from Equation (6.1.1) that the gain of the equivalent plant, G_{eq} , only depends on the gain of G_1 and H_2 . The gain of G_1 is constant (see Equation (7.1.4)), thus the only variation of the gain of G'_{eq} is due to H'_2 . Hence the gain of H'_1 can be adjusted to $h_1 \cos(x_3)$, where h_1 is the gain of this controller.

It can also be checked that with the H'_2 of Equation (7.2.1) the new equivalent plant has two zeros at $\pm\sqrt{w}$. So H'_1 can be set to cancel the two stable zeros of G'_{eq} . The new equivalent plant is

$$G'_{eq} = \frac{\frac{-80k_1}{\cos x_3}(s + \sqrt{w})(s - \sqrt{w})}{s[s^3 + (90 - \sqrt{w})s^2 + (80k_2 - 200 - 90\sqrt{w})s + 200\sqrt{w}]} \quad (7.2.2)$$

From Equations (6.1.3) and (6.1.4) it can be noticed that H_1 was canceling two poles of G_{eq} . So this controller might need to cancel those poles, but their location varies with the variation of some parameters of the plant, such as the angle, x_3 . In order to do such cancellations the variation of the poles of G'_{eq} as x_3 changes from 0 to 90 degrees is calculated while setting u and x_2 (see Equation 7.1.3) to zero. The variation of these poles is tabulated. The table below shows the variation of the angle at several values.

Angle (x_3)	0	5	10	15	20
poles	-68.452	-68.445	-68.422	-68.384	-68.33
	-23.402	-23.422	-23.481	-23.58	-23.72
	-0.68214	-0.68034	-0.67495	-0.666	-0.65354
Angle (x_3)	30	45	60	80	
poles	-68.172	-67.797	-67.206	-65.772	
	-24.125	-25.068	-26.497	-29.718	
	-0.6183	-0.54065	-0.43391	-0.23296	

Table 7.1 Variation of poles of G_{eq}

So it is needed to find functions that describe the variations of the two slower poles. Using Matlab's commands `polyfit` and `polyval` the polynomials which fit the variations of the poles (including negative values of the angle) were computed. So the new controller for the system is

$$H'_1 = \frac{0.35 \cos(x_3)(s + \alpha)(s + \beta)}{(s + 15)(s + \sqrt{w})} \quad (7.2.3)$$

where

$$\begin{aligned} \alpha &= 0.00093273(x_3 \times 180/\pi)^2 + 23.289 \\ &= 3.062 x_3^2 + 23.289 \quad (x_3 \text{ in rad}) \end{aligned}$$

and

$$\begin{aligned} \beta &= -6.9113 \times 10^{-5}(x_3 \times 180/\pi)^2 + 0.68136 \\ &= -0.22688 x_3^2 + 0.68136 \quad (x_3 \text{ in rad}) \end{aligned}$$

7.3 Discussion

The controllers of the previous chapters work properly on the real system (see Section 6.2), but despite the fact that those controllers are robust, their performance decreases as the pendulum angle drifts away from the vertical position. This is because the sensitivity and complementary sensitivity functions are affected by the angle as well as the stability margins which decrease as the angle moves away from zero. This is one of the advantages of the GS approach, since it keeps the stability margins and the robustness of the closed loop system unaffected, or at least between a small range of variation.

It can be checked from simulations that when the initial conditions are close to the equilibrium the transient and steady state response of the closed loop system with the GS controllers is very similar to that of the system with the controllers described in Section 6.2. The advantage as was said above, is that the GS controllers are more robust regarding variations of the plant due to non-linearities. Several tests were performed on the real system with the GS controllers and the controllers of the previous chapters. The initial position of the pendulum was changed. With the controllers of the previous chapter the system could not be stabilized when the initial condition was greater than or equal to 0.2 rad (11° approx), whereas the GS controllers could stabilize the system with initial position of around 0.35 rad (20° approx).

Chapter 8

\mathcal{H}_2 Optimization and Multivariable Control

In this chapter a full MIMO perspective is adopted. As mentioned earlier, some of the tools and definitions used for SISO systems are no longer applicable for MIMO systems. An example of this is discussed in Chapter 2 where the poles and zeros were defined for MIMO systems. There are several methods for designing controllers for multivariable systems, [16] [9], [12], [24]. Here, an approach based on frequency domain \mathcal{H}_2 optimization is considered.

8.1 Introduction

The idea of \mathcal{H}_2 control is to find a controller that stabilizes the system and minimizes a given quadratic cost function. There are many ways in which control design problems can be cast as \mathcal{H}_2 optimization problems. The best known solution of the standard \mathcal{H}_2 problem is described by Doyle et al. [25] but it is only applicable to a limited class of problems and it relies on the solution of Riccati equations.

The approach taken here uses the sensitivity and complementary sensitivity function as a measure of robustness. The sensitivity function, S , determines the effect of disturbances on the closed-loop system. The complementary sensitivity function, T , is important for the closed-loop response, the effect of measurement

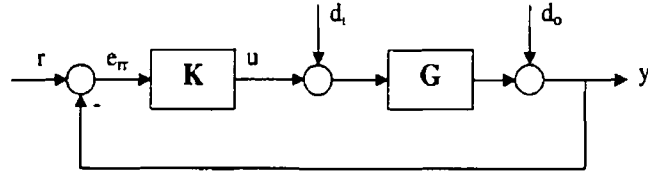


Figure 8.1 Control loop

noise and robust stability. For the configuration of Figure 8.1 these functions are defined as

$$S_o(s) = (I + G(s)K(s))^{-1} \quad (8.1.1)$$

$$T_o(s) = I - S_o(s) = G(s)K(s)(I + G(s)K(s))^{-1} \quad (8.1.2)$$

$$S_i(s) = (I + K(s)G(s))^{-1} \quad (8.1.3)$$

$$T_i(s) = I - S_i(s) = K(s)G(s)(I + K(s)G(s))^{-1} \quad (8.1.4)$$

where the subscripts i and o stand for input and output, respectively. This is to distinguish the functions evaluated at the input and at the output of the plant. Of course, for SISO systems $S_i = S_o$ and $T_i = T_o$. Typically, control system design amounts to shaping these functions aiming for the following objectives

- Make the sensitivity S small at low frequencies
- Make the complementary sensitivity T small at high frequencies
- Prevent both S and T from peaking at crossover frequencies

Therefore the \mathcal{H}_2 problem can be cast in terms of the sensitivity and complementary functions, as follows

Problem The \mathcal{H}_2 problem can be cast as

$$\arg \inf_w \|W_s S(jw)\|_2^2 + \|W_t T(jw)\|_2^2 \quad (8.1.5)$$

where W_s and W_t are weighting functions used to shape S and T , respectively, and the \mathcal{H}_2 -norm is defined as

$$\|F\|_2^2 = \frac{1}{2\pi} \int_{-\infty}^{\infty} \text{Trace}[F^*(jw)F(jw)]dw \quad (8.1.6)$$

The Youla parameterization (Chapter 3) is a useful tool that facilitates the solution of the \mathcal{H}_2 problem, since it allows the cost function (Equation (8.1.5)) to be written in terms of a single parameter, Q . That is, the optimal Q is calculated and then, using the Youla parameterization, the corresponding optimal controller K is found. In this way, closed loop stability is equivalent to the stability of Q .

In this chapter, two different approaches are studied, both of them in the frequency domain. The first uses an optimization of S and T at the input and then at the output of the plant in order to find Q . In the second approach, the cost function is minimized in terms of S_o and T_o , that is the optimization is only done at the output. Again, the procedure is explained based on the inverted pendulum plant (Equations (2.1.24) and (2.1.25)).

8.2 Finding the \mathcal{H}_2 Controller - Approach 1

As stated above, the \mathcal{H}_2 problem is to find the optimal Q which minimizes the two-norm of

$$J = \|W_s S(j\omega)\|_2^2 + \|W_t T(j\omega)\|_2^2$$

where S and T are the sensitivity and complementary sensitivity functions respectively. Notice that in the pendulum system, Q is a 1×2 matrix (i.e. $Q = [Q_1 \ Q_2]$) and by the identity

$$G(I + KG)^{-1} = (I + GK)^{-1}G$$

it can be concluded that $GS_i = S_oG$. Thus the optimal Q at the input of the plant is the same as the output. The solution sought in this section is based on the structure of the pendulum plant.

For the pendulum system the sensitivity at the input is a scalar, therefore it should be easier to find the optimal Q at the input of the plant. To do so, two expressions are needed. They are the sensitivity, $S(s)$ and complementary sensitivity, $T(s)$, functions at the input of the plant. They should be expressed in

terms of the Youla parameter This can be done using Theorem 3 0 1 as follows,

$$\begin{aligned}
S_i &= (I + KG)^{-1} \\
&= (I + Y_l^{-1}X_lN_rD_r^{-1})^{-1} \quad (\text{by Theorem 3 0 1}) \\
&= [Y_l^{-1}(Y_lD_r + X_lN_r)D_r^{-1}]^{-1} \\
&= D_r(Y_lD_r + X_lN_r)^{-1}Y_l \\
&= D_r[V_rD_r + QN_lD_r + U_rN_r - QD_lN_r]^{-1}(V_r + QN_l) \quad (\text{by Th 3 0 1}) \\
&= D_r[I + QN_lD_r - QN_lD_r]^{-1}(V_r + QN_l) \\
&= D_r(V_r + QN_l)
\end{aligned}$$

In the above equations, the identities $G = N_lD_r = D_lN_r$ and $U_rN_r + V_rD_r = I$ (see Theorem 3 0 1) were used Thus S_i in terms of the Q parameter is

$$S_i = D_r(V_r + QN_l) \quad (8 2 1)$$

Following a similar procedure it can easily be proved that

$$T_i = (U_l - D_rQ)N_l \quad (8 2 2)$$

Note also that

$$S_o = (V_l + N_rQ)D_l \quad (8 2 3)$$

$$T_o = N_r(U_r - QD_l) \quad (8 2 4)$$

Now the \mathcal{H}_2 problem can be cast in terms of the Q parameter

8 2.1 Solution via Completion of Squares

Here the term $*$ will denote complex conjugation Notice that

$$|W_sS_i|^2 + |W_tT_i|^2 = (W_sS_i)^*(W_sS_i) + (W_tT_i)^*(W_tT_i)$$

and using Equations (8 2 1) and (8 2 2) in the equation above yields

$$\begin{aligned}
|W_sS_i|^2 + |W_tT_i|^2 &= (W_sD_rV_r + W_sD_rQN_l)^*(W_sD_rV_r + W_sD_rQN_l) \\
&\quad + (W_tU_lN_l - W_tD_rQN_l)^*(W_tU_lN_l - W_tD_rQN_l)
\end{aligned}$$

Notice that N_l is a 2×1 matrix, U_l is 1×2 , Q is a 1×2 and D_r , V_r , W_s and W_t are scalar transfer functions. Thus

$$\begin{aligned}
|W_s S_i|^2 + |W_t T_i|^2 &= W_s^* D_r^* V_r^* W_s D_r V_r + W_s^* D_r^* V_r^* W_s D_r Q N_l \\
&\quad + W_s^* D_r^* N_l^* Q^* W_s D_r V_r + W_s^* D_r^* N_l^* Q^* W_s D_r Q N_l \\
&\quad + W_t^* N_l^* U_l^* W_t U_l N_l - W_t^* N_l^* U_l^* W_t D_r Q N_l \\
&\quad - W_t^* D_r^* N_l^* Q^* W_t U_l N_l + W_t^* D_r^* N_l^* Q^* W_t D_r Q N_l \\
&= D_r^* D_r (W_s^* W_s + W_t^* W_t) N_l^* Q^* Q N_l + D_r^* (W_s^* W_s D_r V_r - W_t^* W_t U_l N_l) N_l^* Q^* \\
&\quad + D_r (W_s^* W_s D_r V_r - W_t^* W_t U_l N_l)^* Q N_l + W_s^* W_s D_r^* D_r V_r^* V_r + W_t^* W_t N_l^* U_l^* U_l N_l
\end{aligned}$$

Let

$$\Lambda_i^* \Lambda_i = D_r^* D_r (W_s^* W_s + W_t^* W_t) \quad (8.2.5)$$

Thus

$$\begin{aligned}
&= \Lambda_i^* \Lambda_i N_l^* Q^* Q N_l + D_r^* (W_s^* W_s D_r V_r - W_t^* W_t U_l N_l) (Q N_l)^* \\
&\quad + D_r (W_s^* W_s D_r V_r - W_t^* W_t U_l N_l)^* Q N_l + W_s^* W_s D_r^* D_r V_r^* V_r \\
&\quad + W_t^* W_t N_l^* U_l^* U_l N_l
\end{aligned}$$

and completing the square

$$\begin{aligned}
&= (\Lambda_i Q N_l + B_i)^* (\Lambda_i Q N_l + B_i) + W_s^* W_s D_r^* D_r V_r^* V_r + W_t^* W_t N_l^* U_l^* U_l N_l \\
&\quad - \left(\frac{D_r^* (W_s^* W_s D_r V_r - W_t^* W_t U_l N_l)}{\Lambda_i^*} \right)^* \left(\frac{D_r^* (W_s^* W_s D_r V_r - W_t^* W_t U_l N_l)}{\Lambda_i^*} \right)
\end{aligned}$$

where

$$B_i = \left(\frac{D_r^* (W_s^* W_s D_r V_r - W_t^* W_t U_l N_l)}{\Lambda_i^*} \right) \quad (8.2.6)$$

After simplifying gives

$$\begin{aligned}
|W_s S_i|^2 + |W_t T_i|^2 &= \\
&(\Lambda_i Q N_l + B_i)^* (\Lambda_i Q N_l + B_i) + \frac{D_r^* D_r W_s^* W_s W_t^* W_t}{\Lambda_i^* \Lambda_i} (D_r V_r + U_l N_l)^* (D_r V_r + U_l N_l)
\end{aligned}$$

Since Q can do nothing to affect the second term in the above equation, only one Q that minimizes the 2-norm of the first term needs to be chosen and this is a

1-block problem which should be easier to solve than the 2-block problem. Thus the problem can be recast as

$$Q_{opt} = \arg \inf_{Q \in \mathcal{H}^\infty} \|\Lambda_i Q N_i + B_i\|^2 \quad (8.2.7)$$

where Λ_i and B_i are given in Equations (8.2.5) and (8.2.6). In the equation above some of the terms are vectors. In order to express that equation in terms of the scalar components of the vectors, let $Q = [Q_1 \ Q_2]$ and $N_i = [N_{i1} \ N_{i2}]^T$ and substituting into Equation (8.2.7) yields

$$\begin{aligned} & (\Lambda_i Q N_i + B_i)^* (\Lambda_i Q N_i + B_i) = \\ & \left(\Lambda_i [Q_1 \ Q_2] \begin{bmatrix} N_{i1} \\ N_{i2} \end{bmatrix} + B_i \right)^* \left(\Lambda_i [Q_1 \ Q_2] \begin{bmatrix} N_{i1} \\ N_{i2} \end{bmatrix} + B_i \right) \end{aligned}$$

Thus

$$(\Lambda_i Q N_i + B_i)^* (\Lambda_i Q N_i + B_i) = (\Lambda_i Q_1 N_{i1} + \Lambda_i Q_2 N_{i2} + B_i)^* (\Lambda_i Q_1 N_{i1} + \Lambda_i Q_2 N_{i2} + B_i) \quad (8.2.8)$$

or equivalently

$$Q_{opt} = \inf_{Q_1, Q_2 \in \mathcal{H}^\infty} \|\Lambda_i Q_1 N_{i1} + \Lambda_i Q_2 N_{i2} + B_i\|^2 \quad (8.2.9)$$

Clearly the problem has been reduced to an optimization problem of two scalar variables Q_1 and Q_2 . Now a solution to this problem is sought.

Finding the Optimal Q_1 and Q_2 - Approach 1

From Equation (8.2.9) and from the well known Projection Theorem ([26]) it is known that $Q_{opt} = [Q_{1opt} \ Q_{2opt}]$ is optimum if and only if

$$\int (A_1 Q_{1opt} + A_2 Q_{2opt} + B_i)^* (A_1 Q_1 + A_2 Q_2) dw = 0 \quad \forall Q_1, Q_2 \in \mathcal{H}^\infty$$

where $A_1 = \Lambda_i N_{i1}$, $A_2 = \Lambda_i N_{i2}$ and B_i are stable and strictly proper. In this case N_{i1} and N_{i2} differ only by a constant (see Equation (3.3.21)) and hence, so do A_1 and A_2 . Therefore, from an inner/outer factorization of A_1 and A_2 it can be seen that the inner products are the same. Now, let $A_1 = A_i A_{1op}$ and $A_2 = A_i A_{2op}$ be

their respective inner/outer factorizations, thus the above integral becomes

$$\begin{aligned}
&= \int (A_1 A_{1op} Q_{1opt} + A_1 A_{2op} Q_{2opt} + B_1)^* (A_1 A_{1op} Q_1) dw + \\
&\quad \int (A_1 A_{1op} Q_{1opt} + A_1 A_{2op} Q_{2opt} + B_1)^* (A_1 A_{2op} Q_2) dw \\
&= \int A_i^* (A_{1op} Q_{1opt} + A_{2op} Q_{2opt} + A_i^{-1} B_i)^* (A_1 A_{1op} Q_1) dw + \\
&\quad \int A_i^* (A_{1op} Q_{1opt} + A_{2op} Q_{2opt} + A_i^{-1} B_i)^* (A_1 A_{2op} Q_2) dw
\end{aligned}$$

but $A_i^* = A_i^{-1}$, hence

$$\begin{aligned}
&\int (A_1 Q_{1opt} + A_2 Q_{2opt} + B_1)^* (A_1 Q_1 + A_2 Q_2) dw \\
&= \int (A_{1op} Q_{1opt} + A_{2op} Q_{2opt} + A_i^{-1} B_i)^* (A_{1op} Q_1) dw + \\
&\quad \int (A_{1op} Q_{1opt} + A_{2op} Q_{2opt} + A_i^{-1} B_i)^* (A_{2op} Q_2) dw
\end{aligned}$$

Now, since A_{1op} and A_{2op} are minimum phase transfer functions, let

$$Q_{1opt} = -\frac{\pi_+(A_i^{-1} B_i)}{A_{1op}} \quad \text{and} \quad Q_{2opt} = 0 \quad (8.2.10)$$

where $\pi_+(\cdot)$ denotes stable projection. Thus replacing this, in the integral above yields

$$\begin{aligned}
&\int (A_1 Q_{1opt} + A_2 Q_{2opt} + B_1)^* (A_1 Q_1 + A_2 Q_2) dw \\
&= \int (\pi_-(A_i^{-1} B_i))^* (A_{1op} Q_1) dw + \int (\pi_-(A_i^{-1} B_i))^* (A_{2op} Q_2) dw \\
&= \int \pi_+(A_i^{-1} B_i) A_{1op} Q_1 dw + \int \pi_+(A_i^{-1} B_i) A_{2op} Q_2 dw
\end{aligned}$$

Since A_{1op} , Q_1 and A_{2op} , Q_2 are stable the integrands of the equation above are analytic in the RHP, therefore the above integrals are zero (by the Cauchy-Goursat Theorem). This shows that Q_{1opt} and Q_{2opt} given by Equation (8.2.10) are optimal. Notice that, in this way, the optimal Q is not unique, since one could have let $Q_{1opt} = 0$ and found an expression for Q_{2opt} .

Finding the Optimal Q_1 and Q_2 - Approach 2

So far, the problem of Equation 8.1.5 has been reduced to find the optimal $Q = [Q'_1 \quad Q'_2]$ of the cost function J see Equation (8.2.9),

$$J = \arg \inf_{Q'_1, Q'_2 \in \mathcal{K}^\infty} \|A_1 Q'_1 + A_2 Q'_2 + B_1\|_2^2$$

where $A_1 = \Lambda_1 N_{l1}$ and $A_2 = \Lambda_1 N_{l2}$. Clearly A_1 and A_2 differ only by the terms N_{l1} and N_{l2} , which, in the pendulum case differ only by a constant, say k . Since A_1 and A_2 differ only by a constant it can be included in either Q'_1 or Q'_2 and then A_1 and A_2 will be the same, say if $Q_1 = Q'_1$ and $Q_2 = kQ'_2$ then $A_1 = A_2 = A$. Thus

$$J = \inf_{Q_1, Q_2 \in \mathcal{H}^\infty} \|A(Q_1 + Q_2) + B_i\|_2^2 \quad (8.2.11)$$

where B_i is given by Equation (8.2.6) and $A = \Lambda_1 N_{l1}$. Let

$$Q_1 = \frac{Q_3 + Q_4}{2}$$

and

$$Q_2 = \frac{Q_3 - Q_4}{2}$$

or equivalently

$$Q_3 = Q_1 + Q_2 \quad \text{and} \quad Q_4 = Q_1 - Q_2 \quad (8.2.12)$$

Notice that Equation (8.2.11) reduces to an optimization problem of one variable when Equation (8.2.12) is used.

Now using Equation (8.2.12) it can be found how the sensitivity and complementary sensitivity depend on these Q 's. Recall that the sensitivity function at the input is given by Equation (8.2.1)

$$S_i = (V_r + QN_l)D_r$$

where, in this case, D_r and V_r are scalars (see Equations (3.3.18) and (3.3.20)), $Q = [Q'_1 \quad Q'_2]$ is a 1×2 vector and $N_l = [N_{l1} \quad N_{l2}]^T$ is a 2×1 vector. Since N_{l1} and N_{l2} differ only by a constant gives

$$\begin{aligned} S_i &= V_r D_r + [Q'_1 \quad Q'_2][N_{l1} \quad N_{l2}]^T D_r \\ &= V_r D_r + Q'_1 N_{l1} D_r + Q'_2 N_{l2} D_r \\ &= V_r D_r + Q_1 N_{l1} D_r + Q_2 N_{l1} D_r \\ &= V_r D_r + (Q_1 + Q_2) N_{l1} D_r \\ &= (V_r + Q_3 N_{l1}) D_r \end{aligned} \quad (8.2.13)$$

The complementary sensitivity function at the input is (see Equation (8.2.2))

$$T_i = (U_i - D_r Q) N_i$$

where, in this case, U_i and $Q = [Q_1 \quad Q_2]$ are 1×2 vectors, D_r is a scalar transfer function and N_i is a 2×1 vector. Again, since N_{i1} and N_{i2} differ only by a constant yields,

$$\begin{aligned} T_i &= U_i N_i - Q N_i D_r \\ &= U_i N_i - Q_3 N_{i1} D_r \end{aligned} \quad (8.2.14)$$

Now analyze the sensitivity and complementary sensitivity functions at the output. Recall from Equation (8.2.3) that the sensitivity at the output is

$$S_o = (V_i + N_r Q) D_i$$

where V_i and D_i are 2×2 matrices and N_r is a 2×1 vector. Here there is no way of simplifying S_o , therefore S_o is a function of Q_1 and Q_2 , or, similarly by Equation (8.2.12) it is a function of Q_3 and Q_4 . The same happens to the complementary sensitivity function (see Equation (8.2.4)),

$$T_o = N_r (U_r - Q D_i)$$

In summary, Q_3 can be found using Equations (8.2.11) and (8.2.12) and then Q_4 can be calculated by optimising S_o and T_o . Thus the minimization of the two-norm of the sensitivity and complementary sensitivity functions at the output is needed.

8.2.2 Optimal Q at the Output

Recall that

$$|W_s S_o|^2 + |W_t T_o|^2 = (W_s S_o)^* (W_s S_o) + (W_t T_o)^* (W_t T_o)$$

Using Equations (8.2.3) and (8.2.4) in the equation above yields

$$\begin{aligned} |W_s S_o|^2 + |W_t T_o|^2 &= (W_s V_i D_i + W_s N_r Q D_i)^* (W_s V_i D_i + W_s N_r Q D_i) \\ &\quad + (W_t N_r U_r - W_t N_r Q D_i)^* (W_t N_r U_r - W_t N_r Q D_i) \end{aligned}$$

Notice that N_r is a 2×1 matrix, U_r is 1×2 , Q is a 1×2 and D_l , V_l , W_s and W_t are 2×2 matrices (see Equations (3 3 17)-(3 3 22)) Thus

$$\begin{aligned}
|W_s S_o|^2 + |W_t T_o|^2 &= D_l^* V_l^* W_s^* W_s V_l D_l + D_l^* V_l^* W_s^* W_s N_r Q D_l \\
&\quad + D_l^* Q^* N_r^* W_s^* W_s V_l D_l + D_l^* Q^* N_r^* W_s^* W_s N_r Q D_l \\
&\quad + U_r^* N_r^* W_t^* W_t N_r U_r - U_r^* N_r^* W_t^* W_t N_r Q D_l \\
&\quad - D_l^* Q^* N_r^* W_t^* W_t N_r U_r + D_l^* Q^* N_r^* W_t^* W_t N_r Q D_l \\
&= D_l^* Q^* N_r^* (W_s^* W_s + W_t^* W_t) N_r Q D_l + D_l^* Q^* N_r^* (W_s^* W_s V_l D_l - W_t^* W_t N_r U_r) \\
&\quad + (D_l^* V_l^* W_s^* W_s - U_r^* N_r^* W_t^* W_t) N_r Q D_l + D_l^* V_l^* W_s^* W_s V_l D_l + U_r^* N_r^* W_t^* W_t N_r U_r
\end{aligned}$$

Let

$$\Lambda_1^* \Lambda_1 = N_r^* (W_s^* W_s + W_t^* W_t) N_r \quad (8 2 15)$$

Thus

$$\begin{aligned}
\|W_s S_o\|^2 + \|W_t T_o\|^2 &\quad (8 2 16) \\
&= D_l^* Q^* \Lambda_1^* \Lambda_1 Q D_l + (Q D_l)^* N_r^* (W_s^* W_s V_l D_l - W_t^* W_t N_r U_r) \\
&\quad + (W_s^* W_s V_l D_l - W_t^* W_t N_r U_r)^* N_r Q D_l + D_l^* V_l^* W_s^* W_s V_l D_l + U_r^* N_r^* W_t^* W_t N_r U_r
\end{aligned}$$

and completing the square

$$\begin{aligned}
&= (\Lambda_1 Q D_l + B)^* (\Lambda_1 Q D_l + B) + D_l^* V_l^* W_s^* W_s V_l D_l + U_r^* N_r^* W_t^* W_t N_r U_r \\
&\quad - [(\Lambda_1^*)^{-1} N_r^* (W_s^* W_s V_l D_l - W_t^* W_t N_r U_r)]^* [(\Lambda_1^*)^{-1} N_r^* (W_s^* W_s V_l D_l - W_t^* W_t N_r U_r)]
\end{aligned}$$

where

$$B_{12} = (\Lambda_1^*)^{-1} N_r^* (W_s^* W_s V_l D_l - W_t^* W_t N_r U_r) \quad (8 2 17)$$

Again since Q can only affect the first term in the previous equation, one Q that minimizes the 2-norm of this term needs to be chosen. Thus, the two block problem has been reduced to a one-block optimization problem. That is, the problem now is

$$Q_{opt} = \arg \inf_{Q \in \mathcal{H}^\infty} \|\Lambda_1 Q D_l + B_{12}\|_2^2 \quad (8 2 18)$$

where Λ_1 (a scalar) and B_{12} (a 1×2 vector) are given by Equations (8 2 15) and (8 2 17). In the equation above, some of the terms are vectors, so in order

to express this equation in terms of the scalar components of the vectors, let $Q = [Q_1 \ Q_2]$ and $B_{12} = [B_1 \ B_2]$ and, using the definition of the 2-norm, it can be shown that

$$\begin{aligned} \|\Lambda_1 Q D_l + B_{12}\|_2^2 &= \|\Lambda_1(Q_1 D_{l11} + Q_2 D_{l21}) + B_1\|_2^2 \\ &\quad + \|\Lambda_1(Q_1 D_{l12} + Q_2 D_{l22}) + B_2\|_2^2 \end{aligned} \quad (8.2.19)$$

From Section 8.2.1 it is known that Q_3 can be found by using Equations (8.2.11) and (8.2.12). Therefore Q_4 can be calculated using Equations (8.2.12) and (8.2.19) taking Q_3 as a constant. That is, following Equation (8.2.19), yields,

$$\begin{aligned} &[\Lambda_1(Q_1 D_{l11} + Q_2 D_{l21}) + B_1]^* [\Lambda_1(Q_1 D_{l11} + Q_2 D_{l21}) + B_1] \\ &+ [\Lambda_1(Q_1 D_{l12} + Q_2 D_{l22}) + B_2]^* [\Lambda_1(Q_1 D_{l12} + Q_2 D_{l22}) + B_2] \\ &= \left[\frac{1}{2} \Lambda_1 [(D_{l11} + D_{l21}) Q_3 + (D_{l11} - D_{l21}) Q_4] + B_1 \right]^* \\ &\quad \times \left[\frac{1}{2} \Lambda_1 [(D_{l11} + D_{l21}) Q_3 + (D_{l11} - D_{l21}) Q_4] + B_1 \right] \\ &\quad + \left[\frac{1}{2} \Lambda_1 [(D_{l12} + D_{l22}) Q_3 + (D_{l12} - D_{l22}) Q_4] + B_2 \right]^* \\ &\quad \times \left[\frac{1}{2} \Lambda_1 [(D_{l12} + D_{l22}) Q_3 + (D_{l12} - D_{l22}) Q_4] + B_2 \right] \\ &= \frac{1}{4} \Lambda_o^* \Lambda_o Q_4^* Q_4 + \frac{1}{2} \left(\frac{1}{2} \Lambda_1 (D_{l11} + D_{l21}) Q_3 + B_1 \right) \Lambda_1^* (D_{l11} - D_{l21})^* Q_4^* \\ &\quad + \frac{1}{2} \left(\frac{1}{2} \Lambda_1 (D_{l12} + D_{l22}) Q_3 + B_2 \right) \Lambda_1^* (D_{l12} - D_{l22})^* Q_4^* \\ &\quad + \frac{1}{2} \left[\left(\frac{1}{2} \Lambda_1 (D_{l11} + D_{l21}) Q_3 + B_1 \right) \Lambda_1^* (D_{l11} - D_{l21})^* \right]^* Q_4 \\ &\quad + \frac{1}{2} \left[\left(\frac{1}{2} \Lambda_1 (D_{l12} + D_{l22}) Q_3 + B_2 \right) \Lambda_1^* (D_{l12} - D_{l22})^* \right]^* Q_4 \\ &\quad + \left[\frac{1}{2} \Lambda_1 (D_{l11} + D_{l21}) Q_3 + B_1 \right]^* \left[\frac{1}{2} \Lambda_1 (D_{l11} + D_{l21}) Q_3 + B_1 \right] \\ &\quad + \left[\frac{1}{2} \Lambda_1 (D_{l12} + D_{l22}) Q_3 + B_2 \right]^* \left[\frac{1}{2} \Lambda_1 (D_{l12} + D_{l22}) Q_3 + B_2 \right] \end{aligned}$$

where

$$\Lambda_o^* \Lambda_o = \Lambda_1^* \Lambda_1 [(D_{l11} - D_{l21})^* (D_{l11} - D_{l21}) + (D_{l12} - D_{l22})^* (D_{l12} - D_{l22})] \quad (8.2.20)$$

Now let

$$B_o = (\Lambda_o^*)^{-1} \left[\left(\frac{1}{2} \Lambda_1 (D_{l11} + D_{l21}) Q_3 + B_1 \right) \Lambda_1^* (D_{l11} - D_{l21})^* + \left(\frac{1}{2} \Lambda_1 (D_{l12} + D_{l22}) Q_3 + B_2 \right) \Lambda_1^* (D_{l12} - D_{l22})^* \right] \quad (8.2.21)$$

and completing the square in Q_4 yields

$$\begin{aligned} &= \left[\frac{1}{2} \Lambda_o Q_4 + B_o \right]^* \left[\frac{1}{2} \Lambda_o Q_4 + B_o \right] \\ &\quad + \left[\frac{1}{2} \Lambda_1 (D_{l11} + D_{l21}) Q_3 + B_1 \right]^* \left[\frac{1}{2} \Lambda_1 (D_{l11} + D_{l21}) Q_3 + B_1 \right] \\ &\quad + \left[\frac{1}{2} \Lambda_1 (D_{l12} + D_{l22}) Q_3 + B_2 \right]^* \left[\frac{1}{2} \Lambda_1 (D_{l12} + D_{l22}) Q_3 + B_2 \right] - B_o^* B_o \end{aligned}$$

Thus the optimal Q_4 can be found from

$$Q_{4opt} = \arg \inf_{Q_4 \in \mathcal{H}^\infty} \left\| \frac{1}{2} \Lambda_o Q_4 + B_o \right\|_2^2 \quad (8.2.22)$$

where Λ_o and B_o are given by Equations (8.2.20) and (8.2.21), respectively. Notice that after finding the optimal Q_3 and Q_4 , Q_1 and Q_2 have to be found and then the substitution $Q_2' = Q_2/k$ needs to be done.

In summary, using approach 2 (Section 8.2.1), one can find the optimal Q_{opt} from the following the steps

- 1 Find the constant k by which N_{l1} and N_{l2} differ. In this case,

$$Q_2' N_{l2} = Q_2' \frac{-k_2}{k_1} N_{l2} \frac{-k_1}{k_2} = Q_2 N_{l1}$$

where

$$Q_2 = Q_2' k \quad \text{and} \quad k = \frac{-k_2}{k_1} \quad (8.2.23)$$

- 2 Let $Q_3 = Q_1 + Q_2$ and $Q_4 = Q_1 - Q_2$ and find the optimum (at the input of the system) of Equation (8.2.11), that is find the optimal Q_3 of

$$J = \inf_{Q_1, Q_2 \in \mathcal{H}^\infty} \|A Q_3 + B_i\|_2^2$$

which is

$$Q_{3opt} = -\frac{\pi_+(A_{inner}^{-1}B_1)}{A_{outer}} \quad (8.2.24)$$

where

$$B_1 = \left(\frac{D_r^*(W_{s1}^*W_{s1}D_rV_r - W_{t1}^*W_{t1}U_tN_t)}{\Lambda_1^*} \right),$$

$$\Lambda_1^*\Lambda_1 = D_r^*D_r(W_{s1}^*W_{s1} + W_{t1}^*W_{t1})$$

and A_{inner} and A_{outer} are the inner and outer part of $A = \Lambda_1 N_{11}$

3 Find the optimum of Equation (8.2.22), that is

$$Q_{4opt} = -\frac{\pi_+(B_o)}{\frac{1}{2}\Lambda_o} \quad (8.2.25)$$

where

$$B_o = (\Lambda_o^*)^{-1} \left[\left(\frac{1}{2}\Lambda_1(D_{l11} + D_{l21})Q_3 + B_1 \right) \Lambda_1^*(D_{l11} - D_{l21})^* \right. \\ \left. + \left(\frac{1}{2}\Lambda_1(D_{l12} + D_{l22})Q_3 + B_2 \right) \Lambda_1^*(D_{l12} - D_{l22})^* \right],$$

$$\Lambda_o^*\Lambda_o = \Lambda_1^*\Lambda_1 [(D_{l11} - D_{l21})^*(D_{l11} - D_{l21}) + (D_{l12} - D_{l22})^*(D_{l12} - D_{l22})]$$

$$B_{12} = [B_1 \quad B_2] = (\Lambda_1^*)^{-1} N_r^*(W_s^*W_s V_l D_l - W_t^*W_t N_r U_r)$$

and

$$\Lambda_1^*\Lambda_1 = N_r^*(W_s^*W_s + W_t^*W_t)N_r$$

4 Find

$$Q_1 = \frac{Q_3 + Q_4}{2} \quad \text{and} \quad Q_2 = \frac{Q_3 - Q_4}{2}$$

5 Find $Q_{opt} = [Q'_1 \quad Q'_2]$ Recall that $Q'_1 = Q_1$ and from Equation (8.2.23) find

$$Q'_2 = \frac{-k_1}{k_2} Q_2$$

Remark 8.2.1 *This approach has the advantage that the algorithm is based on scalar transfer functions, rather than transfer matrices. But it has the disadvantage that two sets of weights are needed, one for the input (W_{s1} and W_{t1}) and one for the output (W_s and W_t). The algorithm was implemented in Matlab, but no appropriate weights were found. For all weights that were tried, the peaks in the maximum singular values of S_o and T_o were very large, see Figure 8.6*

Following the above remark, it is obvious that a new approach is needed

8.3 Finding the \mathcal{H}_2 Controller - Approach 2

In this section the optimization problem given by Equation (8.2.18) is studied. To do so, some further definitions are needed and are stated in this section.

Definition 8.3.1 (All-pass Function) A transfer function matrix, $B(s)$, is called all-pass if $B(s)B(s)^* = I$, which implies that all singular values of $B(j\omega)$ are equal to one.

The next theorem is a result given in [11] and the proof is given there. It uses the definitions given in Section 2.3.2.

Theorem 8.3.1 (Input Factorization of RHP-zeros) A system $G(s)$ containing N_z RHP-zeros z_i , with input directions \hat{u}_{z_i} and \hat{x}_{z_i} defined by

$$\begin{bmatrix} A - zI & B_{i-1} \\ C & D \end{bmatrix} \begin{bmatrix} \hat{x}_{z_i} \\ \hat{u}_{z_i} \end{bmatrix} = 0 \quad (8.3.1)$$

can be factorized in a minimum phase system $G_I(s)$ and an all-pass function $B_I(s)$ which is stable and has zeros coinciding with the RHP-zeros of $G(s)$, $G(s) = G_I(s)B_I(s)$ where

$$G_I(s) = C(sI - A)^{-1}B' + D \quad (8.3.2)$$

The modified input matrix B' can be calculated by applying the following formula repeatedly for $i = 1, \dots, N_z$

$$B_i = B_{i-1} - 2\text{Re}(z_i)\hat{x}_{z_i}\hat{u}_{z_i}^* \quad (8.3.3)$$

with $B_0 = B$ and $B' = B_{N_z}$. The all-pass function $B_I(s)$ is given by

$$\begin{aligned} B_I(s) &= B_{N_z}(s)B_{N_z-1}(s) \dots B_1(s) \\ &= \prod_{i=0}^{N_z-1} B_{i+1}(s) \end{aligned} \quad (8.3.4)$$

where

$$B_i(s) = I - \frac{2\text{Re}(z_i)}{s + \bar{z}_i}\hat{u}_{z_i}\hat{u}_{z_i}^* \quad (8.3.5)$$

Note that a non-minimum phase transfer function also admits an output factorization analogous to the input factorization and it can be expressed in a similar way. For more information about multivariable poles and zeros and factorization of RHP zeros and poles refer to [24], [11], [12], [27] and/or [28].

Now it is possible to prove the next theorem which allows us to find the optimal solution of the optimization problem given by Equation (8.2.18).

Theorem 8.3.2 *Suppose that A and B are strictly proper stable transfer function matrices, where A is 2×2 and B is 1×2 . Then*

$$\arg \inf_{Q \in \mathcal{H}_{\infty}^{1 \times 2}} \|QA + B\|_2^2 = [-\pi_+(BA_1^*)_{(1)} \quad -\pi_+(BA_1^*)_{(2)}] A_o^{-1}$$

where A_i and A_o are the all-pass and minimum phase factors found at the input of A , respectively (see Theorem 8.3.1). That is A can be factored at the input as $A = A_o A_i$ where A_i is an all-pass function and A_o is a minimum phase function. $\pi_+(BA_1^*)_{(i)}$ denotes the stable projection of the i -th element of BA_1^* .

Proof From the Projection Theorem (see Luenberger [26, §3.3]) it is known that Q_{opt} is optimum if and only if $(Q_{opt}A + B)$ is perpendicular to the space generated by QA . That is

$$(Q_{opt}A + B) \perp QA \quad \forall Q \in \mathcal{H}_{\infty}^{1 \times 2}$$

Thus, it is needed to show that

$$\langle Q_{opt}A + B, QA \rangle = \frac{1}{2\pi} \int \text{Tr} \{ (Q_{opt}A + B)(QA)^* \} dw = 0, \quad \forall Q \in \mathcal{H}_{\infty}^{1 \times 2}$$

where $\langle \cdot, \cdot \rangle$, $\text{Tr} \{ \cdot \}$ and $(\cdot)^*$ denote inner product, trace and conjugate transpose, respectively.

Since A is stable, it can be factored as $A = A_o A_i$ (see Theorem 8.3.1) where A_i is an all-pass factor (i.e. $A_i A_i^* = I$) and A_o is a minimum phase factor (i.e. no transmission zeros on the ORHP). Hence

$$\begin{aligned} \int \text{Tr} \{ (Q_{opt}A + B)(QA)^* \} dw &= \int \text{Tr} \{ (Q_{opt}A_o A_i + B)A_i^* A_o^* Q^* \} dw \\ &= \int \text{Tr} \{ (Q_{opt}A_o + BA_i^*)A_o^* Q^* \} dw \end{aligned} \tag{8.3.6}$$

Now let

$$Q_{opt} = [-\pi_+(BA_1^*)_{(1)} \quad -\pi_+(BA_1^*)_{(2)}] A_o^{-1} \quad (8.3.7)$$

and substituting into Equation (8.3.6) yields

$$\int \text{Tr} \{ (Q_{opt}A + B)(QA)^* \} dw = \int \text{Tr} \{ [\pi_-(BA_1^*)_{(1)} \quad \pi_-(BA_1^*)_{(2)}] A_o^* Q^* \} dw \quad (8.3.8)$$

where $\pi_-(\cdot)_{(i)}$ denotes anti-stable projection of the i -th element of the respective matrix. Since $[\pi_-(BA_1^*)_{(1)} \quad \pi_-(BA_1^*)_{(2)}]$, A_o^* and Q^* are all anti-stable, the integrand of Equation (8.3.8) is analytic in the CLHP and it is known, by the Cauchy-Goursat Theorem (see Brown and Churchill [29, ch 4]), that this integral is zero. Thus, it has been proven that Q_{opt} given by Equation (8.3.7) is optimal. \square

Remark 8.3.1 Notice that, in the pendulum case, $A = \Lambda_1 D_1$, thus the existence of the inverse of A_o is guaranteed by the fact that the transfer matrix D_1 has an inverse and Λ_1 is a scalar transfer function. Also, notice that D_1 has a zero at the origin which does not allow to apply the theorem directly, but the poles and zeros of the plant can be shifted into the RHP in order to be able to use the theorem.

Remark 8.3.2 This theorem can easily be extended to higher order matrices provided that the square matrix A has an inverse.

The $n \times n$ case is explained next. First notice that in the $n \times n$ case, all the matrices involved in Equation 8.2.18 have dimension $n \times n$. Therefore, Λ_1 is no longer a scalar. Also, recall that Λ_1 is the solution to a spectral factorization (see Equation (8.2.15)). Hence, Λ_1 is an $n \times n$ minimum phase transfer matrix. Thus the theorem is as follows:

Theorem 8.3.3 Suppose that $\Lambda Q A$ and B are strictly proper stable transfer function matrices, where Λ , Q , A and B are $n \times n$ matrices. Moreover, assume that Λ is minimum phase. Then

$$\arg \inf_{Q \in \mathcal{H}_\infty^{n \times n}} \|\Lambda Q A + B\|_2^2 = \Lambda^{-1} [-\pi_+(BA_1^*)_{(j,k)}]_{n \times n} A_o^{-1} \quad (8.3.9)$$

where A_1 and A_o are the all-pass and minimum phase factors found at the input of A , respectively (see Theorem 8.3.1). That is, A can be factored at the input as

$A = A_o A_i$ where A_i is an all-pass function and A_o is a minimum phase function $[-\pi_+(BA_i^*)]_{n \times n}$ is an $n \times n$ matrix whose element (j, k) with $j = 1, \dots, n$ and $k = 1, \dots, n$ is the stable projection of the element (j, k) of the matrix BA_i^*

Proof From the Projection Theorem (see Luenberger [26, §3.3]) it is known that Q_{opt} is optimum if and only if $(\Lambda Q_{opt} A + B)$ is perpendicular to the space generated by $\Lambda Q A$. That is,

$$(\Lambda Q_{opt} A + B) \perp \Lambda Q A \quad \forall Q \in \mathcal{H}_{\infty}^{n \times n}$$

Thus, it is needed to show that

$$\langle \Lambda Q_{opt} A + B, \Lambda Q A \rangle = \frac{1}{2\pi} \int Tr \{ (\Lambda Q_{opt} A + B)(\Lambda Q A)^* \} dw = 0 \quad \forall Q \in \mathcal{H}_{\infty}^{n \times n}$$

Since A is stable, it can be factored as $A = A_o A_i$ (see Theorem(8.3.1)) where A_i is an all-pass factor (i.e. $A_i A_i^* = I$) and A_o is a minimum phase factor (i.e. no transmission zeros on the ORHP). Hence

$$\begin{aligned} \int Tr \{ (\Lambda Q_{opt} A + B)(\Lambda Q A)^* \} dw &= \int Tr \{ (\Lambda Q_{opt} A_o A_i + B) A_i^* A_o^* Q^* \Lambda^* \} dw \\ &= \int Tr \{ (\Lambda Q_{opt} A_o + B A_i^*) A_o^* Q^* \Lambda^* \} dw \end{aligned} \quad (8.3.10)$$

Now, let

$$Q_{opt} = \Lambda^{-1} [-\pi_+(BA_i^*)]_{n \times n} A_o^{-1} \quad (8.3.11)$$

and substituting into Equation (8.3.10) gives

$$\int Tr \{ (\Lambda Q_{opt} A + B)(\Lambda Q A)^* \} dw = \int Tr \left\{ [\pi_-(BA_i^*)]_{n \times n} A_o^* Q^* \Lambda^* \right\} dw \quad (8.3.12)$$

where $[\pi_-(BA_i^*)]_{n \times n}$ is an $n \times n$ matrix whose element (j, k) with $j = 1, \dots, n$ and $k = 1, \dots, n$ is the anti-stable projection of the element (j, k) of the matrix BA_i^* . Since $[\pi_-(BA_i^*)]_{n \times n}$, Λ^* , A_o^* and Q^* are all anti-stable, the integrand of Equation (8.3.12) is analytic in the CLHP and by the Cauchy-Goursat Theorem (see Brown and Churchill [29, ch. 4]) it is known that this integral is zero. Thus, it has been proven that Q_{opt} given by Equation (8.3.9) is optimum. \square

8.4 \mathcal{H}_2 Control of the Inverted Pendulum

As explained in the previous sections, the approach is to solve the problem given by Equation (8.1.5), which was shown to be equivalent to solving the problem of Equation (8.2.18), which is shown next

$$Q_{opt} = \arg \inf_{Q \in \mathcal{H}^\infty} \|\Lambda_1 Q D_l + B_{12}\|_2^2$$

where

$$\Lambda_1^* \Lambda_1 = N_r^* (W_s^* W_s + W_t^* W_t) N_r$$

$$B_{12} = (\Lambda_1^*)^{-1} N_r^* (W_s^* W_s V_l D_l - W_t^* W_t N_r U_r)$$

and N_r , D_l , V_l and U_r are given in Section 3.3.4. The problem can be extended to include a weight on $R = K(I + GK)^{-1}$ so that it covers the same weighted mixed sensitivity problem as the Robust Control Toolbox for Matlab [30]. To do so, just change the last two equations to

$$\Lambda_1^* \Lambda_1 = N_r^* (W_s^* W_s + W_t^* W_t) N_r + D_r^* W_r^* W_r D_r \quad (8.4.1)$$

$$B_{12} = (\Lambda_1^*)^{-1} [N_r^* (W_s^* W_s V_l D_l - W_t^* W_t N_r U_r) - D_r^* W_r^* W_r U_l D_l] \quad (8.4.2)$$

Thus, the algorithm to find the \mathcal{H}_2 -optimal controller after choosing the appropriate weights can be summarized as

Step 1 Find the solution of the generalised Bezout equation using Theorem 3.2.1

Step 2 Find the inner-outer factorization of $A = \Lambda_1 D_l$ using Theorem 8.3.1

Step 3 Find the optimal Q using Theorem 8.3.2, Equation (8.3.7)

Step 4 Find the optimal controller, K using Theorem 3.0.1

The algorithm was implemented and tested in Matlab. The important question is how to choose the weights W_s and W_t , which is not a trivial task. They are usually chosen based on experience and knowledge of the plant to be controlled.

Sometimes it is a trial and error process. For the pendulum system many sets of weights were tried. The best choices obtained are shown next.

$$W_s = \begin{pmatrix} \frac{(s+50)}{(s+0.1)} & 0 \\ 0 & \frac{10(s+100)}{(s+10)} \end{pmatrix} \quad W_t = \begin{pmatrix} \frac{s}{10000} & 0 \\ 0 & \frac{s}{1000} \end{pmatrix} \quad (8.4.3)$$

The resulting sensitivity and complementary sensitivity functions are shown in Figures 8.2, 8.3, 8.4 and 8.5, respectively.

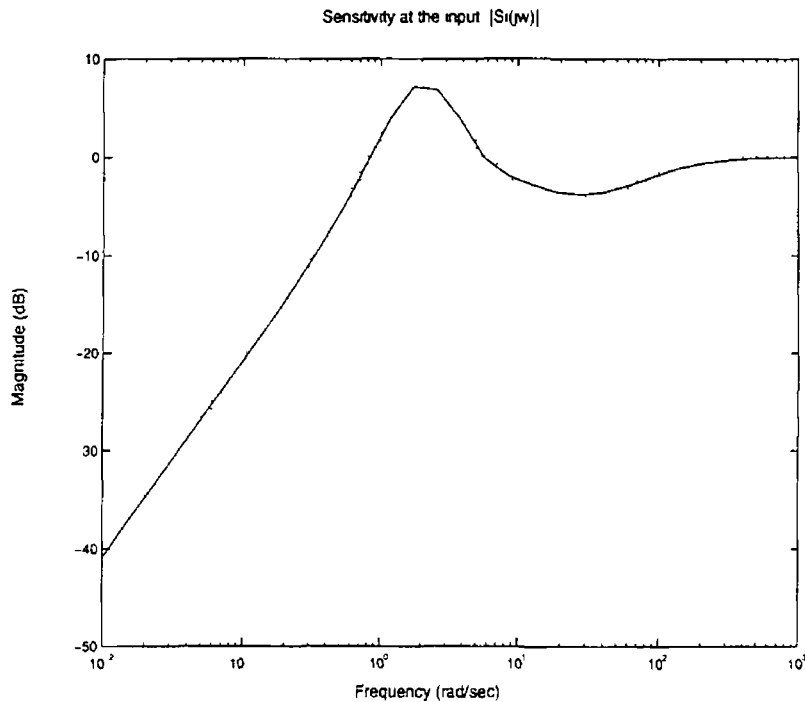


Figure 8.2 Sensitivity function at the input, $|S_1(j\omega)|$

From those figures, note the peaks of the components of the matrix functions. Also, notice that disturbances in a range of about 0.1 to 10 rad/sec applied to the pendulum-angle have a considerable effect on the cart position, since this disturbance is amplified due to the high peak of the component (1,2) of Figure 8.4 at those frequencies. Moreover, a disturbance on the cart of any frequency is attenuated due to the low gain of the element (2,1), making no significant effect on the angle position. From physical considerations, it can be argued that interactions have to exist in this system, since a disturbance on either the cart or the pendulum has to affect the state of the other component. The ideal is to have

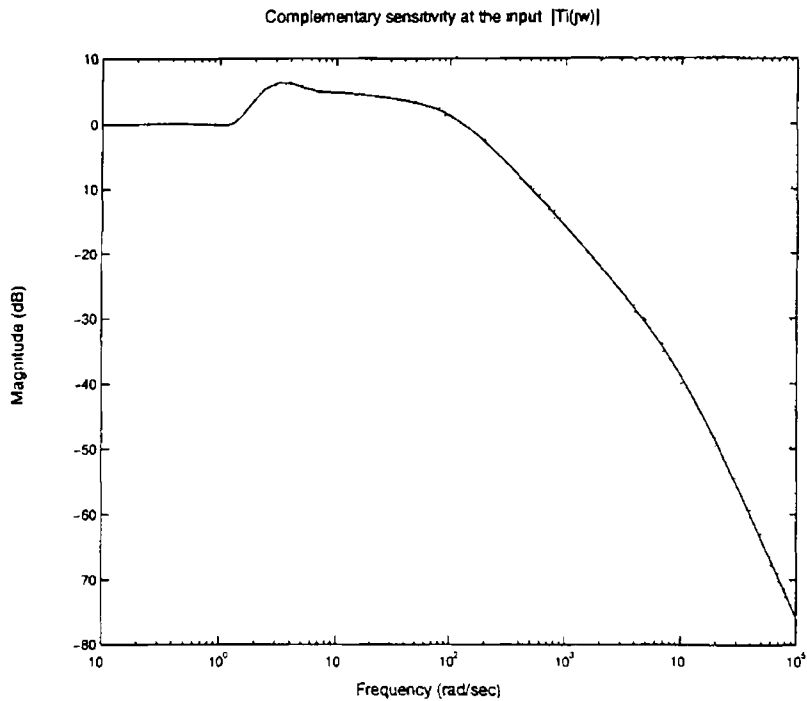


Figure 8.3 Complementary sensitivity function at the input $|T_i(j\omega)|$

a balance between the off-diagonal elements since they represent the interaction inherent in the system. It is important to be aware that these peaks cannot be avoided at all due to limitations imposed by the RHP poles of the plant.

Figures 8.6 and 8.7 show the singular values of S_o and T_o and the step response of the simulation with the linearized plant model, respectively.

8.5 Discussion

As can be seen in this chapter, dealing with MIMO systems is not a trivial task. As is known, there are many different aspects of the control design problem that have to be taken into account. Also there are many new concepts (compared to the theory for SISO systems) that have to be used and some others that have to be further developed. One area that is still under research is the limitations that exist in the design of multivariable control systems.

The pendulum system is not an easy system to control. As shown in Chapters 5

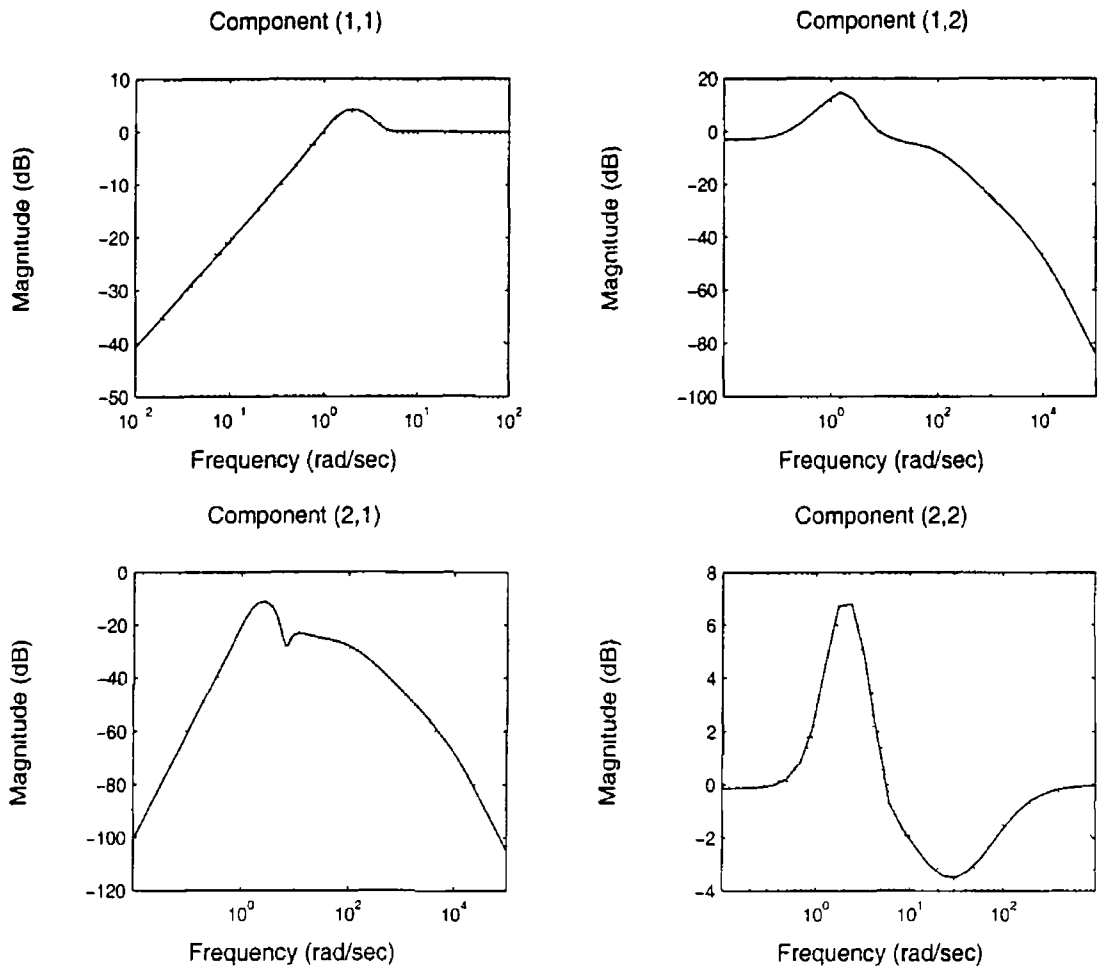


Figure 8.4 Sensitivity function, $|[(S_o(j\omega))_{i,j}]|$

and 9, there are fundamental limitations that apply, especially the ones imposed by RHP poles. These limitations make controller design much more challenging. In this case, they make the selection of weights, i.e. W_s and W_t , more difficult. The right selection of weights is a difficult and tricky part of this design process. Despite the fact that nowadays there is more literature with guidelines on how to choose the weights, [31], [12], [32], this part of the design is often done as a trial and error process. When using the approaches presented here and the \mathcal{H}_2 approach of the Robust Control Toolbox many sets of weights were tried. It was noticed that a change in one of the elements of the weights changes the shape of the overall S and T . This also shows that the selection of weights for multivariable systems is more challenging than the selection of weights for SISO systems.

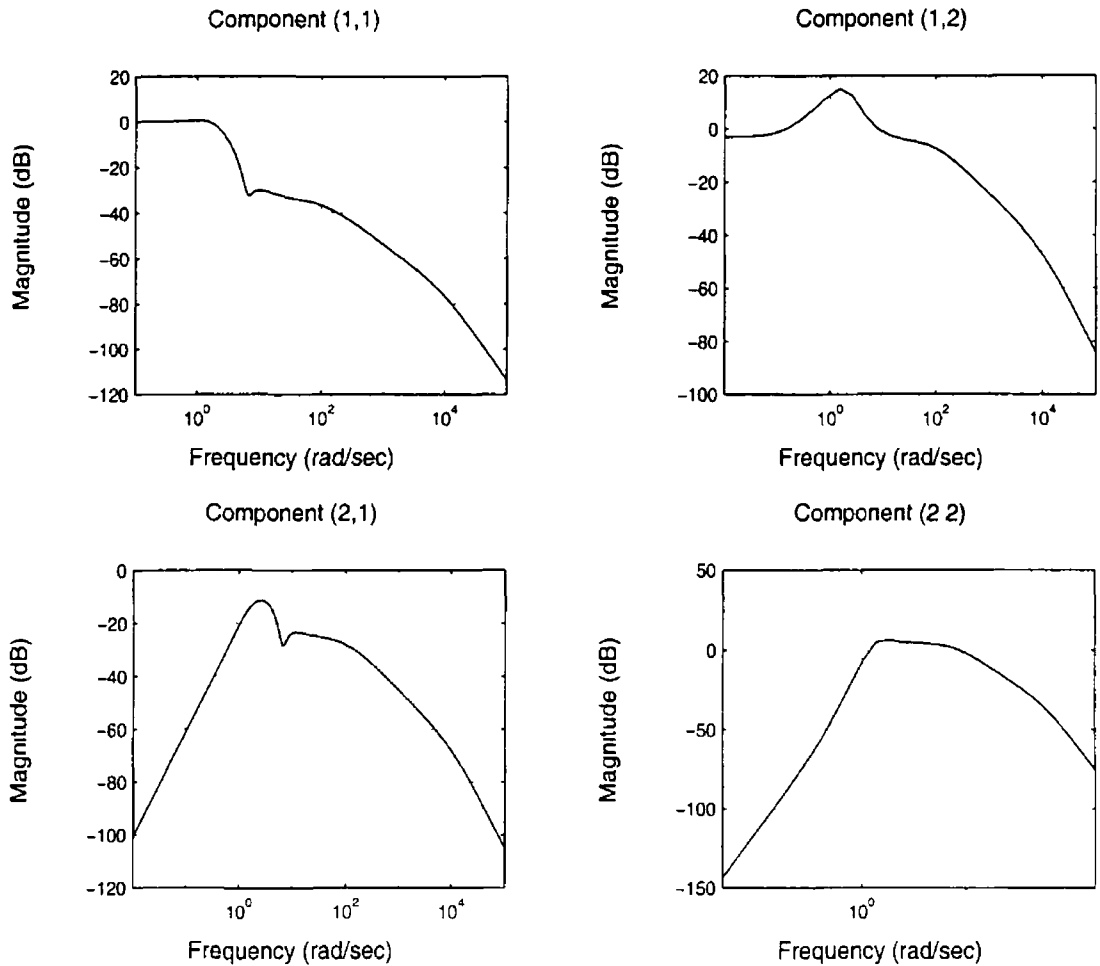


Figure 8.5 Complementary sensitivity function, $|(T_o(j\omega))_{ij}|$

Freudenberg and Looze [31] state that “the real unanswered question is how effective the weighting functions will prove to be as design parameters.” Here, the designed controller with the weights of Equation (8.4.3) was implemented as well as many other controllers obtained with different sets of weights, but even though stability of the real system was achieved with most of the controllers, the performance was not as good as expected. The main reason for this lack of quality performance was the high uncertainty present in this system, since some non-linearities such as saturation and friction, among others, were not taken into account during the modeling process. One of the drawbacks of \mathcal{H}_2 is that it does not deal with large uncertainty compared with \mathcal{H}_∞ control as is mentioned in [33] and [30]. In [33] an application of \mathcal{H}_2 to a dynamically tuned gyroscope (DTG) is presented. The reason why the authors choose \mathcal{H}_2 is that “the \mathcal{H}_∞

methodology is suitable when the uncertainties of the plant are large, and the \mathcal{H}_2 methodology is suitable when the uncertainties are small and the performances are more important” “Because a DTG is a very precise and expensive instrument, the model parameters of the DTG are precisely measured and determined, thus the model uncertainties are very small” This paper is also a proof that \mathcal{H}_2 is still an important tool for control system design

The algorithm presented in Section 8.2 has the disadvantage that two different sets of weights are needed, one for S and T at the input of the plant and the other set for S and T at the output. Indeed, simulations showed that the selection of weights is “easier” with the algorithm of Section 8.3. One disadvantage of the algorithm presented in Section 8.3 is in terms of its implementation. For large systems (i.e. many inputs and/or outputs) or for systems with high order the implementation is difficult. In fact, this algorithm was implemented in Matlab for the pendulum system and a lot of problems were encountered mainly because of round-off errors and imprecision in some functions.

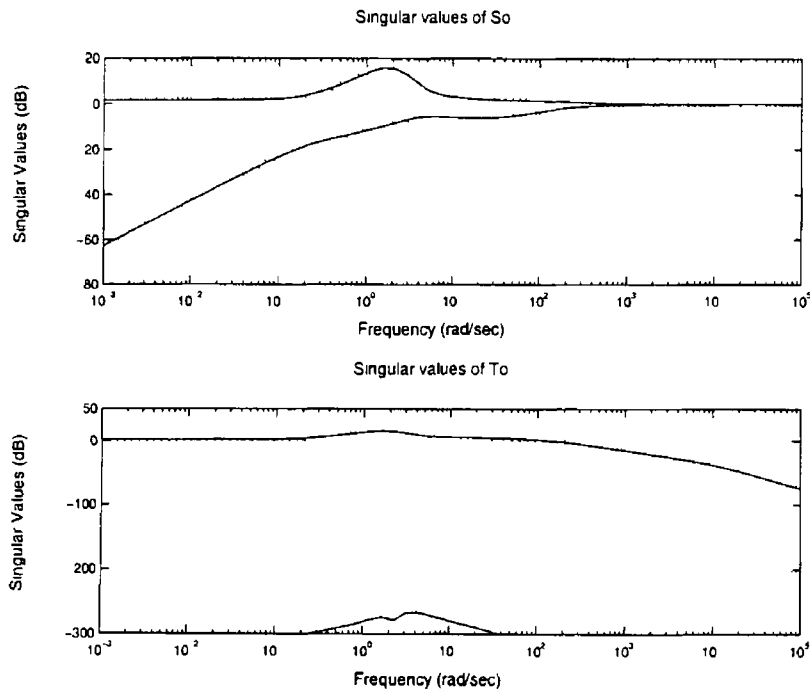


Figure 8.6 Singular values of S_0 and T_0

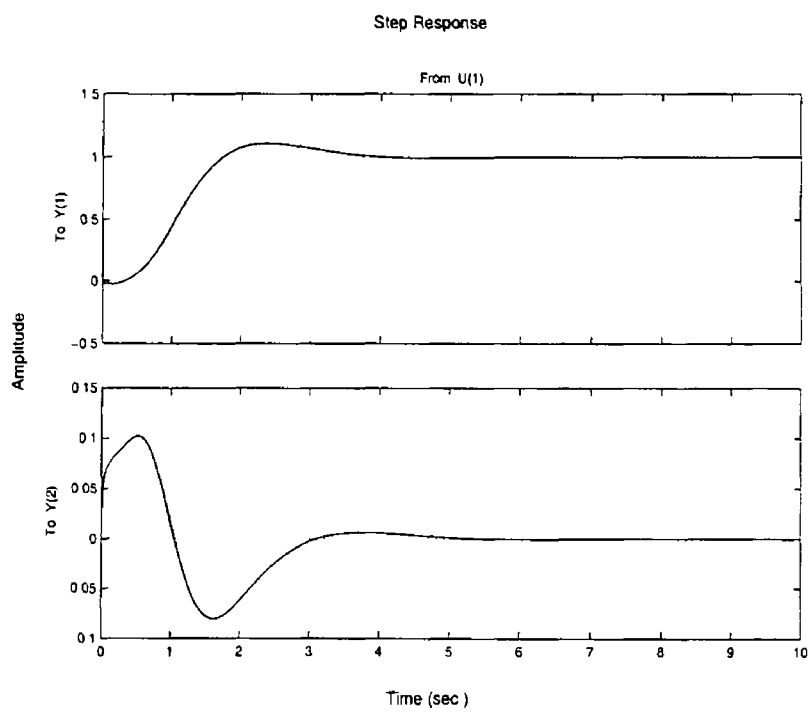


Figure 8 7 Step response of the system $d(t)$ (upper plot) and $\phi(t)$ (lower plot)

Chapter 9

Fundamental Limitations on Control - MIMO case

During the last two decades much attention has been paid to understand the limitations inherent in the design of control systems in both the frequency and the time domain. For some results see [18] [19] [20], [21], [27], [17], [34] and [35]. Nowadays, the trade-offs and design limitations for SISO systems are well understood and the theory is well established. However, despite much progress design limitations for MIMO systems are less well understood compared with their counterparts for SISO systems.

Many design limitations for multivariable systems are phrased as integral inequalities that must be satisfied by the sensitivity and complementary sensitivity functions. Some of the results are either very conservative or not easy to apply since some of the inequalities do not relate S and T directly they are usually given in terms of their logarithms. Some other inequalities involve the singular values of S and T , which have drawbacks in that it may be difficult to relate the singular values to properties of the system under consideration. Another important disadvantage is that some of the inequalities are valid only for square plants. In the paper by Woodyatt et al [34], limitations for a single-input two-output systems are analyzed. It gives inequalities that the complementary sensitivity function has to obey. But, again, they are in terms of the logarithm of T . Also some inequalities concerning elements of T are given in the same paper.

In the next section, the MIMO version of the interpolation constraints stated in Section 5.1 are given

9.1 Interpolation Constraints

The results given in this section have to be obeyed by S and T in order to guarantee stability of the closed-loop system of the pendulum and in general of any system. Only the effect of RHP poles is studied here, since the pendulum does not have RHP zeros, but the result can easily be extended to non-minimum phase zeros by using a similar procedure.

Assume that the plant G and the controller K are represented by a coprime factorization. For ease, the left-coprime factorization given in Theorem 3.0.1 is used, that is $G = D_l^{-1}N_l$. It is obvious that the RHP poles of G are the RHP zeros of D_l . Therefore, there exists at least one vector from the right nullspace and one vector from the left nullspace of D_l such that

$$u_p^* D(p) = 0 \quad D(p) y_p = 0$$

where p is a RHP pole of G . Following Equation (8.2.3) (i.e. $S_o = (V_l + N_r Q) D_l$) and using the equations above, it is easy to show that

$$S_o(p) y_p = 0 \tag{9.1.1}$$

and using the identity $S + T = I$ yields

$$\begin{aligned} (I - T_o(p)) y_p &= 0 \\ \Rightarrow T_o(p) y_p &= y_p \end{aligned} \tag{9.1.2}$$

It can easily be proved that the input direction of the RHP zero of D_l , y_p , is the output direction of the pole at p of G . Thus, for MIMO systems, the interpolation constraints on S_o and T_o not only depend on the location of the pole (or zero) but also on its direction.

Next, limitations inherent in the pendulum system in terms of the individual elements of S and T are studied since they give more insight about the limitations

of the overall system. They also give guidelines on how to choose the weighting functions W_s and W_t , see Chapter 8.

9.2 Limitations in Terms of the Elements of S and T

Here, the limitations inherent in the pendulum system are studied. First, define the plant G and one possible stabilizing controller K in terms of their elements that is $G = (g_1 \ g_2)^T$ and $K = (k_1 \ k_2)$ where g_1 , g_2 , k_1 and k_2 are scalar transfer functions. Notice that they are functions of the complex variable s . The dependence on (s) of transfer functions is not shown explicitly. Thus, the loop gain L , at the output is

$$L_o = GK = \begin{pmatrix} g_1 k_1 & g_1 k_2 \\ g_2 k_1 & g_2 k_2 \end{pmatrix} \quad (9.2.1)$$

Thus, it can be shown, using simple algebra that

$$S_o = (I + L_o)^{-1} = \frac{1}{1 + g_1 k_1 + g_2 k_2} \begin{pmatrix} 1 + g_2 k_2 & -g_1 k_2 \\ -g_2 k_1 & 1 + g_1 k_1 \end{pmatrix} \quad (9.2.2)$$

and

$$\begin{aligned} T_o &= I - S_o = \frac{1}{1 + g_1 k_1 + g_2 k_2} \begin{pmatrix} g_1 k_1 & g_1 k_2 \\ g_2 k_1 & g_2 k_2 \end{pmatrix} \\ &= \frac{g_1 k_1}{1 + g_1 k_1 + g_2 k_2} \begin{pmatrix} 1 & \frac{k_2}{k_1} \\ \frac{g_2}{g_1} & \frac{g_2 k_2}{g_1 k_1} \end{pmatrix} \end{aligned} \quad (9.2.3)$$

To understand the limitations on S and T , these functions can be rewritten in terms of the numerator and denominator of the scalar transfer functions involved. The result is as follows

$$S_o = \frac{1}{\text{den}} \begin{pmatrix} (d_{g_2} d_{k_2} + n_{g_2} n_{k_2}) d_{g_1} d_{k_1} & -n_{g_1} n_{k_2} d_{g_2} d_{k_1} \\ -n_{g_2} n_{k_1} d_{g_1} d_{k_2} & (d_{g_1} d_{k_1} + n_{g_1} n_{k_1}) d_{g_2} d_{k_2} \end{pmatrix} \quad (9.2.4)$$

and

$$T_o = \frac{1}{\text{den}} \begin{pmatrix} n_{g1}n_{k1}d_{g2}d_{k2} & n_{g1}n_{k2}d_{g2}d_{k1} \\ n_{g2}n_{k1}d_{g1}d_{k2} & n_{g2}n_{k2}d_{g1}d_{k1} \end{pmatrix} \quad (9.2.5)$$

and

$$\text{den} = d_{g1}d_{g2}d_{k1}d_{k2} + n_{g2}n_{k2}d_{g1}d_{k1} + n_{g1}n_{k1}d_{g2}d_{k2} \quad (9.2.6)$$

where n_{g_i} and d_{g_i} are the numerator and denominator, respectively, of g_i . Similarly, n_{k_i} and d_{k_i} are the numerator and denominator, respectively, of k_i .

Recall Equations (2.1.24) and (2.1.25). Then, the following conclusions can be drawn from Equations (9.2.4) and (9.2.5)

- First, notice that den is a Hurwitz polynomial (i.e. no roots in the CRHP)
- The element (1,1) of S_o has a zero at the origin as is usually the case, due to d_{g1}
- The magnitude of the off-diagonal elements of S_o and T_o are the same
- The element (2,2) of S_o does not necessarily have a zero at the origin, which makes more difficult the attenuation of low-frequency disturbances on this channel
- The element (1,1) of T_o and the element (1,2) of S_o and T_o have at least one RHP zero. Hence following a similar procedure to that of [17, §4] it can be shown that these elements have an upper bound on its achievable bandwidth
- Because of this upper bound on the element (1,2) and the fact that it does not have any zero at the origin, it can be concluded that there is a range of frequencies for which S_{o12} and T_{o12} are greater than or equal to one. It follows that interactions on this channel cannot be avoided, which from a physical point of view is clear, since a deflection of the pendulum has to affect the position of the cart
- The element (2,2) of T_o has two zeros at the origin, due to n_{g2} and d_{g1}
- T_o is a singular transfer matrix (see Equation (9.2.3)), which means that the minimum singular value is zero (up to numerical precision in Figure 8.6)
- A change on either the numerator or denominator of one of the elements of the controller will affect several elements of S_o and T_o . This makes the selection of weights more difficult since one change in one of the elements of the weights will affect the overall S_o and T_o .

Also notice that the response of the system $Y(s)$ to an input $R(s)$ is given by the complementary sensitivity function, thus

$$\begin{pmatrix} y_1 \\ y_2 \end{pmatrix} = \begin{pmatrix} T_{o11} & T_{o12} \\ T_{o21} & T_{o22} \end{pmatrix} \begin{pmatrix} r_1 \\ 0 \end{pmatrix} = \begin{pmatrix} T_{o11} \\ T_{o21} \end{pmatrix} r_1 \quad (9.2.7)$$

Hence, the response of the system (cart and angle position) to a command input $r(s)$ is determined by the first column of T_o .

9.3 Input vs Output Properties

The algorithm given in Section 8.2 is based on an optimization at the plant input and output. Here, a discussion of the input and output properties is given in order to understand better the implications of such optimization. It will become clear that the input optimization is not independent of the output. This coupling presents design difficulties.

First define the plant/controller alignment angle as

$$\phi(j\omega) = \arccos \left(\frac{|K(j\omega)G(j\omega)|}{\|K(j\omega)\|\|G(j\omega)\|} \right) \quad (9.3.1)$$

where $K(j\omega) \neq 0$ and $G(j\omega) \neq 0$ and $j\omega$ is neither a pole of $K(s)$ nor $G(s)$. The alignment angle satisfies $\phi(j\omega) \in [0^\circ, 90^\circ]$. To analyze the alignment angle at a pole use the numerator polynomial of a right coprime factorization of the plant. The following two theorems are taken from [36]. The norm used in the theorems is the Euclidean norm.

Theorem 9.3.1 *The closed loop transfer functions satisfy*

$$\|S_o\| \leq \sqrt{1 + |T_i(j\omega)|^2 \tan^2 \phi(j\omega)} + |S_i(j\omega)| \quad (9.3.2)$$

$$\|S_o\| \leq \max\{1, |S_i(j\omega)|\} + |T_i(j\omega)| \tan \phi(j\omega) \quad (9.3.3)$$

$$\|S_o\| \geq \max\{\sqrt{1 + |T_i(j\omega)|^2 \tan^2 \phi(j\omega)}, |S_i(j\omega)|\} \quad (9.3.4)$$

$$\|T_o\| = \frac{|T_i(j\omega)|}{\cos \phi(j\omega)} \quad (9.3.5)$$

and

$$\|K(j\omega)S_o(j\omega)\| = \frac{|T_i(j\omega)|}{\cos \phi(j\omega)\|G(j\omega)\|} \quad (9.3.6)$$

Proof See [36] □

Theorem 9 3 2 *The off-diagonal elements of $T_o(j\omega)$ satisfy the bounds*

$$|T_{o12}(j\omega)| + |T_{o21}(j\omega)| \geq |T_i(j\omega)| \tan \phi(j\omega) \quad (9 3 7)$$

and, for $i \neq j$

$$|T_{oj}(j\omega)| \leq \frac{|T_i(j\omega)|}{\cos \phi(j\omega)} \left(1 + \left| \frac{p_j(j\omega)}{p_i(j\omega)} \right|^2 \right)^{-1/2} \quad (9 3 8)$$

Proof See [36] □

Thus, the sensitivity functions at the output of the plant, S_o and T_o , are not independent of those at the input of the plant, S_i and T_i . They depend on plant/controller alignment as well as the magnitude of S_i and T_i . Notice, from Equation (9 3 5), that alignment is important at frequencies where $|T_i(j\omega)| \geq 1$. That is, it is important at frequencies smaller than the bandwidth of $T_i(j\omega)$, since at higher frequencies $|T_i(j\omega)| \ll 1$ and therefore the effect of a bad alignment is attenuated. Bad alignment means $\phi(j\omega) \approx 90^\circ$, and 'good' alignment means $\phi(j\omega) \approx 0^\circ$.

It can also be concluded, from Theorem 9 3 2, that bad alignment will give higher closed loop interactions, since at least one of the off-diagonal elements of T_o will have relatively high gain. From the conclusions about limitations given in Section 9 2, it can be seen that, for the pendulum, the element (1 2) will tend to have a higher gain than the element (2 1), being even higher when the alignment is bad. Hence, interactions of this system are difficult to avoid. Also, notice that the interactions may be very sensitive to small variations of the alignment angle, since $\tan \phi$ increases linearly with small variations of ϕ from zero, whereas, $\cos \phi$ is not that sensitive regarding these variations.

Unfortunately, achieving perfect alignment is not easy, specially if the plant directions change considerably with frequency, as discussed in [37]. The pendulum system changes direction in the frequency range from 1 to 10 rad/sec as shown in Table 9 1. This shows that the system will tend to have large peaks on S_o and T_o within this range. Indeed, during the design of several controllers for this plant,

the system always presented high peaks on these functions within this range Figure 9 1 shows the variation of the plant/controller alignment with respect to frequency when using the controller obtained with the weights of Equation 8 4 3 This shows that alignment is not easily achieved when the direction of the plant varies considerably

Frequency (ω)	0 1	1	5	10	100
Direction	$\begin{pmatrix} -1 \\ 0 0009 \end{pmatrix}$	$\begin{pmatrix} -0 996 \\ 0 088 \end{pmatrix}$	$\begin{pmatrix} -0 627 \\ 0 779 \end{pmatrix}$	$\begin{pmatrix} -0 43 \\ 0 9 \end{pmatrix}$	$\begin{pmatrix} -0 345 \\ 0 938 \end{pmatrix}$

Table 9 1 Frequency vs direction of the plant

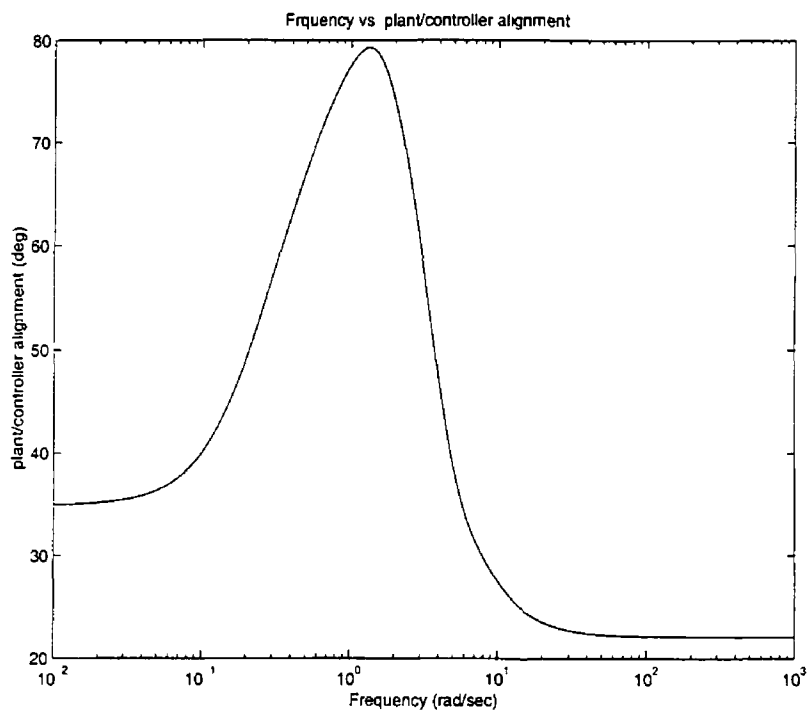


Figure 9 1 Frequency vs plant/controller alignment

9.4 Discussion

It is shown from a MIMO point of view that the pendulum system has strong limitations imposed by RHP poles As is well known, these limitations cannot be avoided, no matter what control design approach is used In fact, several control design methodologies were used to design controllers for the pendulum, among

these are LQR, \mathcal{H}_2 using the approaches of Chapter 8, \mathcal{H}_2 using the Robust Control Toolbox [30], one-loop-at-a-time (Chapter 6) and with all of them these limitations were noticeable

Also, it is shown that the relation between the sensitivity functions at the input and output depend on the plant/controller alignment. But this raises important questions. How choose the weights so that a ‘good’ alignment is achieved? Is it possible to use alignment as a measure of system quality, since it clearly varies with scaling, and with the choice of units for the two system outputs?

Chapter 10

Discussion and Conclusions

In this thesis some multivariable design approaches were presented. The inverted pendulum was used as an application example. It is a non-linear unstable plant characteristics that make it useful for analyzing design methods and trade-offs in control systems design.

Several different approaches were discussed. The first two approaches were based on one-loop-at-a-time SISO design. The second one was better because it was designed taking into consideration the inherent limitations and trade-offs in the system. The third approach was based on a non-linear method, Gain Scheduling, which was combined with the one-loop-at-a-time technique. The fourth was a full 2-norm-optimization MIMO approach. Among all controllers implemented, the Gain Scheduled (GS) controller gave the best performance for this specific system. The author believes that the reason for this is that this method takes into consideration some nonlinearities of the plant. One of the most attractive advantages of the GS approach is its simplicity compared with other design methods for non-linear systems since in the design stage it makes use of linear system theory.

The importance of analysing the fundamental limitations that exist in any system was also discussed, since these limitations were found to give more insight and guidelines on how to improve the performance of the final closed-loop.

Also, a multivariable \mathcal{H}_2 optimization approach was studied. The method presented in this thesis is based on a frequency domain approach. This feature makes

it more transparent in the sense of analysing and interpreting the algorithm, since all the steps are based on linear algebra unlike many other algorithms which depend on the solution of a Riccati equation. The algorithm given in [25] is one of the most popular methods for solving the \mathcal{H}_2 problem, but it is based on several assumptions and conditions that the plant has to obey, i.e. stability and detectability of some state space matrices and the choice of the weighting matrix W_s is restricted to strictly proper transfer functions. The only condition that the algorithm presented here has to obey is that the matrices A and B_{12} are strictly proper. Furthermore, the weight W_s can be biproper as long as A and B_{12} are strictly proper. This gives more flexibility in the choice of the weights. However, the main disadvantage with this algorithm is that the implementation is not easy in cases where the plant is complex or with high order. In those cases serious numerical difficulties were encountered. Also commercially available software (i.e. Robust Control Toolbox [30]) was used to design \mathcal{H}_2 controllers. It uses a state-space approach. It was slightly less flexible since it has some restrictions on the plants and weights to which it can be applied. Once these restrictions were fulfilled, this software presented no numerical problems. However, it has the disadvantage that the set of possible weights was reduced. In general, the results were broadly similar to the author's frequency domain software.

As mentioned above, the GS approach was found to be very effective for the pendulum system since it deals with non-linearities of the plant, which is an important characteristic of this system. The \mathcal{H}_2 MIMO approach was taken because it was expected to give better results than the one-loop-at-a-time approach since it can deal rigorously with multivariable aspects such as interactions or coupling. In practice the designed \mathcal{H}_2 controllers stabilized the system, but the performance was not very good. The conclusion is that the impact of non-linearities outweighed the benefits of a full MIMO optimization design. For future work, the combination of \mathcal{H}_2 and Gain Scheduling would be an obvious direction forward.

The \mathcal{H}_2 approach is still a useful tool for designing multivariable systems. However, it relies on the proper choice of weights. This task is much more difficult when the plant presents high interactions or strong limitations, specially those

coming from RHP poles or zeros. The real theoretical problems seem to be how to select good weights and how to treat non-linearities using \mathcal{H}_2 control. One reason for this is that the benefits that would be expected from a full MIMO optimization-based design may not be realized in practice because of the difficulties in weight selection. Thus, it would be desirable to study in more depth the relation of the weighting functions to some properties of the closed-loop system, such as the relation of weights to plant/controller alignment and/or the relation with respect to some stability margins. Also, it would be desirable to have more theoretical methods and algorithms for the GS approach, since most of the existing literature is based on ad hoc methods or approaches that are not easy to apply.

Bibliography

- [1] H H Rosenbrock, *State-space and Multivariable Theory*, Nelson, London, 1970
- [2] H H Rosenbrock and C Storey *Mathematics of Dynamical Systems*, Nelson, London, 1970
- [3] H H Rosenbrock, *Computer-Aided Control System Design*, Academic Press, London 1974
- [4] Z Lin A Saberi, M Gutmann and Y A Shamash 'Linear controller for an inverted pendulum having restricted travel A high-low gain approach ' *Automatica*, vol 32, no 6, pp 933-937, 1996
- [5] K J Astrom and K Furuta 'Swinging up a pendulum by energy control ' *Automatica* vol 36, pp 287-295, 2000
- [6] H Kwakernaak and R Sivan *Linear Optimal Control Systems*, Wiley-Interscience, New York, 1972
- [7] Feedback *Digital Pendulum System*, Feedback Instruments Ltd , Sussex UK 2000
- [8] A L Stanford and J M Tanner, *Physics for Students of Science and Engineering*, Academic Press, Orlando 1985
- [9] J M Maciejowski, *Multivariable Feedback Design*, Addison-Wesley, Wokingham England, 1989
- [10] F Tadeo, J del Valle, and A Holohan, "Smith-Youla Toolbox," in *III Congreso de Usuarios de MATLAB* Madrid, November 1999
- [11] K Havre and S Skogestad, "Directions and factorizations of zeros and poles in multivariable systems " Tech Rep , Norwegian University of Science and Technology, Trondheim 1996, Internal Report
- [12] S Skogestad and I Postlethwaite, *Multivariable Feedback Control*, John Wiley and Sons, England, 1996
- [13] Fernando Tadeo, "Personal communication," 2000

- [14] C N Nett, C A Jacobson, and M J Balas, "A connection between state-space and doubly coprime fractional representations," *IEEE Trans Automat Contr*, vol 29, no 9, pp 831-832, 1984
- [15] T Kailath *Linear Systems*, McGraw Hill United States of America, 1981
- [16] G C Goodwin, S F Graebe, and M E Salgado *Control System Design*, Prentice Hall, New Jersey, 2001
- [17] K J Astrom, "Limitations on control svstem performance," *European Journal of Control*, vol 6, no 1, pp 1-19 2000
- [18] J S Freudenberg and D P Looze, "Right half plane poles and zeros and design tradeoffs in feedback systems ' *IEEE Trans Automat Contr*, vol 30, no 6 pp 555-565, 1985
- [19] B R Holt and M Morari, "Design of resilient processing plants-vi the effect of right-half-plane zeros on dynamic resilience," *Chemical Eng Science*, vol 40, no 1 pp 59-74, 1985
- [20] R H Middleton, "Trade-offs in linear control svstem design " *Automatica* vol 27 no 2, pp 281-292, 1991
- [21] G I Gomez and G C Goodwin, 'Integral constraints on sensitivity vectors for multivariable linear systems,' *Automatica* vol 32, no 4, pp 499-518 1996
- [22] D C Youla J J Bongiorno and C N Lu, "Single-loop feedback stabilization of linear multivariable dynamical plants " *Automatica*, vol 10 pp 159-173 1974
- [23] W J Rugh and J S Shamma, "Research on gain scheduling " *Automatica*, vol 36, no 10, pp 1401-1425, October 2000
- [24] K Zhou J C Doyle and K Glover *Robust and Optimal Control*, Prentice Hall, New Jersey, USA, 1996
- [25] J Doyle K Glover, P P Khargonekar, and B A Francis, "State-space solutions to the standard \mathcal{H}_2 and \mathcal{H}_∞ control problems," *IEEE Trans Automat Contr*, vol 34, no 8 pp 831-846 August 1989
- [26] D Luenberger, *Optimization by Vector Space Methods*, John Wiley and Sons, USA, 1969
- [27] K Havre and S Skogestad, "Effect of RHP zeros and poles on the sensitivity functions in multivariable systems ' *J Proc Cont*, vol 8, no 3, pp 155-164, 1998
- [28] Z Zhang and J S Freudenberg, 'Loop transfer recovery for nonmimumum phase plants," *IEEE Trans Automat Contr*, vol 35, no 5, pp 547-553, 1990

- [29] J W Brown and R V Churchill *Complex Variables and Applications*, McGraw-Hill, Singapore, 1996
- [30] R Y Chiang and M G Safonov, *Robust Control Toolbox, User's Guide*, 2nd edition, January 1998
- [31] J S Freudenberg and D P Looze, "An analysis of \mathcal{H}_∞ -optimization design methods," *IEEE Trans Aut Control*, vol 31, no 3, pp 194–200, March 1986
- [32] H Kwakernaak, "Robust control and \mathcal{H}_∞ -optimization – tutorial paper," *Automatica*, vol 29, no 2, pp 255–273, 1993
- [33] J W Song, J G Lee, and T Kang, "Digital rebalance loop design for a dynamically tuned gyroscope using \mathcal{H}_2 methodology," *Control Eng Practice*, vol 10 pp 1127–1140, October 2002
- [34] A R Woodyatt, J S Freudenberg, and R H Middleton "An integral constraint for single input two output feedback systems" *Automatica*, vol 37, pp 1717–1726, 2001
- [35] K H Johanson, "Interaction bounds in multivariable control systems," *Automatica*, vol 39, no 6 pp 1045–1051 2002
- [36] J S Freudenberg and R H Middleton "Properties of single-input two-output feedback systems" *Int J Control* vol 72 no 16 pp 1446–1465, 1999
- [37] J M Maciejowski, "Design of multivariable feedback systems," Cambridge University, February 1982, Lecture Notes